Tailoring Fluorene-based Oligomers for micron and sub-micron sized Photopatterning

DISSERTATION

for the award of the academic degree of
Doctor of Natural Science (Dr. rer. nat.)
from the Faculty of Biology, Chemistry and Geosciences
University of Bayreuth

submitted by

Esther Scheler

born in Sonneberg/Thür.

Bayreuth, 2009

Die vorliegende Arbeit wurde in der Zeit von Januar 2006 bis Juli 2009 am Lehrstuhl für Makromolekulare Chemie I der Universität Bayreuth unter der Betreuung von Prof. Dr. Peter Strohriegl angefertigt.

Vollständiger Abdruck der von der Fakultät für Biologie, Chemie und Geowissenschaften der Universität Bayreuth genehmigten Dissertation zur Erlangung des akademischen Grades Doktor der Naturwissenschaften (Dr. rer. Nat.)

Datum der Einreichung der Arbeit: 29.07.2009

Datum des wissenschaftlichen Kolloquiums: 13.11.2009

Prüfungsausschuss:

Vorsitzender: Prof. Dr. Hans-Werner Schmidt

Erstgutachter: Prof. Dr. Peter Strohriegl

Zweitgutachter: Prof. Dr. Rainer Schobert

                    Prof. Dr. Andreas Fery

„Wer kämpft, kann verlieren.

Wer nicht kämpft, hat schon verloren.“

- Bertolt Brecht -

Table of contents

1   Summary

This thesis describes the work on tailor-made synthesis, characterization and application of well-defined fluorene oligomers for photoptatterning. Two types of fluorene oligomers are presented: pure fluorene oligomers and fluorene cooligomers incorporating various comonomers for adjusting the conductive properties towards electron and hole conduction. Since possible applications for these materials feature organic light emitting diodes and organic field effect transistors we focused on the preparation of well-defined and defect free oligomers and the preservation of their electro-optical properties during photopatterning. Further on the requirements for material synthesis are easy procedures and large quantities. Therefore we developed an approach, which produces large quantities combined with the adjustment of the desired properties in one single step. The synthetic strategy throughout the thesis comprises the addition of an endcapping species in aryl-aryl polymerization reactions. The tailormade endcapper fulfils three tasks at once, the control of the molecular weight, the introduction of polymerizable acrylate moieties and the avoidance of undesired endgroups. As aryl-aryl coupling methods the nickel catalyzed Yamamoto and palladium catalyzed Suzuki condensations were applied. The completeness of the aryl-aryl coupling and the endcapping was proven with Maldi-ToF mass spectrometry. With this approach the properties of the oligomers can be easily adjusted in view of the optimization of their photopolymerization behaviour.

The first oligomer series deals with the effect of the molecular weight on the properties and photopatterning behaviour of pure fluorene oligomers. The molecular weights were controlled by the amount of functionalized endcapper, which carried the polymerizable acrylate groups. As coupling method the Yamamoto coupling was applied. The molecular weights defined the temperature range of the nematic mesophases. An increase of the average chain length leads to higher transition temperatures $T_{i,n}$ and to better film forming properties. The photopolymerization is usually performed in the nematic state to achieve a sufficient mobility of the acrylates. The irradiation conditions had major consequences on the preservation of the characteristic electro-optical properties of the fluorenes, the harsher the conditions the higher was the probability to destroy the chemical structure by photooxidation. Further on since each chain only carries two acrylate functionalities attached to the endcappers the total number of acrylates is different for high molecular weight and low molecular weight mixtures. The

lowest molecular weight mixture contains the most acrylates and shows the lowest transition temperature, which leads to the best micron sized photopatterns.

The second generation of pure fluorene oligomers demonstrate how different contents of polymerizable groups affect the photopolymerization behaviour. Here the molecular weights were kept constant around 5000 g/mol by equal amounts of endcapper and the acrylate groups were introduced by the fluorene monomers. The Yamamoto coupling was used and upon cooligomerization with a non-acrylate fluorene monomer the acrylate content was changed from 10% to 100%. The photopolymerization times strongly depend on the acrylate content, the 100% acrylate oligomer could be photopatterned in 30 seconds, whereas the 80% and 60% mixtures needed 2-5 minutes. In the best case crosslinking is 20 times faster than found for the preceding series, which ensures the preservation of the electro-optical properties. With the highest acrylate content a photocrosslinking even at room temperature became possible.

The third oligomer series describes the incorporation of various comonomers such as TPD and bithiophene via Yamamoto reaction. Taking the knowledge of the two preceding generations into account we exploited the acrylate monomer from series two and introduced 30% comonomer. This ensured a sufficient content of acrylates for a fast photopatterning and enough comonomer for a shift of the electronic properties. We found that the electronic structure of the comonomer strongly affected the behaviour in the Yamamoto reaction. The HOMO and LUMO energy values were shifted towards hole or electron conduction. The photopatterning conditions were similar as found for the corresponding pure oligofluorenes with a 60% acrylate content. 2-5 minutes exposure produced highly emissive micro patterns. Thus a change of the electro-optical properties does not affect the photopolymerization behaviour and vice versa.

Since we found differences in the incorporation of comonomers during Yamamoto coupling we applied the Suzuki coupling, which ensures an alternately linkage of monomers. Here protective groups had to be used since the Pd-catalyst does not tolerate acrylate functionalities. We found that the comonomers were incorporated quantitatively, but the major difficulty proved to be the polymeranalogous reactions following the polycondensation. The energy values were shifted towards electron and hole conduction and the photopolymerization behaviour was similar to the Yamamoto oligomers. An exposure time of 2-5 minutes produced patterns with a maximum resolution of 700 nm.

To conclude the endcapping strategy combined with the Yamamoto coupling is a most effective tool for the adjustment of properties within one single step. The acrylate content as

well as the molecular weight can be precisely tuned, which allows a good control of the photopatterning properties. In some cases e.g. with electron withdrawing comonomers the Suzuki cross coupling is the method of choice.

Zusammenfassung

Diese Arbeit beschreibt die maßgeschneiderte Synthese, Charakterisierung und Anwendung von wohl definierten Fluorenoligomeren für die Photostrukturierung. Zwei Arten von Fluorenoligomeren werden vorgestellt: reine Fluorenoligomere und Oligomere mit verschiedenen Comonomeren für verbesserte Loch- und Elektronenleitungseigenschaften. Mögliche Anwendungen dieser Materialien sind organische Leuchtdioden und organische Feldeffekttransistoren, weshalb wir uns auf die Synthese von wohl definierten und defekt-freien Oligomeren und den Erhalt ihrer elektro-optischen Eigenschaften während der Photopolymerisation konzentriert haben. Weitere Voraussetzungen für eine Materialsynthese sind einfache Verfahren und große Mengen. Deswegen wurde ein Ansatz entwickelt, der in einem Schritt größere Mengen produziert und gleichzeitig die gewünschten Eigenschaften einstellt. Die Synthesestrategie, die sich in der ganzen Doktorarbeit findet, ist der Einsatz eines maßgeschneiderten Endcappers, der drei Aufgaben gleichzeitig erfüllt, das Regulieren des Molekulargewichts, die Einführung von polymerisierbaren Acrylaten und das Vermeiden von unerwünschten Endgruppen. Als Aryl-Aryl-Kupplungsmethoden wurden die Nickel katalysierte Yamamoto- und die Palladium katalysierte Suzuki-Kupplung verwendet. Die Effektivität der Kupplungen und des Endcappings wurden mittels Maldi-ToF Massenspektrometrie überprüft. Dieser Ansatz erlaubt die Anpassung der Oligomereigenschaften im Hinblick auf eine Optimierung der Photopolymerisation in einem einzigen Schritt.

Die erste Serie umfasst reine Fluorenoligomere und zeigt den Effekt des Molekulargewichts auf die Eigenschaften und das Photopolymerisationsverhalten. Die Moleklargewichte wurden über die Menge an Endcapper, der die polymerisierbaren Acrylate trug, gesteuert. Als Kupplungsmethode wurde die Yamamoto-Reaktion verwendet. Mit den Molekulargewichten der Oligomere veränderte sich die Lage ihrer flüssigkristallinen nematischen Phase. Ein höheres Molekulargewicht führt zu einer höheren isotrop-nematischen Übergangstemperatur. Die Photovernetzung wird gewöhnlich im flüssigkristallinen Zustand durchgeführt, weil dort

die Acrylate genügend Beweglichkeit aufweisen. Es zeigte sich, dass die Belichtungsbedingungen großen Einfluss auf den Erhalt der charakteristischen elektro-optischen Eigenschaften der Fluorene haben: je härter die Bedingungen desto höher die Wahrscheinlichkeit für eine Zerstörung der chemischen Struktur. Desweiteren trägt jede Oligomerkette nur zwei Acrylate, weshalb der Acrylatgehalt in den Mischungen verschieden ist. Die niedermolekularste Mischung enthält die meisten Acrylate und zeigt die niedrigste Übergangstemperatur was zu den besten Mikrostrukturen führt.

Die zweite Generation reiner Fluorenoligomere zeigt wie stark verschiedene Acrylatgehalte die Photopolymerisation beeinflussen. Hier wurden die Molekulargewichte konstant bei 5000 g/mol durch gleiche Mengen an Endcapper gehalten. Die Acrylate wurden mit jedem Fluorenmonomer eingeführt. Die Yamamoto-Kupplung wurde angewandt und durch Cooligomerisierung mit einem Fluorenmonomer ohne Acrylat wurde der Gehalt an Acrylat von 10-100% verändert. Es zeigte sich, dass die Photovernetzungszeit stark vom Acrylatgehalt abhängt. Das 100%-Acrylatoligomer konnte in 30 Sekunden strukturiert werden, während für die 80%- und 60%-Oligomere 2-5 Minuten nötig waren. Im besten Fall wurde eine Verkürzung der Belichtungszeit um das 20-fache im Vergleich zur ersten Serie gefunden, was erheblich zum Erhalt der elektro-optischen Eigenschaften der Oligomere beitrug. Mit dem 100%-Acrylatoligomer war die Photovernetzung sogar bei Raumtemperatur möglich.

Die dritte Oligomerserie beschreibt die Einführung von verschiedenen Comonomeren, z.B. TPD oder Bithiophen. Unter Berücksichtigung der Ergebnisse der vorangegangenen Generationen wurde ein Gehalt an 30% Comonomer gewählt und das Acrylatmonomer der zweiten Serie verwendet. Somit wurde ein ausreichender Gehalt an Acrylat und genügend Comonomer für das Verändern der elektronischen Eigenschaften garantiert. Wir stellten fest, dass die elektronische Struktur des Comonomeren das Polymerisationsverhalten in der Yamamoto-Kupplung stark beeinflusst. Die HOMO und LUMO Niveaus konnten zur besseren Elektronen- oder Lochleitung verändert werden. Das Photopolymerisationsverhalten der Oligomere war ähnlich dem des 60%-Acrylat-Gegenstücks aus Generation zwei und eine Belichtung von 2-5 Minuten produzierte stark fluoreszierende Mikrostrukturen. Demnach führen veränderte elektronischen Eigenschaften der Oligomere nicht zu einer Veränderung der Photopolymerisation und umgekehrt.

Weil wir starke Unterschiede in der Reaktivität der Comonomere in der Yamamoto-Kupplung feststellten, haben wir die Suzuki-Kupplung angewandt, die einen abwechselnden Einbau an Monomeren garantiert. Hier mussten Schutzgruppen verwendet werden, da der Pd-

Katalysator keine Acrylate toleriert. Die Comonomere wurden quantitativ in die Oligomerkette eingebaut, aber die größte Herausforderung waren die nachfolgenden polymeranalogen Umsetzungen. Die Photovernetzung war ähnlich zu den Yamamoto-Oligomeren, eine Belichtung von 2-5 Minuten führte zu Strukturen mit einer maximalen Auflösung von 600 nm.

Zusammenfassend ist die Kombination von Endcapping Technik und Yamamoto-Reaktion ein sehr effektives Verfahren für das Anpassen der Eigenschaften in einem einzigen Schritt. Sowohl der Acrylatgehalt als auch das Molekulargewicht können leicht eingestellt werden, was eine gute Kontrolle der Photopolymerisation bedeutet. In einigen Fällen jedoch, z.B. bei elektronenziehenden Comonomeren, ist die Suzuki-Kupplung die Methode der Wahl.

2   Introduction

In the past decade nanotechnology revolutionarily emerged as a fast growing field of research. The great evolution in nanotechnology is strongly driven by academic as well as industrial interests. The academic desire to reach the minimum size and resolution of working devices goes along with the constant industrial interest of driving forward the product performances. Especially the semiconductor industry is steadily increasing the computing power by the incorporation of more and more transistors on a single chip. In 1965 Gordon Earl Moore, who co-funded Intel® in 1968, formulated a law describing the extent of this growth. This law is known as Moore´s law and it says that the number of integrated circuits on a chip doubles within two years time. To give an idea of the dimensions of the number and size of transistors on a chip some examples of Intel® processors are presented. For example the Intel® 4004 processor, which emerged on the market in 1971, was equipped with 2300 transistors with a minimum gate length of 10 μm. In 1993 the Intel® Pentium with 3.1 Mio transistors and a gate length of 0.8 μm came onto the market and in 2007 Intel® released a Quad-Core Intel® Xeon® Processor with 820 Mio transistors and a gate length of only 45 nm.[1] Figure 2-1 pictures the development of the number of transistors and their gate dimensions versus time. The graphic shows that Moore´s law is still valid. The gate length decreases by a factor 0.7 in a two year period and the minimal gate length accessible at the moment is 32 nm.
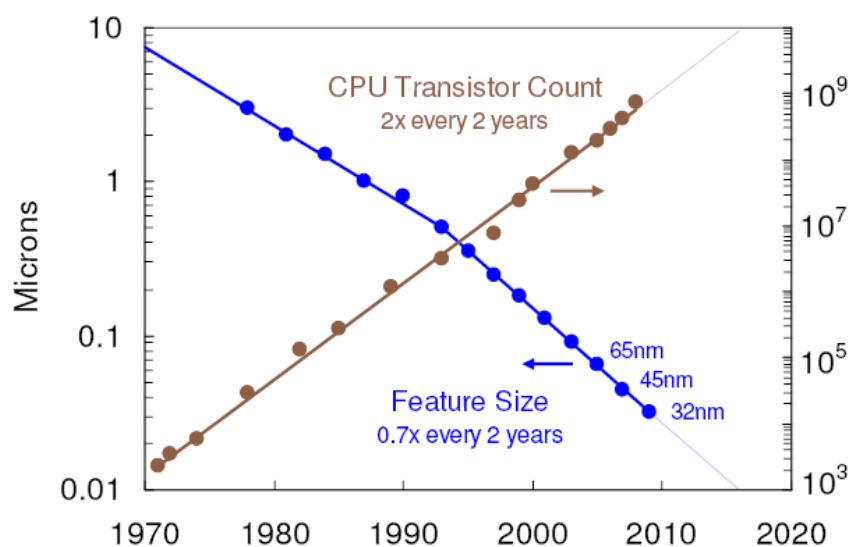
Figure 2-1. *Development of the number of transistors on a central processing unit (CPU, brown circles) and the feature sizes of the transistor gates (blue circles) over time.*[1]

Due to their power and size, microprocessors are nowadays found in many consumer electronic applications, such as mobile phones, MP3-players or GPS receivers. Thus the increasing computing power of the chips opens up new markets, which is a strong driving force for industrial research.

For the fabrication of these transistors mainly photolithographic techniques are used. Photolithography is a so-called top-down approach, where external forces, for example light, are applied for the creation of small patterns. A detailed description of lithographic techniques is found in the following paragraph. There are further top-down patterning methods such as printing or thermal evaporation techniques. Both techniques have advantages and are in use for different purposes, but they suffer from limited resolutions and are therefore not suitable to create structures in the nanometer range.[2] A different approach is the so-called bottom-up approach. Here the intrinsic properties of the materials themselves are exploited. Some materials, for example block copolymers, strongly tend to form particular patterns. In the case of the block copolymers a micro phase separation of the different polymer blocks takes place due to their immiscibility. Depending on the length of the blocks different nanometer sized structures are formed.[3] However the size and shape of the structures are predetermined by the intrinsic properties of the material, which makes the formation of arbitrary sizes and shapes difficult. Thus with this approach very small feature sizes become accessible, but there is only a limited number of patterns available. Therefore the only technique for the generation of well-defined geometric structures in the nanometer range with arbitrary shape is photolithography.
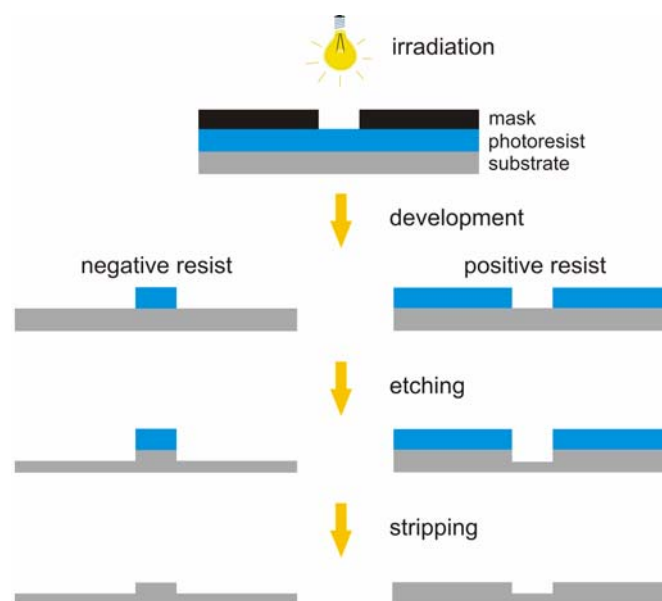
2.1 Patterning using photolithography

2.1.1 Principle and development of photolithography

In the semiconducting industry photolithography is exploited for the fabrication of micro(nano)-electronic devices based on inorganic transistors. The transistors are fabricated on silicon wafers and to pattern those wafers, the silicon or the upper silicon dioxid layer has to be structured.

In general photolithography is a method to transfer geometric shapes onto a substrate by optical means. A radiation sensitive organic layer on top of a substrate is exposed using a mask and the pattern of the mask is transferred to the organic layer. The light sensitive

organic layer is called photoresist. Upon illumination photoresists undergo chemical reactions and the solubilities of the exposed and the unexposed areas of the film become different. Afterwards, by applying a selective solvent, one of the parts, the exposed or the unexposed one, can be removed (Figure 2-2).[4]

In general there are two different types of photoresist, which produce different images of the applied mask. The positive-type resists produce an exact copy of the mask. The exposed areas become better soluble and are washed away in the developing step, which produces an exact image of the mask. Negative-type resists produce a negative image of the mask. Here, the illuminated parts become insoluble and remain on the substrate upon development. With the resist structure a number of processing steps are carried out. Among these are the etching of the SiO_2 layer, implantation of ions (doping) or metallization to realize the electrical contacts.[5] In Figure 2-2 etching is shown as third processing step, where the unprotected parts of the SiO_2 are removed. The last processing step is the complete removal of the residual photoresist. Thus a photoresist is a very important auxiliary agent, which transfers a pattern onto a silicon wafer (see Figure 2-2).

Figure 2-2. *Conventional photolithographic processing: 1. Irradiation applying a mask. 2. Developing the pattern using a selective solvent. 3. Etching the parts, which are unprotected by the photoresist. 4. Stripping off the residual photoresist.*

Researchers have been optimizing each processing step and over the years the patterns produced by photolithography were steadily decreasing in size. That is mainly due to various changes in the exposure wavelengths and the associated optics. The first technique, which

was used from 1970-1980, was the contact alignment. Here, the light sensitive material had direct physical contact with the mask and a 1x image was transferred. The resolutions were around 5 microns and the main disadvantage was the steady contamination of the mask during illumination. Later on 1x projection aligners were used. Here, the image of the mask is projected onto the wafer by optical systems. The contamination of the mask was suppressed and the resolutions were around 1 micron. In the late 1980s step and repeat systems, so-called `steppers`, were developed. In this case the pattern of the mask is projected onto the wafer with reduction optics. The patterns on the mask are about 4-5 times larger than they appear on the wafer and the substrate is stepwise illuminated. This allows an easier inspection and repair of the mask in view of defects. This method mainly came up due to the increasing wafer sizes, which drastically increased the costs for the 1x projection optics. Resolutions of 0.25 microns became accessible. The last evolution were step and scan systems, so-called `scanners`. Here, only a slit of the mask is projected onto the wafer and mask and wafer were scanned in a synchronized way to complete the image, which further reduces the complexity of the optics. With this technique feature sizes of 45 nm are produced at the moment and it is expected that the size will decrease down to at least 32 nm.[6,7]

For optical projection systems there is a simple theory, the Rayleigh equation (Eq. I), which determines the accessible resolution R:

$$R = k_1\lambda/\text{NA} \qquad \text{with } k_1 > 0.5 \qquad\qquad \text{(Eq. I)}$$

This equation expresses resolution as a function of three main lithographic parameters:
- The resolution improves with a smaller exposure wavelength λ.
- The resolution improves with a larger numerical aperture NA. The numerical aperture itself depends on the refractive index of the lens material.
- The resolution improves with a smaller k_1. This factor was originally introduced to describe the quality of the resist process, but it also commonly represents all resolution enhancement techniques such as phase shift masks etc.

Until today the most important parameter for minimizing the feature sizes is the reduction of the exposure wavelength. Here we note that with the reduction of the exposure wavelength the optics and in some cases the optical materials (lens materials etc.) have to be modified,

which is expensive and thus the key step in view of an economic use. The technical improvements leading to a lower k_1 factor will not be discussed here in detail.
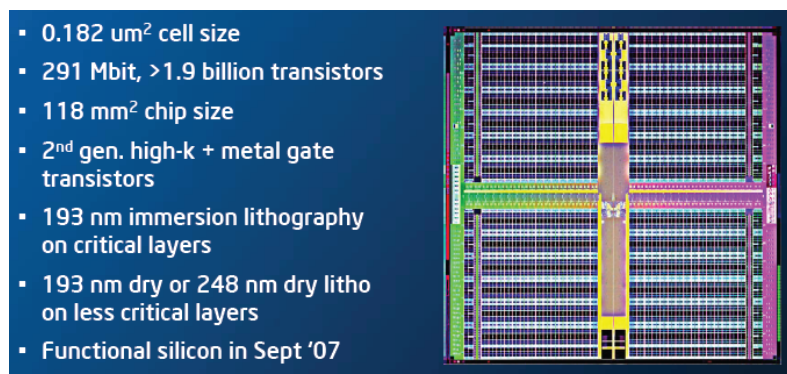
The first light sources used for photolithography were mercury lamps exhibiting a strong emission line at 365 nm (`i-line`). Therefore most of the commercially available resist systems, which are based on novolac polymers, are patterned using a wavelength of 365 nm. Then the exposure wavelength was decreased to the deep-UV region (248 nm) and new resist materials were developed. The light sources for 248 nm were mercury lamps and KrF excimer lasers, which show a ten times lower intensity at 248 nm compared to the 365 nm mercury emission. The next important step was the introduction of 193 nm lithography, which exploits the 193 nm emission of an ArF laser. The 193 nm lithography was mainly developed to reach the 90 nm technology node. The next wavelength, which was considered to improve the resolution of optical lithography, was 157 nm. The development of this technology started in the late 1990s and was stopped in 2004. There were too many challenges regarding the mask and especially lens materials. Here the most important problem was to achieve sufficient transparency at 157 nm. The production of highly transparent lenses was a very difficult and expensive process and with the evolution of a new 193 nm immersion technology the research on 157 nm was stopped. The 193 nm immersion method enhances the resolution by replacing the usual air gap between final lens and wafer surface with a liquid medium that has a refractive index greater than one (see Figure 2-3). This increases the lens numerical aperture NA and thus the resolution by a factor equal to the refractive index of the liquid. As liquid highly purified water is used, which has a refractive index of 1.44, and with this technique the minimum resolution in production today is 45 nm.[6]
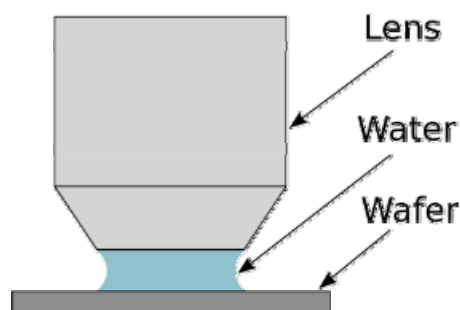
Figure 2-3. The principle of immersion lithography, the gap between lens and wafer is filled with a liquid.

The high potential of the 193 nm immersion technology has driven research to gate widths of 32 nm and it is believed that the resolution will further improve with this technology. Figure *2-4* shows an image and the characteristic data of a test chip with 32 nm gate transistors. It was presented by Intel® in September 2007 and incorporates over 1.9 billion transistors, which is over 2.3 times more than the Quad-Core Intel® Xeon® Processor released on the market in 2007.[1]

One of the leading candidates for next generation lithography is the extreme ultraviolet (EUV) lithography. This technique uses high-energy photons with a wavelength of 13.4 nm, which is in the range of soft X-rays. The EUV technique is expected to immediately improve the resolution by a factor of 3 compared to the 193 nm immersion technology. Here the main challenge is the design of new resist materials due to the high absorption of current photoresist compounds at 13.4 nm.[6,7,8]


- 0.182 um² cell size
- 291 Mbit, >1.9 billion transistors
- 118 mm² chip size
- 2nd gen. high-k + metal gate transistors
- 193 nm immersion lithography on critical layers
- 193 nm dry or 248 nm dry litho on less critical layers
- Functional silicon in Sept '07

Figure 2-4. *Characteristic data of the new 32 nm test-chip fabricated by 193 nm immersion technology by Intel®.[1]*

Another powerful lithographic technique is electron beam (e-beam) lithography. Here the chemical modification of the exposed material is induced by electrons. These electrons have a much higher energy and a much lower wavelength compared to the photons used in photolithography. Thus the achievable resolution is much higher. The factors, which limit the resolution, are electron scattering and aberrations in the resist. However the feature sizes produced by e-beam lithography are smaller than produced by photolithography, but until today this technology is not used for transistor mass production due to its low throughput.[4] However e-beam technology is utilized for the production of high resolution masks.

2.1.2   Materials used for photoresist applications

As already mentioned in the preceding paragraph there are two categories for resist materials (see Figure 2-2). Positive resists produce an exact image of the mask. Here the exposed areas are removed in the development step. Negative tone photoresists produce an inverted image of the mask pattern. Here the exposed areas remain on the substrate upon development. In general during irradiation a chemical modification has to take place to generate differences in solubility of the exposed and unexposed parts. The solubility difference can be induced for example through cutting off a protecting group to form hydroxyl groups. These types of resists are called scission resists and most of them are positive tone. Another strategy is to induce a crosslinking reaction to obtain an insoluble network. Here the classic example is the (2+2) cycloaddition of cinnamoyl groups as shown in Scheme 2-1.[9] Afterwards upon applying an appropriate solvent during development the desired areas can be washed away.
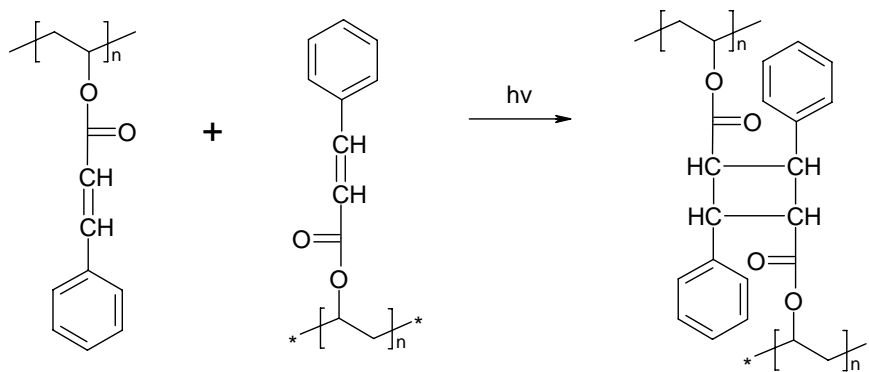
Scheme 2-1. (2+2) cycloaddition of Poly(vinyl cinnamate).

Further on there are some criteria a resist material should also fulfil.[10]
-   *Excellent film forming properties* are essential for the formation of small structures. Segregation, dewetting or defects will not lead to patterns in the nm range.
-   The resist material has to be *highly transparent* at the exposure wavelength to ensure the formation of the image through the whole film thickness.
-   A sufficient *dissolution contrast* between the exposed and unexposed areas is required to generate precise patterns.
-   The material should be *stable during the etching procedure*. Otherwise the generated pattern can not be satisfactorily transferred to the silicon wafer.

In general with the steady reduction of the exposure wavelength new photoresist materials had to be developed to ensure sufficient transparencies.

The first generation resists (365 nm `i-line` resists) were based on a novolac polymer and the sensitizer diazonaphthochinon (DNQ, Scheme 2-2).

novolac polymer   diazonaphthochinon

UV initiated reaction of diazonaphthochinon
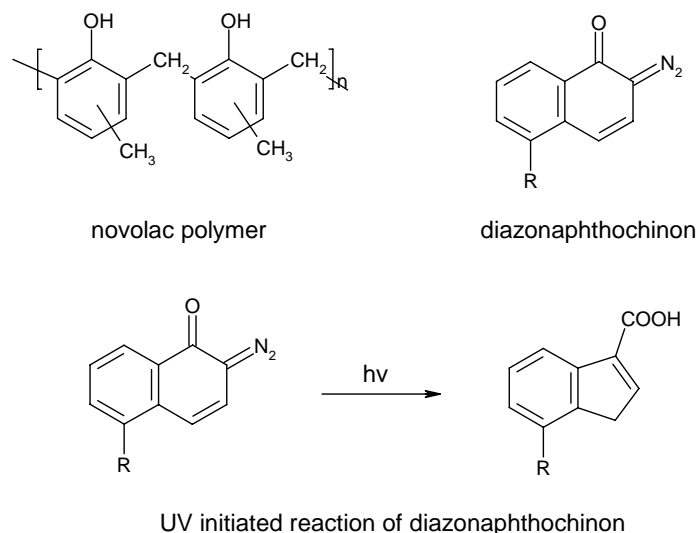
Scheme 2-2. *Top: Novolac-DNQ photoresist system. Bottom: Photoinitiated reaction of DNQ.[11]*

The novolac polymer itself is soluble in common organic solvents and in aqueous base due to its phenolic functionalities. The addition of DNQ to the novolac polymer reduces the dissolution rate in aqueous base relative to the dissolution rate of the pure polymer. Upon UV exposure the DNQ undergoes a series of reactions and indene carboxylic acid is formed, which is now well soluble in aqueous base. This leads to an increasing dissolution of the novolac-DNQ mixture in aqueous base of several orders of magnitude (Figure 2-5).[11] The novolac system therefore is a positive type photoresist.
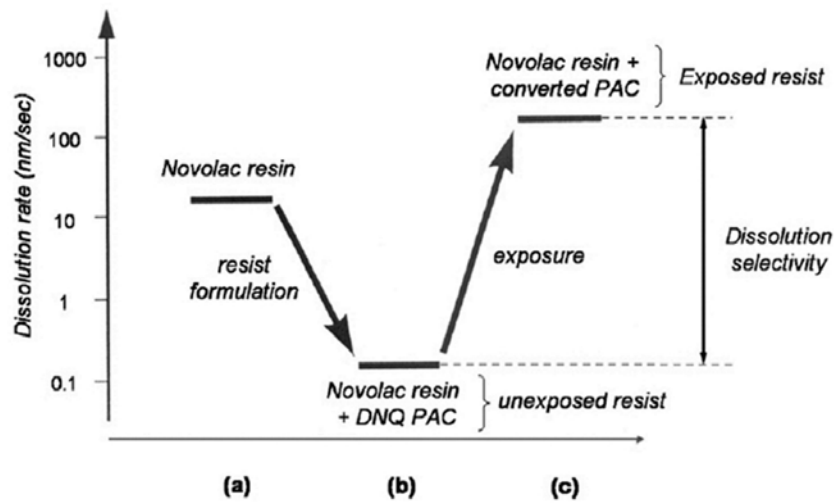
Figure 2-5. *Different dissolution rates in aqueous base for the pure novolac polymer (a), the novolac-DNQ mixture before (b) and after (c) UV exposure.*[11]

For the deep-UV (248 nm, 193 nm), novolac resins could not longer be used due to their high absorption at 248 nm and below. As mentioned before the 248 nm light sources had less power than the mercury lamps at 365 nm and hence resists with higher sensitivities were needed. Therefore so-called chemically amplified systems were introduced. Here the exposure reaction consists of two steps. Step one is the generation of small amounts of protons from a cationic photoinitiator during the light exposure and step two is a post-exposure bake to initiate a chemical reaction with the released protons. Only catalytic amounts of protons are necessary to cleave thousands of t-butyloxycarbonyl (t-BOC) protecting groups from the polymer backbone. This is the key to increase the sensitivity of an order of magnitude. With the deprotection reaction the solubility difference is induced in the exposed areas. Early examples of chemically amplified resists are poly(hydroxystyrene) (PSH) derivatives. Scheme 2-3 shows an acid catalyzed deprotection reaction of a t-BOC carbonate protected poly-4-hydroxystyrene. The protected PSH is base insoluble and the deprotected derivative is soluble in base. PSH-based resists are positive tone resists.[6,10]
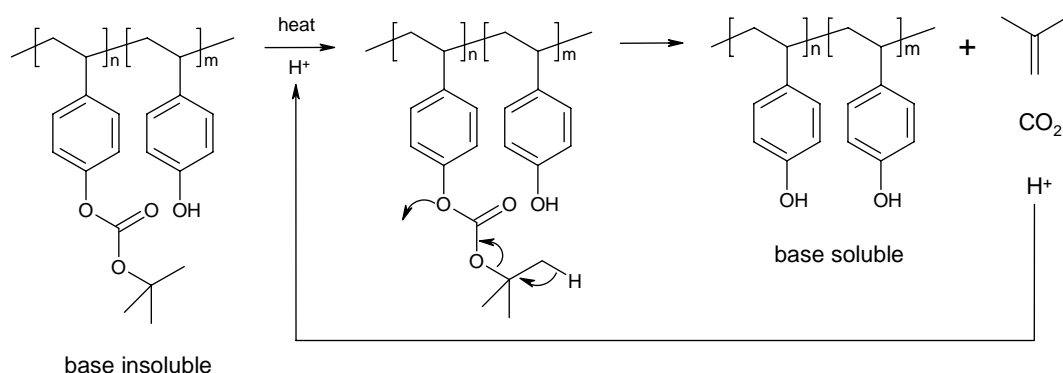
Scheme 2-3. *Acid catalyzed deprotection of a chemically amplified PSH-based resist.*[10]

For the 193 nm resist technology polystyrene derivatives were no longer used due to their insufficient transparency at 193 nm. Acrylate chemistry was applied instead and the incorporation of alicyclic adamantane or norbornene groups led to polymers with higher glass transition temperatures. These functionalized acrylate polymers are also positive tone resists and have the same working principle as the PSH-based resists.[10]
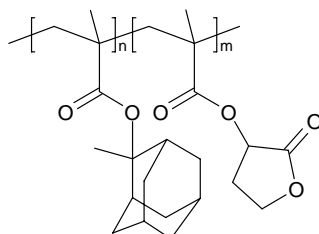
**Scheme 2-4.** *Adamantyl functionalized polymeric photoresist for 193 nm technology.*[10]

Recent research on photoresist materials focuses on amorphous molecular glass compounds. These compounds are a new class of materials for lithographic applications and are expected to improve the pattern quality. In principle they consist of arrays of phenyl rings equipped with typical resist functionalities. Their molecular weights are in the range of 1000-2000 g/mol, they are monodispers and carry many cleavable or crosslinkable functionalities. Thus molecular glasses combine the characteristic properties of small molecules, such as high purity and well-defined structures, with the beneficial aspects of polymers, such as high thermal stability and good film forming properties. Due to the defined and smaller size of the resist molecule itself it is expected that the line edge roughness and thus the pattern quality improves. Figure 2-6 shows two examples of positive tone molecular glass photoresists. The

pattern formation proceeds in the same way as described for the PSH resist upon acid catalyzed cleavage of the t-BOC group.[7,12]
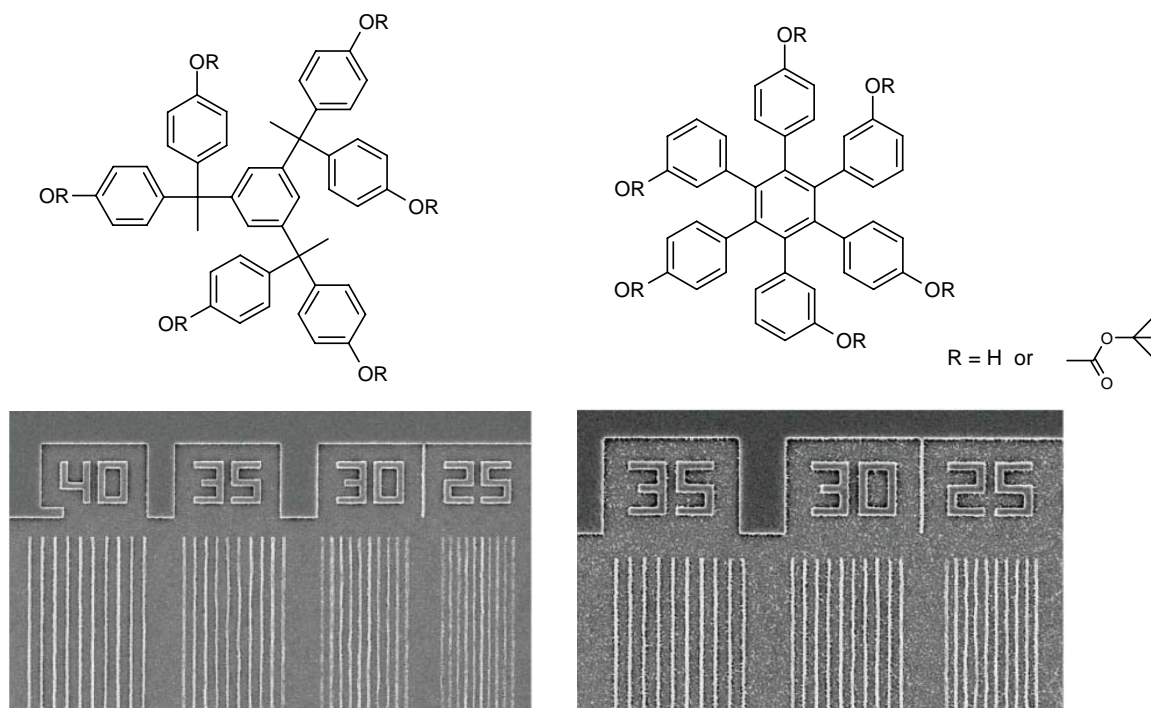
Figure 2-6. *Two types of molecular glass resists and their nano structures obtained by EUV lithography. The numbers above the lines represent their width in nm.*[12]

Some negative type molecular glass photoresists are also found in the literature. Here, upon exposure a crosslinking reaction is induced and the irradiated areas become insoluble, an example is shown in Scheme 2-5. Here the protons released from the PAG catalyze the formation of ethers. The crosslinker trisphenol has three hydroxyl functionalitites and so a three-dimensional insoluble network is formed.[13]
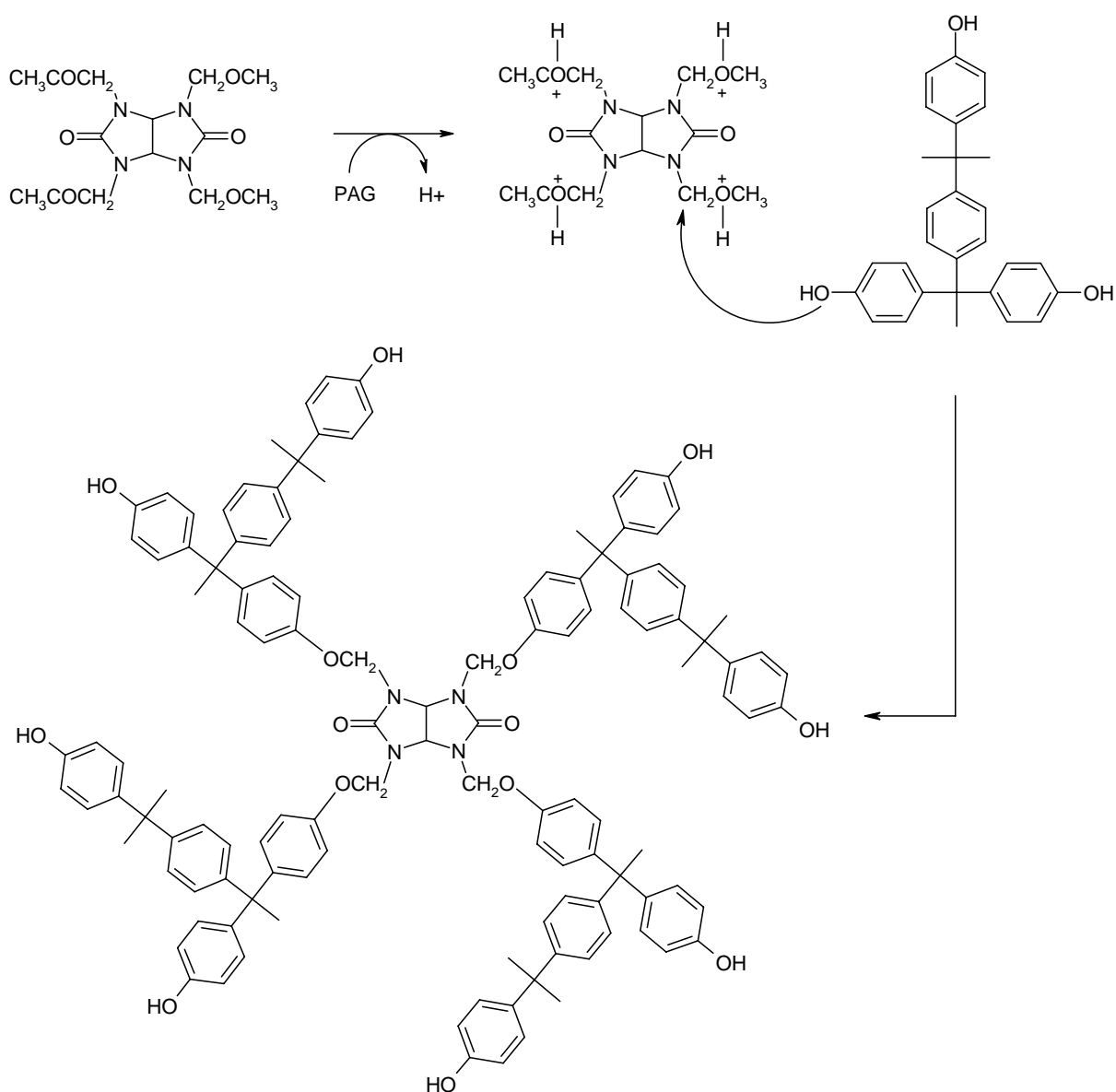
Scheme 2-5. *Working principle of a negative tone molecular glass photoresist system. Compound 1(top left) is the acid labile crosslinker Powderlink®, compound 2 is a glass forming trisphenol (top right).*

The UV sensitive compounds, which start the chemical reactions, are either radical photoinitiators, photo acid generators (PAGs) or photo base generators (PBGs). These materials do either form radicals, release protons or amine bases and are usually added in catalytic amounts.

2.2 Organic electronics

The role of polymers in the electric industry has traditionally been associated with insulating properties. Yet in 1977 Alan J. Heeger, Alan G. MacDiarmid and Hideki Shirakawa fundamentally changed this view with their discovery of electrical conductivity of doped polyacetylene.[14] For their pioneering work that has revolutionized the development of electrically conductive polymers they received the Nobel Prize in Chemistry in the year 2000.[15] Since then semiconducting organic materials have gained great interest in academic and industrial research due to their various applications in opto-electronics and the display industry. Easy processability, e.g. from solution, large area coverage and the possibility to use flexible substrates make organic semiconductors ideal candidates for low cost electronic applications. During the last decades a rapid progress took place in the field of device design, deposition techniques and molecular modeling.[16] Nowadays research on semiconducting organic materials is concentrated on organic thin film devices like organic light emitting diodes (OLEDs)[17], organic field-effect transistors (OFETs)[18], sensors[19] and organic photovoltaics.[20]

Organic light emitting diodes have undergone the fastest development. The first commercially available product based on OLEDs was launched in 1998 by Pioneer. It was an OLED display incorporated in a car radio. Five years later Kodak introduced a digital camera featured with a full color active matrix OLED display. Today a variety of mobile phones and MP3 players with OLED displays are available and some recently launched products are shown in Figure 2-7.[21]

Figure 2-7. Left: Samsung Omnia Pro mobile phone with a 3.5 inch full active matrix OLED display. Right: Sony Walkman with a 3 inch OLED display.

However prototypes of larger flat screens based on OLED technology have been under development for a rather long period of time. In December 2007 Sony introduced the industry´s first OLED television in Japan. It features an 11-inch OLED display with a thickness of only 3 millimeters and a contrast ratio of 1 000 000 : 1 (Figure 2-8).[21] In contrast to traditional liquid crystal displays (LCDs) the construction of OLED based displays does not involve the integration of a backlight for illumination. Due to this circumstance several major advantages can be obtained. OLED panels exhibit low power consumption and allow the realization of extremely thin displays. Additionally OLED displays show no viewing angle dependence which makes them an important competitor to liquid crystal displays. For the OLED technology a large expansion of the market shares has been forecasted for the next years. Nowadays OLED displays are fabricated by physical vapor deposition, which is a very expensive technique and thus raises the prices for large area displays. In order to get competitive to LC displays the OLED processing methods have to become cheaper and more efficient. Seiko Epson recently announced that they have developed an inkjet printing micro-piezo technique for the production of large area displays and they are about to present a 14 inch printed OLED display.[21,22] This would be a big step towards an economic mass production of OLED displays.

Figure 2-8. *Commercially available 11-inch OLED TV (XEL-1) from Sony.*

Besides the display market the research on organic light emitting diodes as solid-state light sources, which are flat, thin, and very lightweight is currently gaining more and more interest. Due to its freedom of design, OLED lighting technology offers many possibilities for new lighting applications while achieving substantial energy savings.[23] A lot of companies such as Osram, BASF and Philips have been working on the development of large area lighting for

several years and the first table lamp based on white OLEDs was presented by Osram.[21] Further on Philips Research recently showed a white transparent OLED lighting modulus, which could be used in window applications. They believe that this application could come onto the market in 3-5 years.[21] In general it is predicted that the real mass production of white OLED lighting applications will start around the year 2011 depending on the current progress of the different companies.


Figure 2-9: *Left: The first white light OLED table lamp introduced by Osram. Right: A transparent modulus for window applications presented by Philips Research.*

Although huge progress has been made in the area of organic electronics, all OLED devices are still driven by traditional silicon based backplanes and control electronics.[16] Current research particularly focuses on all-organic devices for the realization of flexible displays. Here the main problem is the performance of the control electronics based on organic field effect transistors (OFETs). Organic transistors usually suffer from low charge carrier mobilities and thus only low frequencies can be achieved. However in 2005 Philips presented a prototype of a flexible display driven by OFETs. This so-called e-reader had a rollable 5-inch display with a resolution of 320x240 pixels.[24] In december 2008 Hewlett-Packard (HP) and the Arizona State University introduced an unbreakable flexible prototype display driven by thin film transistors (Figure 2-10). By a new self-aligned imprint lithography (SIL) technique, which was invented by HP, the patterns are imprinted on the substrate and a perfect alignment regardless of distortion is achieved.[25] This new technology may pave the way to the mass production of all-organic flexible displays.

Another interesting field of application for OFETs are radio frequency identification (RFID) tags widely used in logistics and security applications. On these tags information can be

stored and read out contactless with a wireless read/write system. The driving voltage for the RFID tag is supplied by the radio waves from the reading/writing unit. These `smart labels` receive the radio waves with a built in antenna and therefore do not require an internal power supply. Nowadays RFID tags based on silicon circuits are quite expensive and prices of around 15 cents per tag make them still uneconomical for many applications. It is widely accepted that the availability of RFID tags at a rate of around 5 cents a piece will be the catalyst for large-scale RFID adoption.[26] This problem however could be solved with RFID tags based on organic semiconductors. Here the prices might drop below 1 cent per piece as the production costs are much lower. Liquid phase processing methods like roll-to-roll printing allow a cheap mass production of RFID tags.[27]

The company PolyIC, specialized in the printing of organic electronics, presented in september 2007 two product lines in the field of organic electronics, one in the field of printed organic RFIDs and a second line in the field of smart objects. Figure 2-10 shows a transponder chip that was prepared by this new printing technique.[28] Organic RFIDs might be the price labels in supermarkets of the future and replace the barcodes that are in use today.
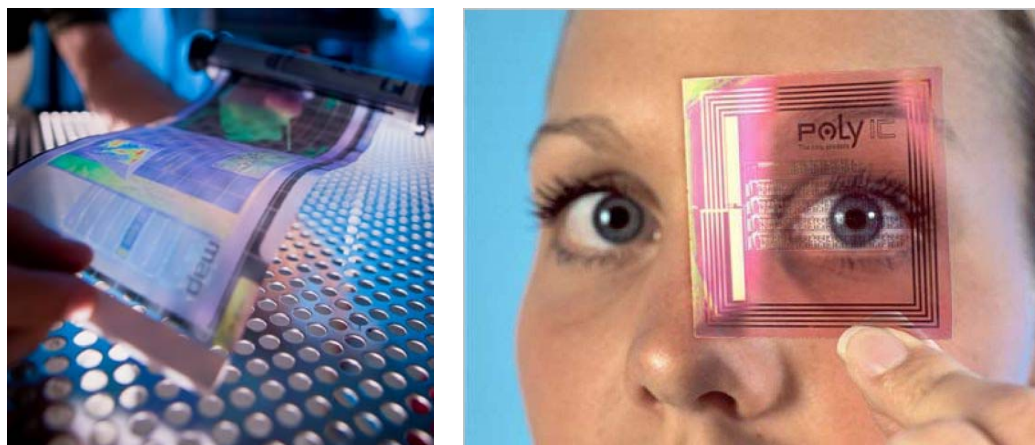

Figure 2-10: *Left: Unbreakable flexible display containing OFETs. Right: RFID prototype also based on organic field-effect transistors produced by PolyIC.*

2.3   Organic light emitting diodes (OLEDs)

2.3.1   Electroluminescence

In general luminescence is the emission in the ultraviolet, visible and infrared region. Different types of luminescence can be distinguished by different excitations. For example excitation by irradiation is called photoluminescence (PL). Chemical reactions can also lead to the emission of as light, which is called chemo- or bioluminescence. If a material is optically excited, an electron from the highest occupied molecular orbital (HOMO, S_0) is excited to the lowest unoccupied molecular orbital (LUMO, S_1). The excited electron rapidly relaxes into the vibrational ground state. Then the electron returns into its ground state S_0 under the emission of light. Due to an energy loss in the excited state S_1, the wavelength of the emitted light is longer than the absorption wavelength. The lifetime of the excited state is very short (1-1000 ns) and the phenomenon is called fluorescence. A second path for an excited electron to return to its ground state is phosphorescence. Here, the excited electron can be transferred from the singlet S_1 to its triplet T_1 state under spin reversal, which is called intersystem crossing. For this triplet state it is spin forbidden to fall back into the ground state and the relaxation therefore is a slow process (1-1000 μs). The principles of photoluminescence are shown in the Jablonski diagram (Figure 2-11).
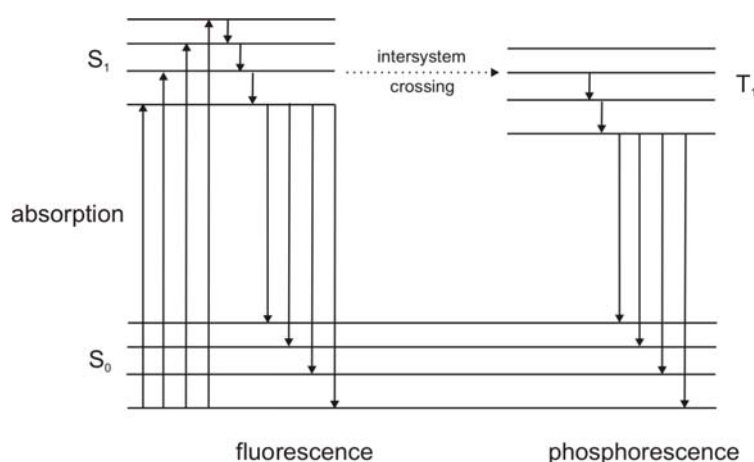
Figure 2-11. *Term scheme of optical excitation and relaxation (Jablonski diagram).*

Electrical excitation is another possibility to obtain luminescence. This electrical excitation takes place by means of an impact of charge carriers from a cathode or an anode. An electron moves from the cathode to the LUMO level of the semiconductor and a radical anion is

generated. On the other side at the anode a hole is formed by removing an electron from the HOMO level leaving the semiconductor positively charged. In an electric field these charges move by so-called hopping processes from one molecule to another. Upon recombination of a positive and negative charge an exciton is formed. An exciton is an electron hole pair with a definite binding energy called exciton binding energy. If the recombination of electron and hole results in the emission of light the phenomenon is called electroluminescence (EL). Now the difference in the LUMO energy of the negative charge and the HOMO energy of the positive charge determines the energy of the emitted light and therewith the wavelength.

This process can also occur in the opposite direction. An exciton may be formed in a dye upon irradiation and if the electron and hole can be separated, a current flows. That is the principle of organic solar cells.

Electroluminescence was first discovered by Pope[29] and Helfrich[30] et al. in the 1960s. An emission of blue light was observed by applying voltages of around 400 V to an anthracene single crystal. Since Tang and van Slyke found electroluminescence from a thin two layer OLED consisting of tris(8-hydroxyquinoline)aluminium (Alq_3) and an aromatic amine in 1987, huge progress has been made in this field.

2.3.2 Principle of organic LEDs

A single layer device architecture is the simplest OLED structure. Here, the organic semiconductor is sandwiched between two metal electrodes and acts as emitter and charge transport material (hole and electron transport) at the same time. The anode typically consists of semitransparent indium-tin-oxide (ITO), which has a relatively high ionization potential of around 5 eV. ITO can be sputtered onto different substrates, for example glass or flexible PET foil. The requirement for the cathode material is a low ionization potential so that electrons can be easily removed. Typical cathode materials are magnesium or calcium. Due to their low ionization potentials these materials are easily oxidized by air or water and thus the processing has to be performed under exclusion of air/water. The cathode is usually vapour deposited on top of the emitting layer. The emitting layer itself can be processed either from solution by spin coating or via vacuum evaporation. The deposition technique of the semiconducting layer strongly depends on the material used. If high molecular weight compounds such as oligomers or polymers are used, they are processed from solution. Low molecular weight compounds, which do not show good film formation from solution, are

usually deposited via thermal evaporation. A typical single layer OLED device is shown in Figure 2-12.
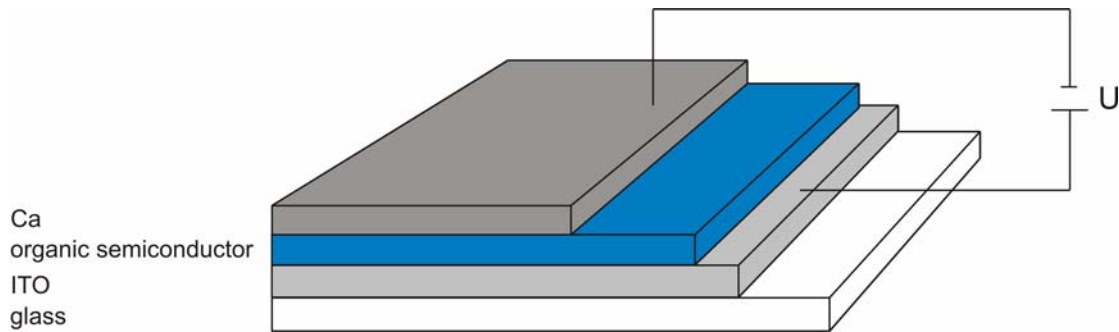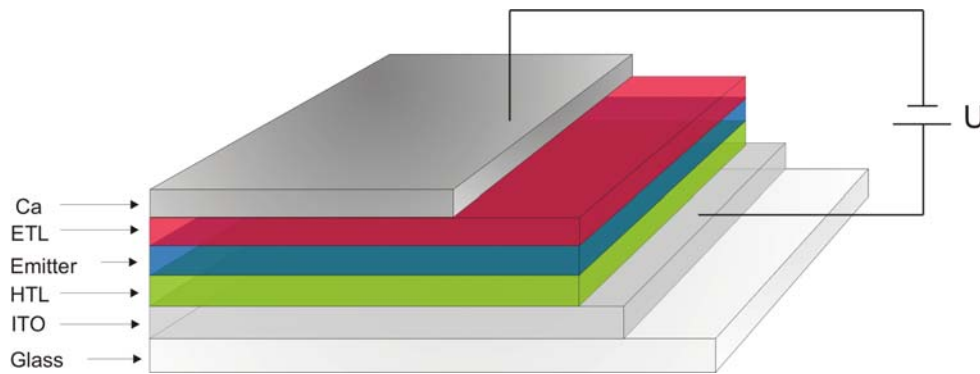

Figure 2-12. *Single layer OLED architecture. Here the organic semiconductor serves as both transport and emission layer.*

If a voltage is applied to the electrodes of the OLED device as depicted in Figure 2-12 electrons from the cathode and holes from the anode are injected into the organic semiconductor. Due to the electric field between the two electrodes the positive and negative charges move through the organic layer. As soon as they recombine in the emitting layer, light is generated.

The efficiency of an OLED is determined by the number of charge carriers that are injected and the number of holes and electrons that actually recombine under the emission of light. There is a special area where the recombination occurs, which is called the recombination zone. The position of this zone depends on the velocity of the moving holes and electrons and usually the hole mobility is higher than the electron mobility.[31] Therefore in a single layer device the recombination zone is not located in the middle of the organic layer, but is shifted towards the cathode, which leads to non-radiative losses.[32] Consequently, the efficiency of the device decreases.[33]

To improve the device efficiency a multi-layer architecture was developed and is now frequently used in OLED manufacturing. Here, additional hole (HTL) and electron (ETL) transport layers are introduced for a balanced charge carrier transport (Figure 2-13). By a variation of the different layer thicknesses the position of the recombination zone can be shifted towards the middle of the emissive layer. This drastically increases the device efficiency. However this architecture demands a careful adaptation of energy levels to insure an efficient charge carrier transport. The HOMO and LUMO levels of the different materials have to match (Figure 2-14). The LUMO level of the ETL has to be in the same range as the

cathode material and the HOMO level of the HTL has to match the ITO ionization potential.[31] Even more layers, e.g. electron injection or blocking layers, can be incorporated to further improve and balance the charge carrier injection and transport.[34]


Figure 2-13. Multi layer OLED architecture incorporating hole (named HTL) and electron (named ETL) transport layers.
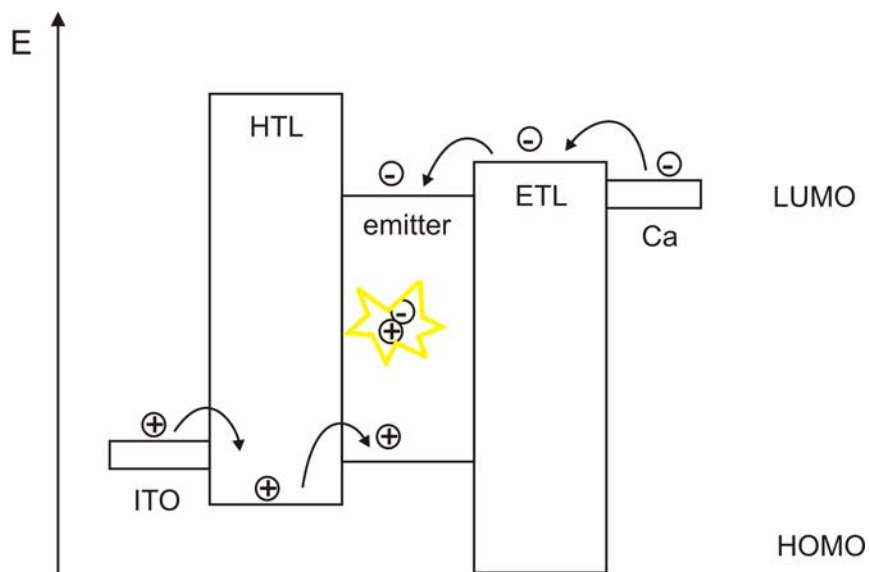
*Figure 2-14.* Energy levels of the different materials used in multi layer OLEDs.

2.3.3   Materials for OLED applications

Active materials in OLEDs have to fulfil a variety of requirements. First of all they have to emit light with suitable colour coordinates of the CIE-system (Commission International de L´ Eclairage) and have to ensure a sufficient transport of charge carriers. A good chemical and electrochemical stability as well as a high thermal stability are also important prerequisites for OLED materials.[35,36] Furthermore the compounds should exhibit good film forming properties. Crystallization of the thin film may lead to a decrease of charge carrier mobilities and finally to a short-circuit in the device.[37,38] Small molecules are therefore equipped with bulky side groups to reduce their crystallization tendency. Such materials form stable amorphous films and are called molecular glasses.[39] These small molecules are either deposited from solution or via vapour deposition. Polymers however usually show good film forming properties and thin films are prepared from solution by spin coating or doctor blading. Additionally the hole and electron transporting materials have to fulfil further requirements. Materials used as HTL have to exhibit HOMO levels around 5.3 eV to ensure a good hole injection from the ITO anode. These materials usually are electron rich compounds and typical hole conductors are aromatic amines as shown in Scheme 2-6.[40,41]

TCTA   TDAB   α-NPD
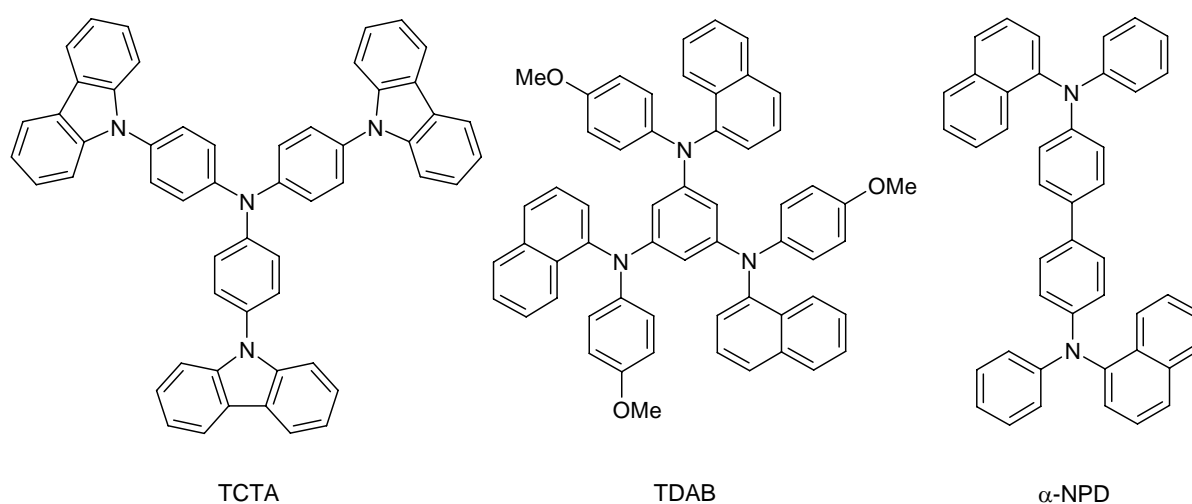
Scheme 2-6. *Typical aromatic amines used as hole transport materials. Tris-(4-carbazol-9-yl-phenyl)-amine (TCTA), 1,3,5-Tris-(diarylamino)benzene (TDAB) and N,N`-di(naphthalen-1-yl)-N,N`diphenyl-diphenyl-4,4`-diamine (α-NPD).*

Compounds used as ETL have to exhibit LUMO levels in the range of the work function of the cathode material to ensure a good electron injection from the cathode. These materials usually are electron deficient compounds and some typical electron conductors are shown in Scheme 2-7.[42,43,44]
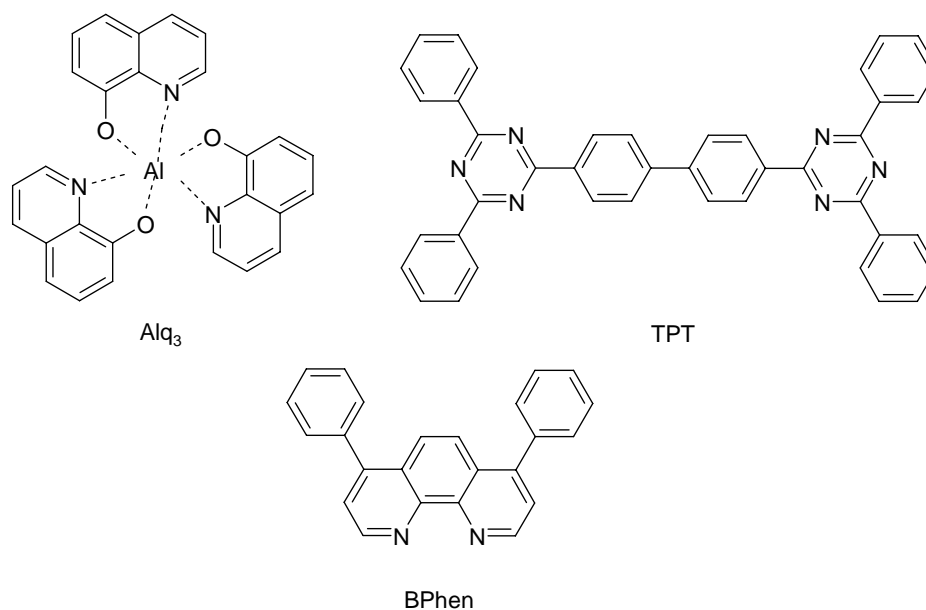

Scheme 2-7. Typical examples for ETL materials: tris(8-hydroquinoline) aluminium (Alq₃), 4,4'-Bis[2-(4,6-diphenyl-1,3,5-triazinyl)]-1,1'-biphenyl (TPT) and 4,7-Diphenyl-[1,10]phenantroline (BPhen).

The emitting material itself is a conjugated polymer or low molecular weight material. In 1990 the group of Richard Friend was the first who used a conjugated polymer as emitter in a solution processed single layer device.[45] They used the highly fluorescent poly(p-phenylenvinylene) (PPV), which was insoluble and therefore hard to work with. A few years later soluble PPV derivatives like MeH-PPV [46] or PPV-copolymers [47] were developed. The solubility could be improved by the introduction of alkoxy substituents. These substituents also influence the emission colour, PPV is a green emitting and MeH-PPV an orange emitting material. All these compounds are shown in Scheme 2-8. To shift the emission wavelength to the blue region the band gap between HOMO and LUMO has to be increased. Poly(9,9-dioctylfluorenes) are frequently used as blue emitting polymers, since they are easily synthesized and processible (Scheme 2-8).[48] Due to the large energy gap between HOMO and LUMO level in blue emitters, the long term stability of blue OLEDs is still a problem.

In fluorescent OLEDs the internal quantum efficiency is limited to 25% due to spin statistics. With phosphorescent emitters both singlet- and triplet excitons contribute to the electroluminescence and hence the theoretical limit of the quantum efficiency rises to 100%. In 1999 Forrest and Thompson introduced the green phosphorescent complex $Ir(ppy)_3$ which is used as a dopant in a CBP matrix[49]. CBP has a high S_0-T_1 band gap of 2.55 eV and is therefore well suited as matrix material for the green emitter $Ir(ppy)_3$ (see Scheme 2-9). FIrpic is a phosphorescent greenish-blue emitter with a higher S_0-T_1 energy level difference. For such emitters, matrix materials with a S_0-T_1 band gap of almost 3 eV, like CzSi[50], are necessary. All these phosphorescent complex emitters are doped into suitable matrix materials to avoid concentration quenching and to ensure an efficient energy transfer. Research in this field is a hot topic at the moment in view of future lighting applications. Here, upon combination of the colours red, green and blue, white light OLEDs are fabricated. To achieve an adequate colour stability of the white light the lifetimes of the three colours have to be similar. However there are still some problems concerning the lifetimes of the blue light emitting species.
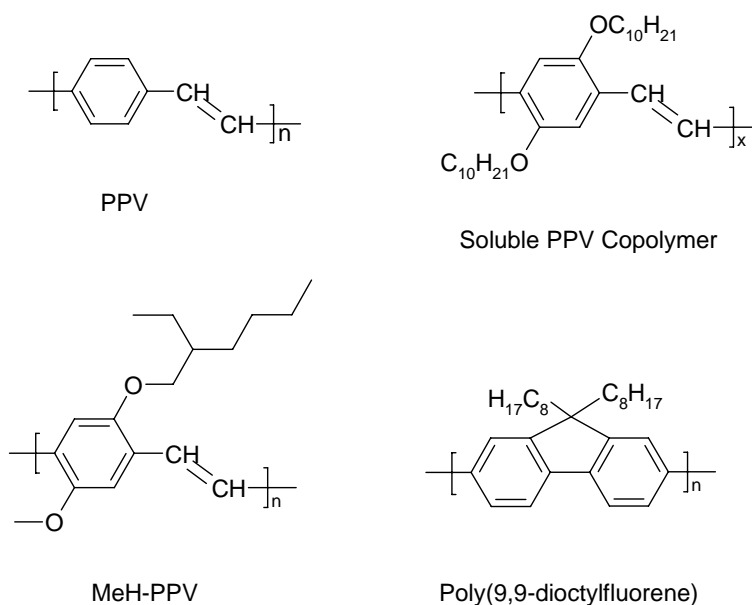

Scheme 2-8. *Chemical structures of PPV and some PPV derivatives and the blue emitting polymer Poly(9,9-dioctylfluorene).*

Ir(ppy)$_3$

FIrpic

CBP

CzSi
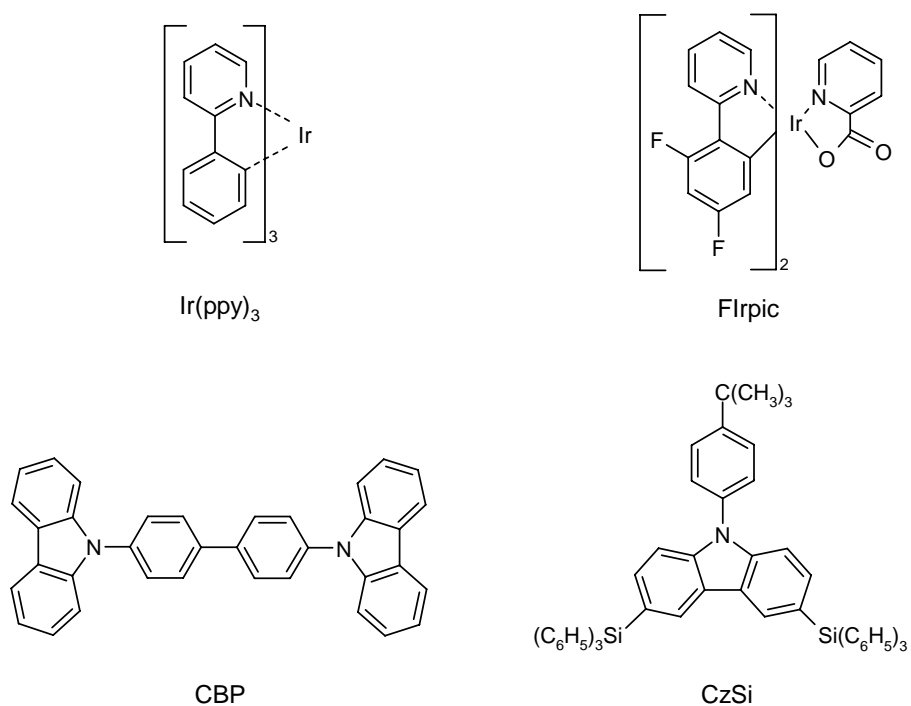
Scheme 2-9. *Chemical structures of some common phosphorescent emitters (top) and their corresponding matrix materials (bottom).*

3   Aim of the thesis

The aim of this thesis was the synthesis, characterization and processing of novel light emitting fluorene oligomers with photocrosslinkable moieties. For the preservation of the characteristic semiconducting properties it is very important that the photocrosslinking does not change the functional conjugated structure.[51] Thus the main task throughout the thesis was to adjust the photopolymerization behaviour by the oligomer composition, so that the electro-optical properties of the material are not changed. Since the requirements for material synthesis are easy procedures and large quantities we were looking for a simple synthesis combined with the control and adjustment of the chemical structure and material properties. For the formation of well-defined fluorene oligomers the transition metal mediated Yamamoto and Suzuki reactions are well- suited.[52] We also know that a powerful approach to easily tune the properties of oligomers is the endcapping technique.[53] Here a monofunctional endcapper is added during polymerization, which terminates the chain growth, regulates the molecular weight, introduces special functional groups and avoids ill defined endgroups. For electro-optical applications well-defined and defect free compounds have to be formed. We now combined the aryl-aryl coupling methods with the endcapping approach and looked at the effectiveness of both reactions. If both reactions are complete well-defined oligomers are formed within one single step. Here the choice of monomers (acrylate-containing, electron donating or withdrawing) and coupling method determines the chain composition and the endcapper regulates the molecular weights. Thus this thesis addresses the effectiveness of aryl-aryl coupling and endcapping reactions, the resulting oligomer compositions and their photopatterning and electro-optical behaviour.
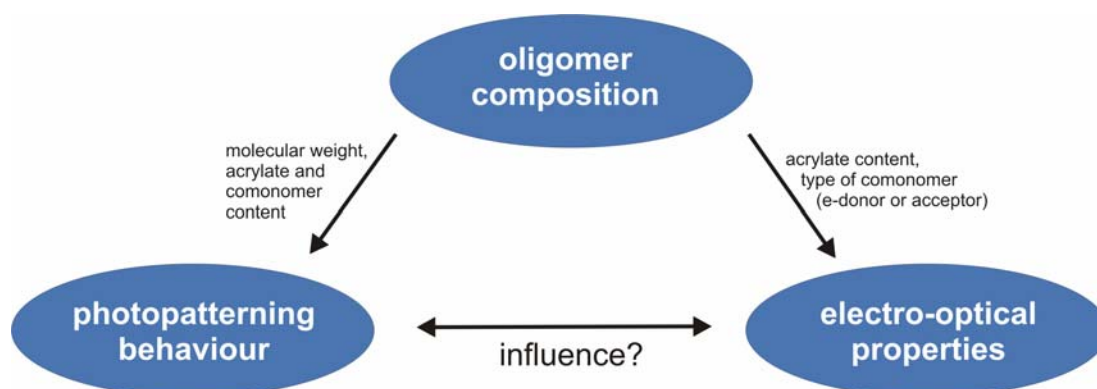
Figure 3-1. *Dependence of the photopatterning and electro-optical properties on the oligomer composition.*

4   Overview of the thesis

This thesis contains six publications, four of them are presented in chapters 7-10. Two more appear in the appendix (chapters 11, 12) since the synthetic work was performed during my diploma thesis, but the important experiments leading to the publications were performed during the PhD thesis. Four publications are already published, one is submitted to Chemistry of Materials and one is intended for submission.

I was mainly interested in developing simple synthetic strategies leading to different photopatternable fluorene oligomers. The central point through my thesis is the adjustment and improvement of the desired properties of the semiconducting materials. The properties were adjusted in two directions, at first towards an optimized photocrosslinking behaviour and secondly towards electron and hole conduction to expand the application spectrum. The experiences with each material series consequently led to the development of the following series. The publications in chapters 7-10 are presented chronologically in the way they evolved during the thesis. Every series of oligomers profited from the preceding one. The optimized parameters found for one series were exploited in the following while varying other parameters. Each new generation of oligomers involved the syntheses of new monomers and/or comonomers while we tried to keep the syntheses as simple as possible. All series of oligomers were characterized thoroughly using standard methods. For the characterization of the micro and sub-micro patterns microscopic methods were applied.

In the first generation oligofluorenes the molecular weights were varied while keeping the number of acrylate units per oligomer constant. As cross coupling reaction the Yamamoto coupling was chosen due to excellent results I obtained during my preceding diploma thesis. The molecular weight was adjusted using endcapping technique and with this endcapper the functional acrylates were introduced. The first important finding was that acrylates can be polymerized directly in the Yamamoto coupling. This simplifies the synthesis and was exploited in the following publications. The molecular weights of the oligomers were tuned and with an increasing molecular weight the nematic-isotropic transition temperatures increased. Since the photocrosslinking is usually performed in the nematic state different temperatures were necessary during irradiation. The different temperatures applied had a major influence on the optical properties afterwards. We obtained the best results with the lowest molecular weight compound and attribute that to the highest number of acrylates und

to the lowest crosslinking temperature (chapter 7). The maximal lateral resolution was 1 micron.

In the second generation oligomers we kept the molecular weights constant by equal amounts of endcapper, but varied the acrylate content. The fluorene monomer itself was modified so that every monomer carries an acrylate unit. Thus upon cooligomerization with a non-functionalized fluorene monomer the variation of the acrylate content became possible. We prepared six different cooligomers and found a complete insertion of both endcapper and comonomer. Thus there is a total freedom in the variation of the molecular weight and acrylate content within one synthetic step. Further on we studied the photopatterning properties and discovered an over 20 times faster photocrosslinking reaction of the oligomer having the highest acrylate content compared to the first generation oligomers (chapter 8). A photopolymerization even at room temperature was possible and lateral resolutions of 700 nm were obtained.

In the third generation the electro-optical properties were altered. The molecular weights were again kept constant by an endcapper, but different comonomers such as TPD or bithiophene were introduced. The best compromise between introducing a sufficient amount of comonomer while having many acrylates was found to be 70% fluorene acrylate and 30% comonomer. The Yamamoto reaction was applied and we found that only electron rich aromates were inserted quantitatively. Electron poor monomers were only incorporated with major monomer modifications. The optical properties were strongly governed by the compositions of the mixtures and upon optical excitation energy transfer reactions were observed. The HOMO and LUMO energy levels were shifted towards hole and electron conductive properties. The photopatterning took roughly the same time as found for the oligofluorene counterpart from the preceding series with 60% acrylate. The lateral resolutions were in the range of 1 micron (chapter 9).

Since the incorporation of electron poor comonomers in the Yamamoto reaction proved to be problematic we applied another prominent cross coupling, the Suzuki coupling. The Suzuki reaction takes place between a bromine and a borolane and thus ensures an alternating incorporation of the monomers and both types, electron poor as well as electron rich monomers, are inserted. The strict alternating arrangement of the monomers also leads to
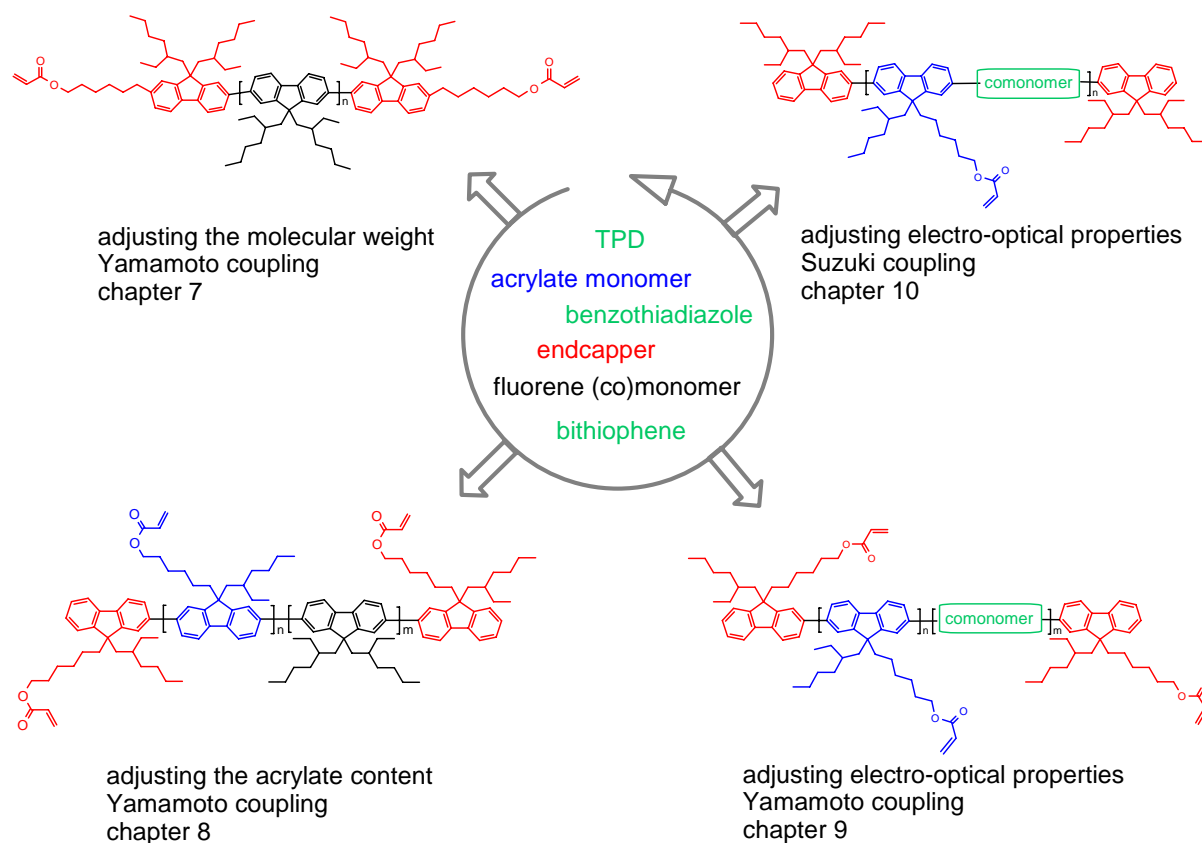
different electro-optical properties compared to the random Yamamoto oligomers. However acrylate functionalities are not tolerated in the Suzuki coupling and we had to use protective groups during the coupling. The acrylate was introduced afterwards by a polymeranalogous conversion. This proved to be the most challenging step due to solubility issues. The optical properties were determined and compared to those of the preceding random Yamamoto oligomers. We found, that they strongly differ in dilute solutions, but are almost the same in thin films. This makes both oligomer series ideal candidates for thin film applications. The photopatterning behaviour was similar to the Yamamoto oligomers, but resulted in a better resolution of up to 600 nm (chapter 10).

Within the framework of this thesis some additional experiments based on unfunctionalized oligofluorenes were performed and two publications evolved. Since the synthetic work was done in my diploma thesis these publications appear as appendices at the end of the thesis (chapters 11, 12) However the key experiments leading to these publications were performed during my PhD thesis and are therefore presented here.

Chapter 11 describes the synthesis and characterization of polydisperse oligofluorenes. The Yamamoto coupling was applied and the results paved the way for the synthetic strategy of the PhD thesis. Another important experiment described in this chapter was the construction of a GPC (gel permeation chromatography) calibration curve from the synthesized fluorene oligomers. This calibration was used to determine the molecular weights of all the acrylate oligomers presented in this thesis.

Chapter 12 describes the determination of the conformation of fluorene oligomers by single molecule spectroscopy. A polydisperse oligofluorene as described in chapter 11 was separated using preparative GPC. Narrowly distributed fractions were obtained and the composition of each fraction and the exact molecular weights of the distinct oligomers were determined. Single molecule spectroscopy of the different fractions was then performed. The phase dependent emission was detected and a shift was observed. Single oligomer chains were therefore isolated and fixed in a transparent matrix. Upon measuring the emission of the isolated chains the total number of molecules and their corresponding phases were determined. Since we know the exact composition of each GPC fraction a dependence of the phases on the chain lengths was found and two phase shifts were observed.

Scheme 4-1 illustrates the various cooligomer compositions synthesized by Yamamoto and Suzuki coupling presented in this thesis. The circular arrow in the centre describes the advances and the increasing complexity in the thesis.


adjusting the molecular weight
Yamamoto coupling
chapter 7

TPD
acrylate monomer
benzothiadiazole
endcapper
fluorene (co)monomer
bithiophene

adjusting electro-optical properties
Suzuki coupling
chapter 10

adjusting the acrylate content
Yamamoto coupling
chapter 8

adjusting electro-optical properties
Yamamoto coupling
chapter 9

Scheme 4-1. Monomers, polymerization techniques used and cooligomer compositions described in this thesis. Upon following the circular arrow from top left the first set of fluorene oligomers shows a variation in the molecular weight. The second series (bottom left) comprises an adjustment of the acrylate content. In the third series (bottom right) new comonomers were introduced to tune the electro-optical properties. The fourth set (top right) comprises the incorporation of the new comonomers via Suzuki coupling.

4.1   Unfunctionalized fluorene oligomers – narrow standards for GPC calibration and single molecule spectroscopy (Chapters 11, 12)

In macromolecular chemistry a standard method for the determination of molecular weights is gel permeation chromatography (GPC). This technique is based on the distribution of the polydisperse macromolecules between the pores of a crosslinked polystyrene matrix and an eluent. The polymer chains penetrate into the pores according to their hydrodynamic volume. Long chains can not infiltrate the pores and are eluted first, short chains can infiltrate into the pores and are eluted at last and therefore a separation takes place. For calibration narrowly distributed standard materials, such as polystyrene standards, with known molecular weights are used. Thus GPC is a relative method and absolute molecular weight values are not obtained. If the hydrodynamic volume of the polymer sample is similar to the calibration standards, GPC provides a good estimation of the molecular weight. If the hydrodynamic volumes differ a lot the measured molecular weights are over- or underestimated. Especially for rigid or semi-rigid polymers such as polyfluorene the molecular weights are overestimated (up to a factor of 2.7) using the standard polystyrene calibration.[54] For a better estimation of the molecular weights by GPC we utilized polydisperse oligofluorene samples for the construction of a calibration curve. This calibration was then used to determine the molecular weights of the (co)oligomers described in this thesis.

For the construction of a calibration curve narrowly distributed standards with known molecular weights had to be prepared. Therefore we separated an oligomeric mixture with a relatively broad molecular weight distribution (PDI = 1.64) by preparative GPC. The synthesis and characterization of the polydisperse fluorene oligomers is described in chapter 11 in detail. Figure 4-1 (top black curve) shows the oligofluorene mixture before separation and the fractions after separation (bottom coloured curves). 13 fractions were obtained and their exact molecular weights and compositions were determined using Maldi-ToF (see Figure 4-1 bottom). Now the elution volume of each (distinct) oligomer in the GPC can be assigned to an exact molecular weight and a calibration curve can be constructed.

The separation produces narrowly distributed samples with PDIs around 1.04, but the fractions still consist of at least four distinct oligomers. A separation of the single oligomers was not obtained by the preparative GPC columns.
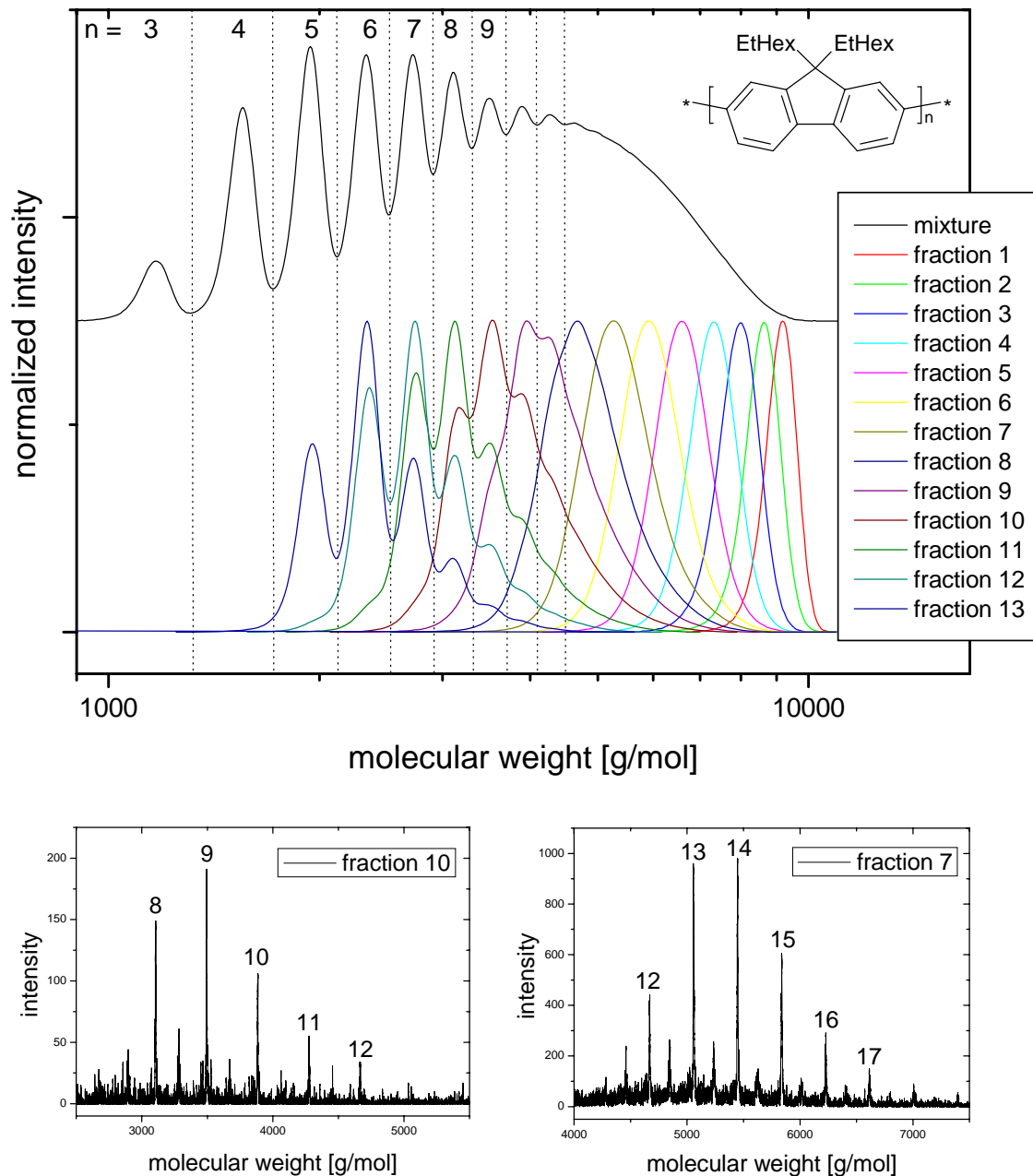
Figure 4-1. *Top: GPC scans of a polydisperse oligofluorene and the narrowly distributed fractions obtained by preparative GPC (named fractions 1-13). Bottom: Maldi-ToF spectra of the separated fractions 7 and 10. The numbers above the signals correspond to the degrees of polymerization (8=fluorene octamer).*

Figure 4-2 shows the oligofluorene versus the standard oligostyrene calibration curve. For molecular weights below 2000 g/mol both curves give identical values. Here, the oligomeric styrene can not be described as random coil and behaves therefore similar to the semi-rigid oligofluorene. At a molecular weight of 2000 g/mol the oligostyrene chain starts to coil and its hydrodynamic volume deviates from the hydrodynamic volume of an oligofluorene chain. The difference between both curves increases with an increasing molecular weight from

2000 g/mol onwards (chapter 11). This calibration curve now allows a very good determination of the molecular weights of oligofluorenes.
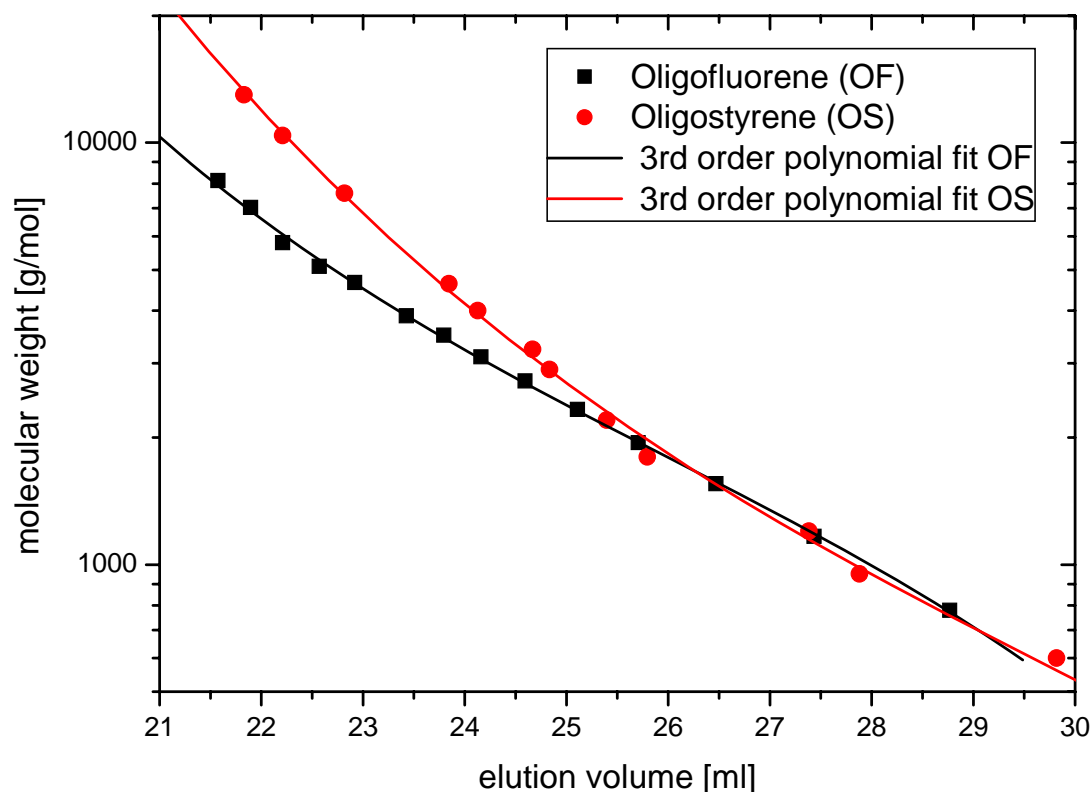
Figure 4-2. *GPC calibration curves constructed from oligostyrene (red) and oligofluorene (black) standards. The dots and squares represent the measured standards and the lines represent the third order polynomial fits.*

Further on n-octyl substituted fluorene oligomers show different bulk morphologies named glassy, γ- and β-phase depending on their intramolecular conformation. These different conformations change the electrical and optical properties and can be measured by low-temperature single-molecule spectroscopy. We therefore prepared narrowly distributed samples of oligo(9,9-dioctyl)fluorenes by preparative GPC as described before. The samples were then fixed in a transparent matrix at very low concentrations (10^{-8} g/l) and cooled down to 5K. With this method the single oligomers are well distributed in the matrix and due to the low concentration they are well separated from one another, which opens up the possibility for the optical excitation of single molecules. Single oligomers were now excited at 398 nm and their photoluminescence (PL) was detected. Depending on their intramolecular conformation the oligomers emit light with maxima at 413 nm (glassy phase), 428 nm

(γ-phase) or 446 nm (β-phase). The PL of several (~100) oligomers was detected within one fraction and histrograms were constructed. The histograms now display the numbers of chains and their corresponding emission wavelength. From the association of emission wavelength and phase behaviour we know the number of chains having a distinct conformation. Since the exact composition (or the most abundant oligomer) of each fraction was determined by GPC and Maldi-ToF we can assign the conformations to distinct oligomers. We found that the transition from the disordered glassy- to the γ-phase takes place from the heptamer (7-FO sample in Figure 4-3) to the octamer (8-FO). The β-phase was predominantly formed by the mixture containing mostly nonamers. Therefore 9 or more fluorene units are necessary for an extended planarization and thus the formation of the β-phase (chapter 12).
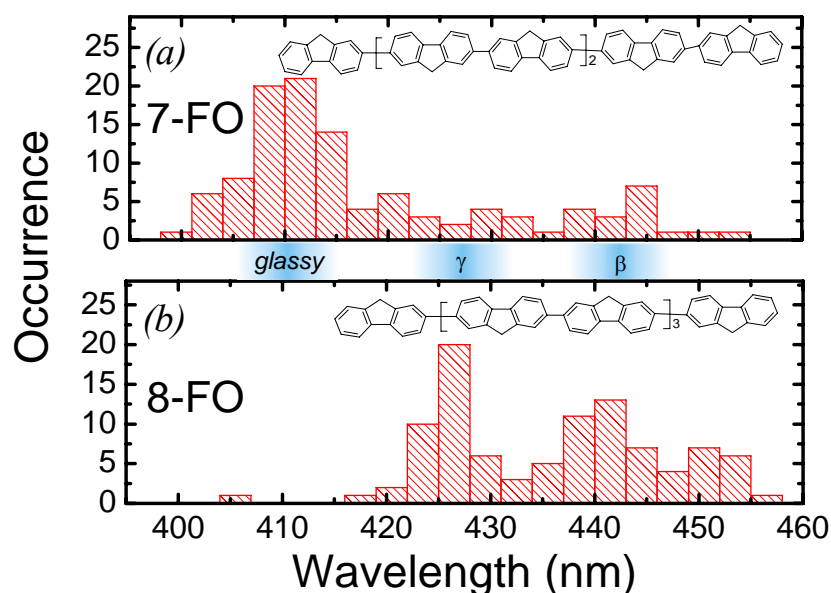
Figure 4-3. *0-0 emission wavelength histograms for 110 single molecules from the 7-FO fraction (a) and 97 single molecules from the 8-FO fraction (b). The insets show the chemical structures for the most abundant oligomer in the respective fractions.*

4.2   Fluorene oligomers with two pendant acrylate groups (Chapter 7)

Since we know from my diploma thesis that with a simple one-step endcapping procedure well defined fluorene compounds are accessible (see chapter 11) we adopted this concept for acrylate functionalized compounds.

In general an endcapper is a molecule, which terminates a polymerization reaction. It is often used to avoid residual functionalities such as bromine at the end of a polymer chain and/or to attach certain molecules. The amount of endcapping species determines the chain length and to obtain well defined products a controlled and complete endcapping process is indispensable. Here the Yamamoto coupling was applied, which uses bromine units as functional groups. For the polymerization 9,9-di(2-ethylhexyl)-2,7-dibromofluorene **A** served as monomer and with the amount of endcapper **B** the molecular weights were adjusted (see Scheme 4-2).
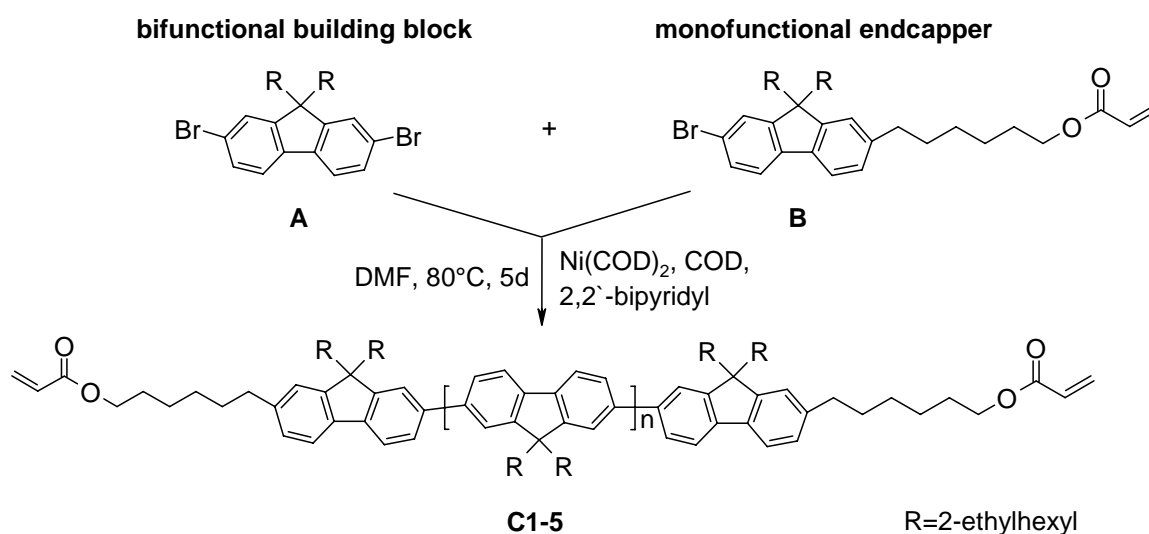
*Scheme 4-2. Yamamoto condensation of a dibromofluorene **A** terminated by an acrylate functionalized endcapper **B**. The ratio of **A** to **B** determines the chain length of **C1-5**.*

Here the endcapper **B** fulfils two tasks at once, the controlled reduction of the molecular weight and the introduction of the crosslinkable acrylate. The acrylate was attached with a C6-spacer to provide a sufficient mobility for the photocrosslinking reaction later on. Five products **C1-5** were synthesized, the molecular weights ranging from 4100-1900 g/mol. We observed that in this narrow molecular weight range the isotropic-nematic transition

temperatures $T_{i,n}$ strongly depend on the chain length, they increase with increasing molecular weight from 65°C to 250°C (Table 4-1).

Table 4-1. *Molecular weights, degrees of polymerisation and isotropic-nematic transition temperatures $T_{i,n}$ of C1-5.*

	ratio **A:B**	M_n^a [g/mol]	M_w^a [g/mol]	P_n(GPC)	$T_{i,n}$ [°C][b]
C1	2:1	4100	6500	9.7	-
C2	3:2	3800	5600	8.9	250
C3	1:1	3100	4400	7.1	190
C4	1:2	2000	2500	4.3	85
C5	1:3	1900	2200	4.1	65

[a] Determined with GPC, polystyrene calibration. [b] Determined with polarization microscopy.

The molecular weights of **C1-5** were determined with oligomer GPC. The GPC scans are shown in Figure 4-4. Since the endcapping process yields in polydisperse mixtures each product mixture contains several distinct oligomers. These different compositions can be nicely observed in the GPC, because the single oligomer signals (trimer n=1, tetramer n=2, ...) are well resolved. The lowest molecular weight mixture **C5** consists of six different oligomers (dimer-heptamer), whereas the highest molecular weight mixture **C1** consists of many more oligomers, especially of high molecular weight chains around 10000 g/mol. Here we note that the number of acrylates is two for each chain, which means that the lowest molecular weight mixture has the highest acrylate content.
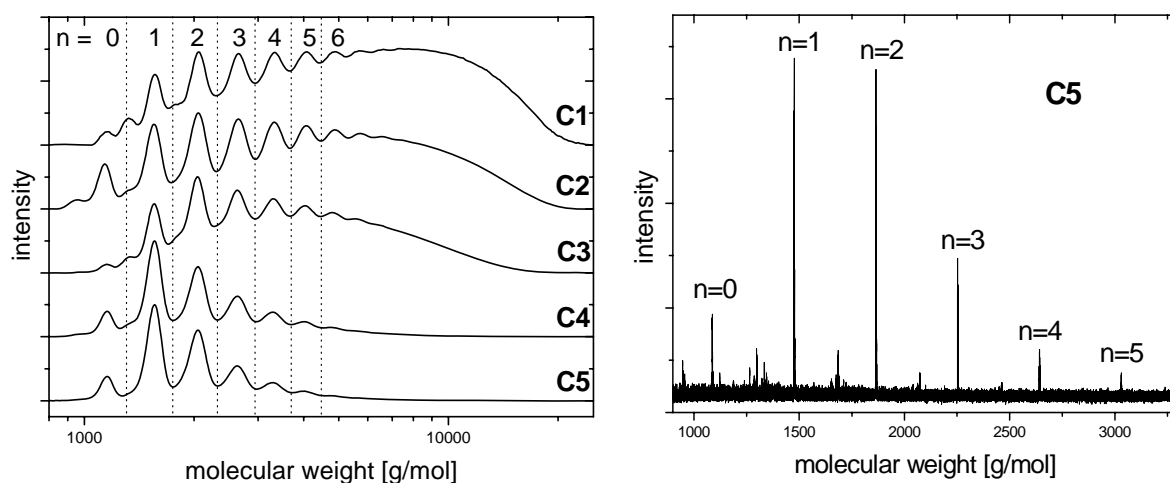
Figure 4-4. *Left: GPC scans of the oligomers C1-5 (n refers to Scheme 4-2). Right: Maldi-ToF spectrum of C5 recorded with 2,2`-p-phenylene-bis(5-phenyloxazole) (POPOP) as matrix.*

Since the GPC scans of the higher molecular weight mixtures show some shoulders next to the main signals we took a closer look with Maldi-ToF spectrometry. The Maldi-ToF spectrum of **C5** is shown in Figure 4-4 right and shows a homologous row of oligomers. The Maldi-ToFs of **C1-2** however show additional signals between the main peaks, which can be assigned to mono-endcapped oligomers. We conclude that the endcapper **B** has a low reactivity in the Yamamoto condensation and only high amounts lead to a complete endcapping. Thus only at low molecular weights a precise endgroup control is possible.

To examine the crosslinking and patterning behaviour we performed photopatterning experiments. Therefore thin films were prepared by spin coating containing 1wt% radical photoinitiator. The films were then annealed in their nematic phase (25°C below $T_{i,n}$) for 20 minutes and afterwards irradiated with UV light using a Xenon-mercury lamp while holding the temperature. Additionally the whole annealing-irradiation procedure was done in a nitrogen chamber to exclude any oxygen. Upon applying a mask the non-irradiated areas do not undergo a crosslinking reaction and can be washed away in the development step. Since the exposure is done in the nematic phase the mixtures **C4-5** seemed to be the most promising candidates due to their low $T_{i,n}$ transition temperature and high overall number of acrylates. At higher temperatures thermal crosslinking starts and a precise UV induced patterning is not possible. We found ~10 minutes irradiation for **C5** and ~20 minutes for **C4** sufficient. The structures were developed for 10 seconds in THF and their quality was checked by

fluorescence microscopy (see Figure 4-5). The fluorescence microscope images also show if oxidation processes took place during irradiation by a colour change from blue to green fluorescence. Figure 4-5 shows that the 5 μm line is slightly green and thus oxidation processes took place. We point that to the long exposure time of 13 minutes. The maximum resolution observed was 1 micron.
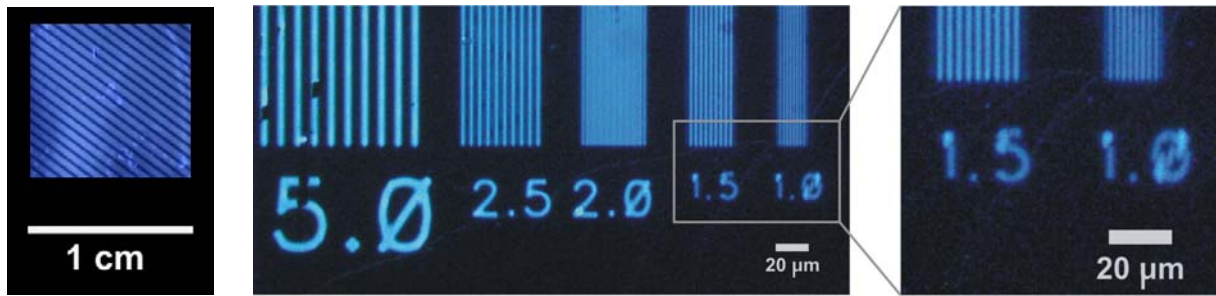
Figure 4-5. *Patterns of a thin film of **C5** (+1wt% irgacure 819, 13 min exposure time at 60°C), pictures taken with a fluorescence microscope. The image left shows a macrostructure and both pictures right show micron sized stripes with the numbers under the lines representing their width in microns.*

4.3 Fluorene oligomers with tunable acrylate content (Chapter 8)

The preceding oligomer series revealed that the irradiation time is an important parameter in view of the preservation of the characteristic blue photoluminescence of oligofluorenes. Two acrylate units per oligomer chain are not sufficient for a fast photocrosslinking. Therefore we developed the new strategy to equip the fluorene oligomers with more acrylates per chain. We attached acrylate moieties to each fluorene monomer and to each endcapper and now the number of acrylates per chain depends on the degree of polymerization. As we have shown before the degree of polymerization can easily be regulated by endcapping. Furthermore upon adding a certain amount of a non-functionalized fluorene monomer the content of acrylate can be adjusted. Scheme 4-3 shows the different monomers used here, **A** is the bifunctional acrylate-monomer, **B** is the bifunctional non-acrylate monomer and **C** is the acrylate-endcapper.
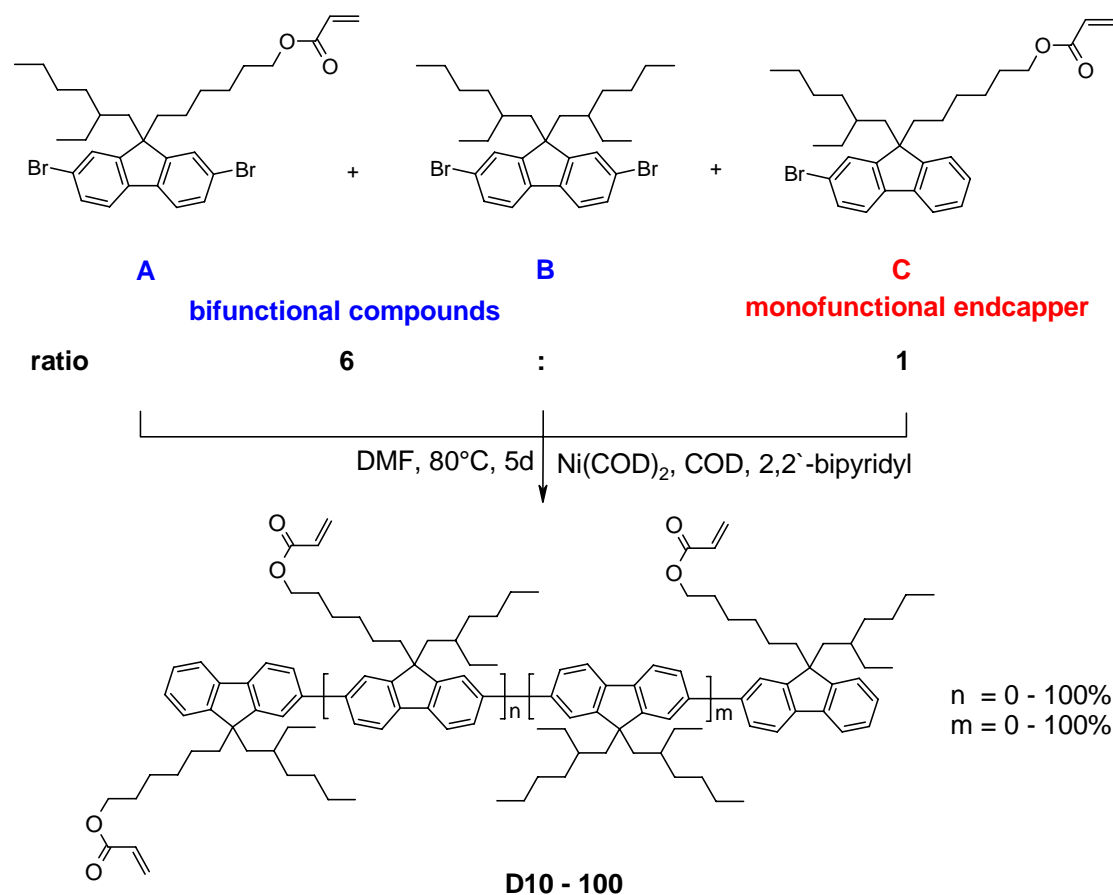
Scheme 4-3. *Synthesis of fluorene oligomers **D10-100** with variable acrylate content. The ratio of **(A+B):C** was 6:1 and the acrylate contents range from n=0% to n=100%. The average degree of polymerization (n+m+2) was ~ 13.*

An asymmetric substitution at the 9-position of the fluorene acrylates **A** and **C** was chosen due to solubility reasons. The ratio of bifunctional compounds **(A+B)** to endcapper **C** was 6:1 in order to obtain processable, but highly photo-reactive oligomers. The ratio of **A** to **B** determines the average content of acrylates in the oligomer chains and we prepared six different mixtures ranging from **A**=100% to **B**=100%. The exact amounts of **A** and **B** used are found in Table 4-2. The Nickel catalyzed Yamamoto reaction was applied as aryl-aryl coupling method, which produces random cooligomers.

The oligomers **D10-100** were thoroughly characterized using NMR, GPC and Maldi-ToF. The acrylate contents found in the oligomers correspond well with the feeds of monomer **A**. The molecular weights of the mixtures **D10-100** are all in the same range of around 5000 g/mol, which shows that the endcapper **C** efficiently adjusts the molecular weights. This points to an equal reactivity of all three components **A**, **B** and **C**. The average number of acrylates per chain range from 12 for the **D100** mixture to 1 for **D10**. The glass transition temperatures were determined by DSC and are all around 35°C.

Table 4-2. *Acrylate contents and molecular weights of the mixtures **D10-100**.*

	feed **A** [%]	**A** found in polymer[a] [%]	$M_n{}^b$ [g/mol]	P_n	average number of acrylates per chain
D 100	100	100	5100	12	12
D 80	83	80	5900	14	11
D 60	55	60	5200	13	8
D 40	48	44	5300	13	6
D 20	30	28	4700	12	3
D 10	14	11	4900	13	1

[a] Determined by NMR. [b] Determined by GPC, oligofluorene calibration.

Figure 4-6 shows the GPC scan of **D100** (left) and the Maldi-ToF spectrum of **D80** (right). In the GPC scan the single oligomers are well resolved from the trimer on and no shoulders are observed. The Maldi-ToF spectrum of **D80** further reveals the different compositions of thesingle oligomers and shows that monomer **A** and **B** are equally incorporated. No bromine endgroups are found, which points to a complete endcapping reaction. This makes the oligomers ideal candidates for OLED applications.
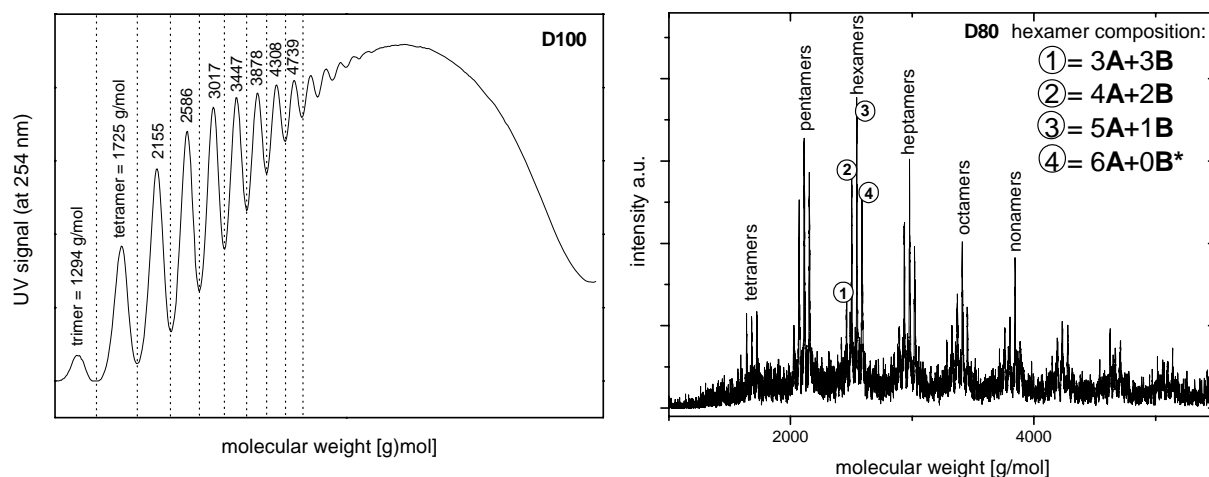
*Figure 4-6. Left: Oligomer GPC of **D100**. In the low molecular weight region the single oligomers (trimer, tetramer ...) are well resolved and the exact molecular weights can be assigned by Maldi-ToF spectrometry. Right: Maldi-ToF spectrum of **D80** (recorded in the linear mode with POPOP as matrix). The inset top right shows the composition of the different hexamers. *refers to Scheme 4-3.*

To absolutely exclude any oxygen during irradiation we designed a new vacuum-irradiation chamber and the modified exposure set-up is shown in Figure 4-7. Since during irradiation a temperature $T > T_g$ is applied to provide a sufficient mobility of the acrylates the whole procedure is done on a hot stage. Hence for a reasonable heat conductivity the chamber was made from stainless steel. For a good (UV)-light transmittance a quartz glass was included in the metal cover. Two gas/vacuum inlets allow an irradiation in vacuum or under inert gas. Furthermore a temperature sensor was fixed at the bottom of the chamber near the substrate to ensure a precise temperature control.

*Figure 4-7. Irradiation set-up for the photopatterning of **D10-100** including vacuum chamber and hot stage.*

Thin films of the oligomers were spin coated onto cleaned glass substrates from toluene solutions including 1wt% radical photoinitiator. The films were then placed in the vacuum chamber together with a mask and selective filters. They were annealed for several minutes at $T > T_g$ and subsequently irradiated for several minutes with a Xe-Hg lamp. Upon development for 10 s with THF the patterns became visible. A minimum crosslinking time of 30 seconds was found for **D100**, which is 20 times faster than the minimum exposure time observed with the first generation oligofluorenes (chapter 7). Well resolved patterns with reasonable exposure times of around 2-5 minutes were found for the mixtures **D80-60**. Even an irradiation at room temperature is now possible and leads to well resolved micropatterns (see Figure 4-8 right). The mixtures **D40-10** with low acrylate contents showed irradiation times comparable to the first generation oligomers. Photooxidation did not take place, which was validated by fluorescence microscopy. The quality of the patterns was checked by scanning electron microscopy (SEM) and the maximum resolution obtained was 700 nm (see Figure 4-8).
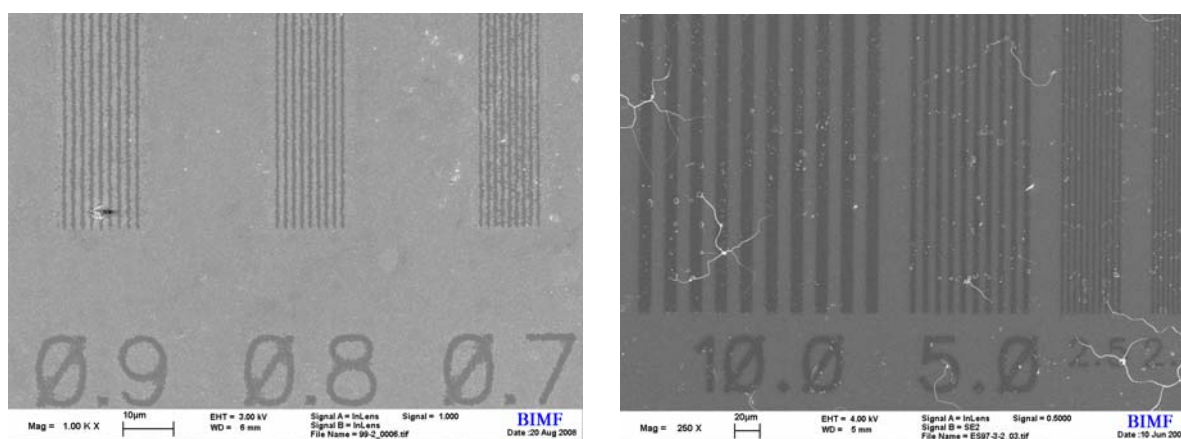

Figure 4-8. *SEM images of photopatterned **D60** (left) and **D100** (right). **D60** was irradiated for 2 minutes at 50°C and **D100** was irradiated at room temperature for 2 minutes. The numbers under the lines represent their width in μm.*

Thus we showed that with an easy 1-step Yamamoto reaction fluorene oligomers with variable acrylate contents are accessible. The photocrosslinking properties were adjusted by the amount of crosslinkable species and the irradiation time was improved by a factor of 20 compared to the first generation oligomers.

4.4   Random functional cooligomers by Yamamoto coupling (Chapter 9)

To extend the application spectrum of the crosslinkable oligomers towards hole and electron conduction we incorporated various comonomers into the oligofluorene chain. For an improved hole conduction we have chosen TPD (*N,N`*-bis(4-methylphenyl)-*N,N`*-diphenyl-benzidine) and bithiophene as comonomers and for a better electron conduction we introduced 2,1,3-benzothiadiazole moieties (**C1-3** see Scheme 4-4). We exploited the Yamamoto condensation because the acrylates can be polymerized directly and a total variation of acrylate and comonomer contents is possible. From the second generation we know that a molecular weight of ~5000 g/mol and acrylate contents of > 60% lead to well processible and highly photo sensitive oligomers. Thus for a shift of the electro-optical properties combined with a fast crosslinking we have chosen to apply 70% fluorene acrylate **F** and 30% comonomer **C1-3**. The ratio of bifunctional monomers (**F+C**) to endcapper **E** was 6:1. Scheme 4-4 displays an overview over the synthesis and the (co)monomers used. 2,1,3-benzothiadiazole was not incorporated into the oligomer chain directly and the more reactive trimer **C2** had to be designed, which was now fully incorporated.
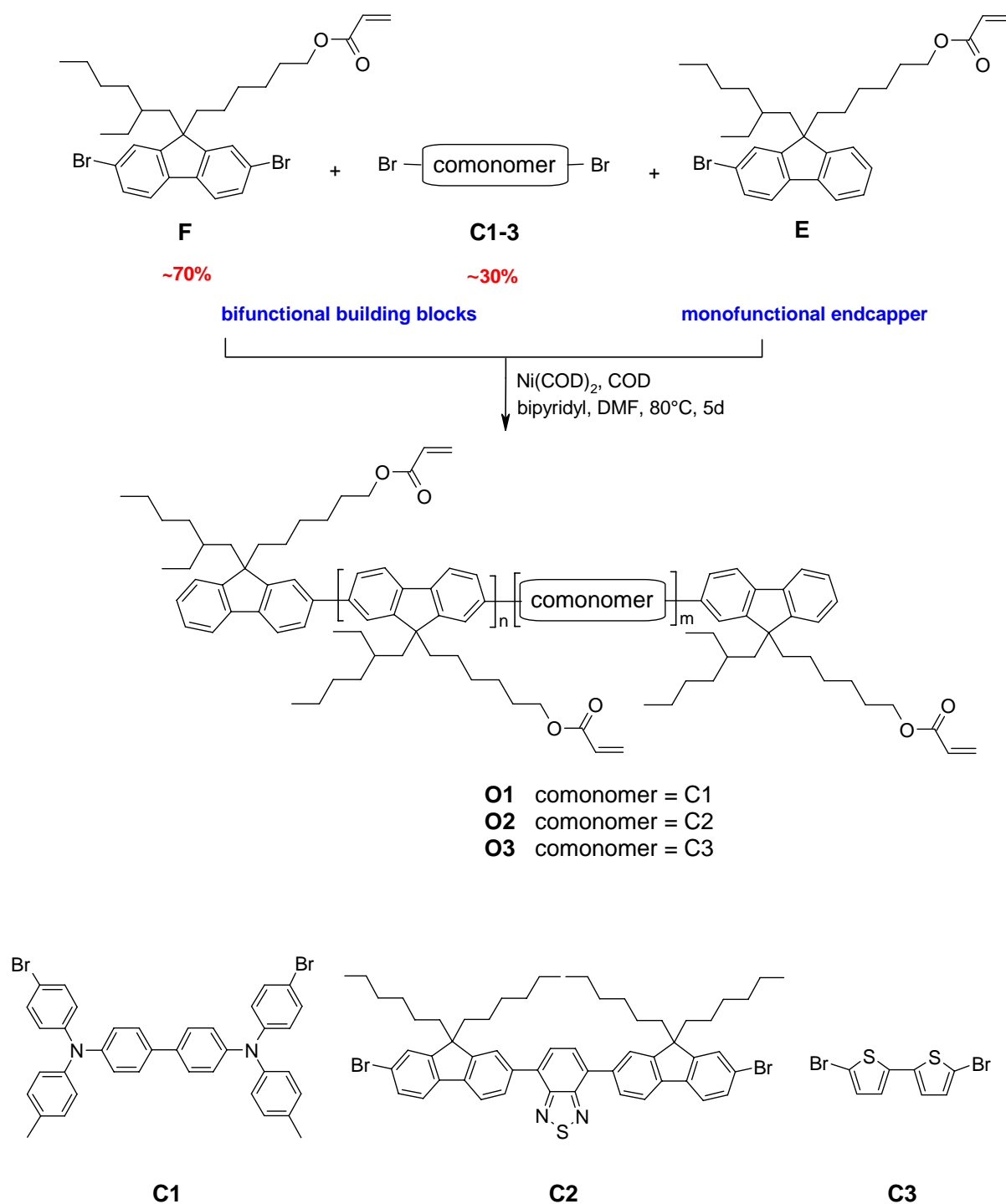
Scheme 4-4. *Synthetic route for the preparation of the acrylate containing fluorene cooligomers **O1-3**.*

We thoroughly characterized the oligomers **O1-3** with NMR, GPC and Maldi-ToF and the data are presented in Table 4-3. The molecular weights were efficiently decreased to ~5000 g/mol and the acrylate feeds correspond well to the amounts found in the oligomers. The thermal characterization was performed with DSC and TGA and low glass transition temperatures of around 50°C and decomposition temperatures of around 350°C were found.

Table 4-3. *Composition, molecular weights and thermal analyses of **O1-3**.*

| oligomer	comonomer	ratio (F+C):E	feed C1-3 [mol%]	found C1-3 [mol%]^a	M_n [g/mol]^b	M_w [g/mol]^b	T_g [°C]^c	$T_{d,onset}$ [°C]^d
O1	**C1**	**6:1**	30	30.5	5200	7900	119	340
O2	**C2**	**4:1**	20	25	5800	7400	50	355
O3	**C3**	**6:1**	30	33	5500	6100	58	350

^{a} Comonomer content determined by NMR. ^{b} Values determined by GPC, oligofluorene calibration. ^{c} Measured with DSC upon heating with a rate of 40 K/min. ^{d} Onset of decomposition determined by thermogravimetry with a heating rate of 10 K/min under N_2.

Maldi-ToF measurements gave a further insight into the chain compositions and revealed, that fluorene-only oligomers were built in low quantities (named F_5, F_6, F_7 in Figure 4-9 right). The occurrence of these pure fluorene oligomers is not unexpected if mathematical considerations are performed, because the probability of adding a fluorene monomer to a growing chain is assumed to be 70% according to the monomer feed. However the probability for the formation of the fluorene-only oligomers decreases with increasing molecular weight. This fact can be observed in the Maldi-ToF, the content of fluorene-only oligomers decreases from the pentamers to the heptamers. Oligomer chains with bromine endgroups were not found.
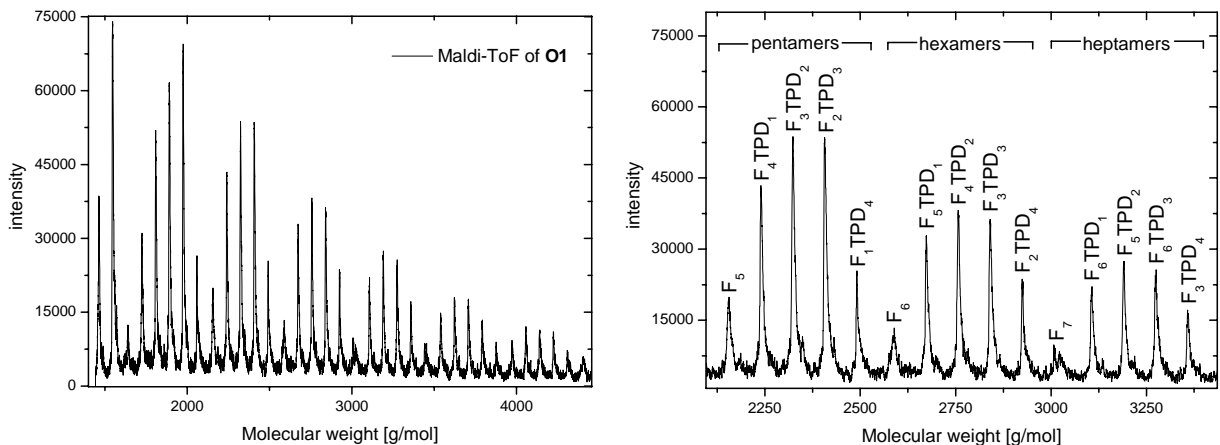
Figure 4-9. *Left: Maldi-ToF spectrum of **O1**. Right: Magnification and assignment of the signals between 2100 and 3400 g/mol. The spectrum was recorded in the linear mode using POPOP as matrix. **F** corresponds to a fluorene and **TPD** to a C1 unit according to Scheme 4-4. **F₄TPD₂** e.g. is an oligomer consisting of four fluorene and two **TPD** repeat units.*

The optical properties were determined in thin film and chloroform solution. The spectra of **O2** are displayed in Figure 4-10. In solution **O2** shows two absorption maxima, a dominant one at 373 nm and a weak one at 430 nm. Upon excitation at 373 nm three PL maxima are observed, the first two at 415 and 437 nm corresponding to the typical oligofluorene emission pattern and the third one at 537 corresponding to the benzothiadiazole cooligomers. The typical blue emission originates from the fluorene-only oligomers present in the mixture. Upon excitation at 430 nm only the benzothiadiazole oligomers emit yellow light. The film spectra on the right are much simpler, there is only one PL maximum at 534 nm
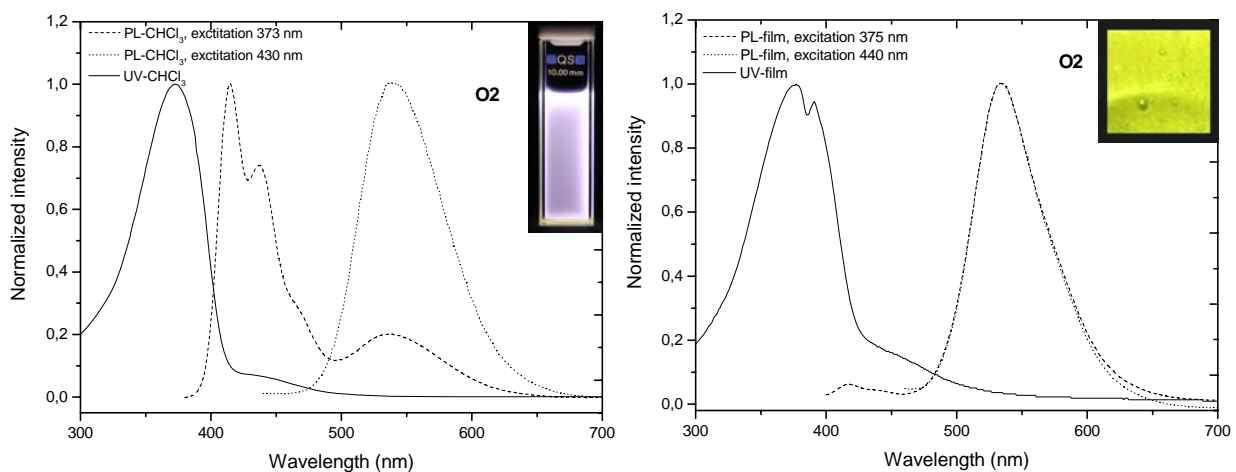
Figure 4-10. *Normalized absorption and emission spectra of **O2** in chloroform solution (left) and as thin film (right). The photographical insets show the chloroform solutions and thin films upon excitation at 366 nm.*

independently from excitation wavelength. In conclusion an intermolecular energy transfer from the pure oligofluorenes to the benzothiadiazole containing oligomers has to take place. This energy transfer is not possible in solution due to dilution.

The HOMO and LUMO values of **O1-3** were measured with photoelectron spectrometry and are shifted in comparison to a pure oligofluorene with energy values of 5.7 eV (HOMO) and 2.73 eV (LUMO). The oligomers **O1** and **O3** with electron donating comonomers show higher HOMO values of 5.25 and 5.31 eV respectively. The oligomer **O2** with the electron withdrawing comonomer shows a lower HOMO value of 5.85 eV and a lower LUMO value of 3.29 eV. Thus the properties are shifted towards hole and electron conduction respectively.

Thin films of **O1-3** were spin coated from toluene solutions and subsequent photopolymerized in the vacuum chamber displayed in Figure 4-7. For a selective excitation of the initiator the Schott filter UG5 was applied in addition. The irradiation times were around 2-6 minutes and feature sizes of around 1 micron were obtained. The quality of the structures was again checked by SEM and fluorescence spectroscopy (Figure 4-11).


Figure 4-11. *Fluorescent microstructures of **O1-3** observed under a fluorescence microscope with an excitation wavelength of 340-380nm. Upon crosslinking the filter UG5 was used and the detailed conditions were: **O1**: exposure at 40°C for 2 min; **O2**: exposure at 50°C for 6 min; **O3**: exposure at 50°C for 4.5 min. The numbers next to the stripes represent their width in μm.*

4.5   Alternating functional cooligomers with Suzuki coupling (Chapter 10)

Since pure fluorene oligomers are formed in the Yamamoto coupling as described in chapter 9 we have chosen to exploit the Suzuki coupling for the introduction of comonomers. The Suzuki coupling uses bromine and boronic acid/borolane functionalities and the monomers are linked in a strictly alternating manner in the polymer chain. This ensures that the comonomers are fully incorporated into the oligomer chain. The palladium catalyzed Suzuki coupling does not tolerate acrylate functionalities and thus protective groups have to be used during polymerization. As protective group tetrahydro-2*H*-pyran (THP) was used, which is stable against bases and can be removed easily under mild acidic conditions. Afterwards a cleavage of the protective groups and a conversion into acrylates is necessary. Scheme 4-5 shows an overview over the Suzuki coupling and the polymeranalogous conversions leading to acrylate functionalized oligomers **O1-3**.

The monomers used in the Suzuki coupling were the bisborolane fluorene **F**, the dibromo comonomers **C1-3** and the monobromo endcapper **E**. The ratio of **F** to **C1-3** was 1:1. Since the ratio of monomers to endcapper (**F:E**) determines the chain length a ratio of 5:1 was chosen for **C2-3** and 3:1 for the high molecular weight comonomer **C1**. The oligomerization reaction proceeded well for all three comonomers. The removal of the THP groups after the oligomerization was quantitatively and the corresponding hydroxyl oligomers were formed. Then the hydroxy groups were converted into acrylates using acryloyl chloride. This step proved to be most challenging due to the moderate solubility of the hydroxy compounds.
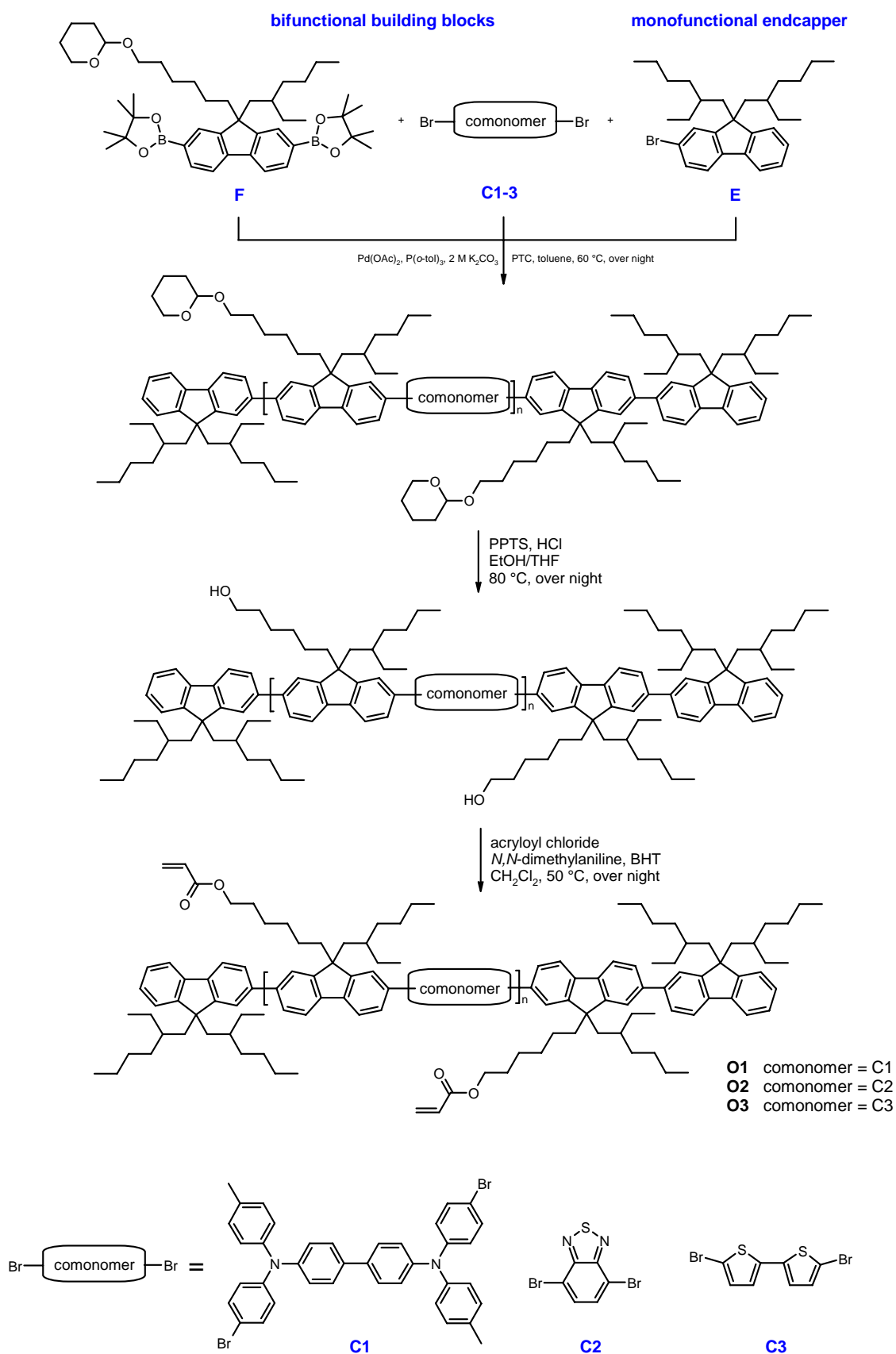
Scheme 4-5. *Overall reaction pathway to acrylate functionalized oligomers **O1-3** via Suzuki coupling. The comonomers **C1-3** used here are shown at the bottom.*

We thoroughly characterized the oligomers **O1-3** with NMR, GPC and Maldi-ToF and the data are presented in Table 4-4. The molecular weights were efficiently decreased. The thermal characterization was performed with DSC and TGA and low T_gs of 53-63°C and decomposition temperatures of 300-350°C were found.

Table 4-4. *Ratios **F:E**, molecular weights and thermal analyses of **O1-3**.*

	ratio **F:E**	M_n [g·mol^{-1}]^b	M_w [g·mol^{-1}]^b	T_g [°C]^c	$T_{d,onset}$ [°C]^d
O1	3:1^a	3600	4000	-	-
O2	5:1	4200	5100	63	340
O3	5:1	6150	8700	53	300

^{a} A lower ratio F:E was chosen due to the high molecular weight of **C1**. ^{b} Determined with GPC, oligofluorene calibration. ^{c} Determined with DSC upon heating with a rate of 40 K/min. ^{d} Onset of decomposition determined by thermogravimetry with a heating rate of 10 K/min under N_2.

Maldi-ToF measurements were performed to get a deeper insight into the chain compositions and revealed that the endcapping process was not complete. Figure 4-12 displays the Maldi-ToF spectrum of oligomer **O2.** The magnification of the signals on the right shows that three different series named a, b and c are formed. Series a comprises the desired products with two endcapper molecules **E** on both ends of the oligomer chain. Series b contains mono
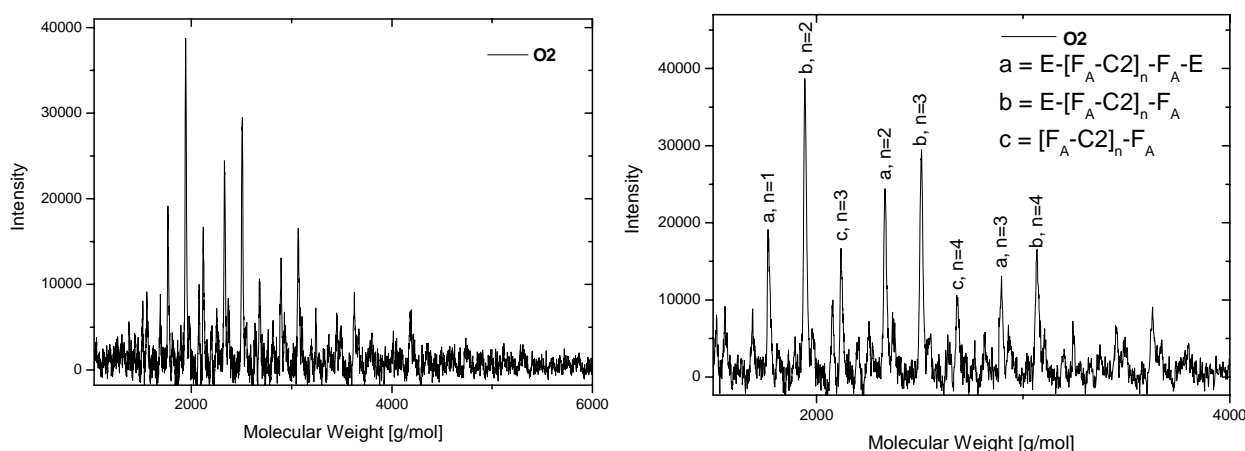
Figure 4-12. *Left: Maldi-ToF spectrum of **O2**. Right: Magnification and assignment of the signals between 1500 and 4000 g/mol. The spectrum was recorded in the linear mode using POPOP as matrix. The assignment of the peaks is named as follows: E=Endcapper, F_A=Fluorene acrylate monomer, C2=C2 monomer, n=degree of polymerization.*

endcapped oligomers and the oligomers in series c do not carry endcappers at all. The signals of series b have the highest intensity and the signals of series c the lowest. We point these results to loss of borolane groups during Suzuki coupling, which has been observed and described before.[55]

The optical properties of **O1-3** were determined in thin film and chloroform solution and the spectra of oligomer **O3** are displayed in Figure 4-13. In solution **O3** exhibits one absorption maximum at 446 nm and upon excitation at 446 nm one emission maximum at 525 nm. In thin films **O3** shows an absorption maximum at 451 nm and one emission maximum at 565 nm. The 40 nm red shift of the fluorescence maximum in thin films originates from well known packing phenomena reported for thiophene compounds.[56]
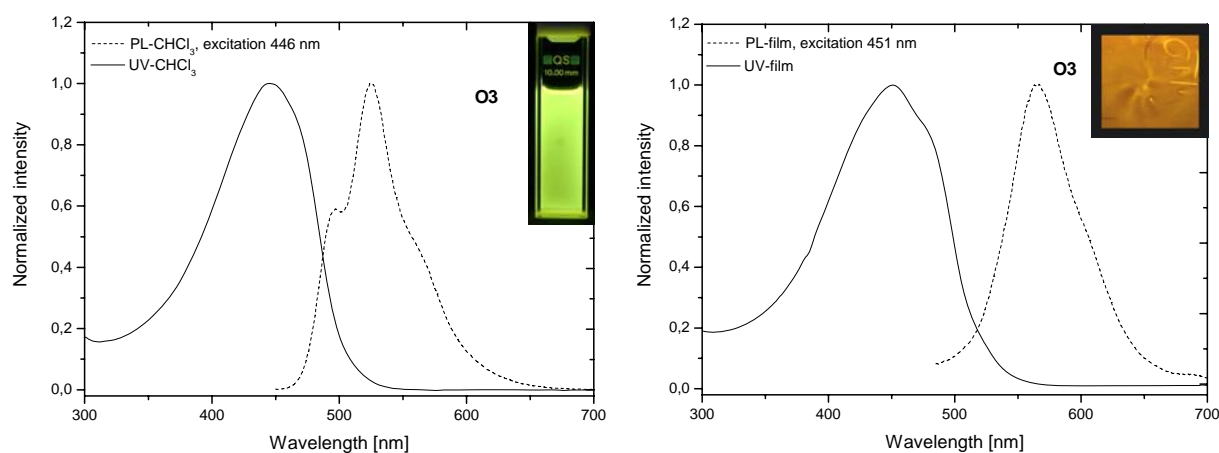

Figure 4-13. *Normalized absorption and emission spectra of **O3** in chloroform solution (left) and thin film (right). The photographical insets show the chloroform solutions and thin films upon excitation at 366 nm.*

The HOMO values of **O1-3** were determined with photoelectron spectrometry. The introduction of the electron donating comonomers **C1** and **C3** lead to an increase of the HOMO level up to 5.25 eV and 5.46 eV respectively (compared to a pure oligofluorene with a HOMO level of 5.70 eV). The electron withdrawing comonomer **C2** leads to a slight decrease of the HOMO value to 5.80 eV and to a decrease of the LUMO value to 3.27 eV. A comparison with the HOMO and LUMO levels of the randomly linked counterparts described in chapter 9 shows that the energy levels are almost identical. Thus the type of linkage (random or alternating) does not influence the energy levels (see Figure 4-14).
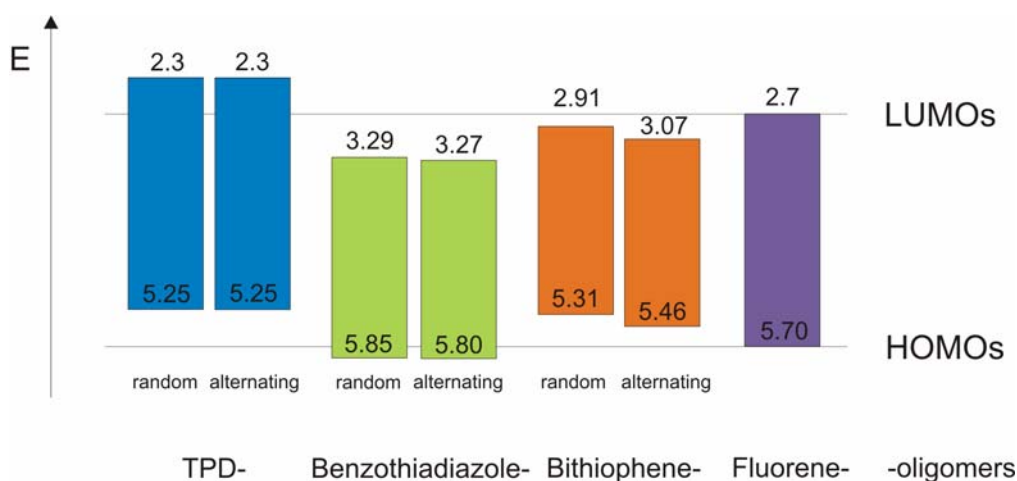
Figure 4-14. *Energy levels of the oligomers **O1-3** and their randomly linked counterparts from chapter 9. Additionally the properties of a pure fluorene oligomer (described in chapter 8) with a similar molecular weight are displayed on the right. The energy levels were measured with photoelectron spectrometry (Riken Keiki AC-2) from thin films.*

Photopolymerization experiments were carried out using the vacuum chamber described in chapter 8. Thin films of the oligomers were spin coated on cleaned silicon wafers. They were annealed at $T > T_g$ and irradiated with a Xe-Hg lamp. The irradiation conditions were almost identical to those found for the randomly linked oligomers. 2-5 minutes were sufficient for the pattern formation. The resolution was improved to 600 nm for the benzothiadiazole oligomer **O2** and a fluorescence and SEM image of the 600 nm stripes is shown in Figure 4-15. The yellow fluorescence is preserved during exposure.
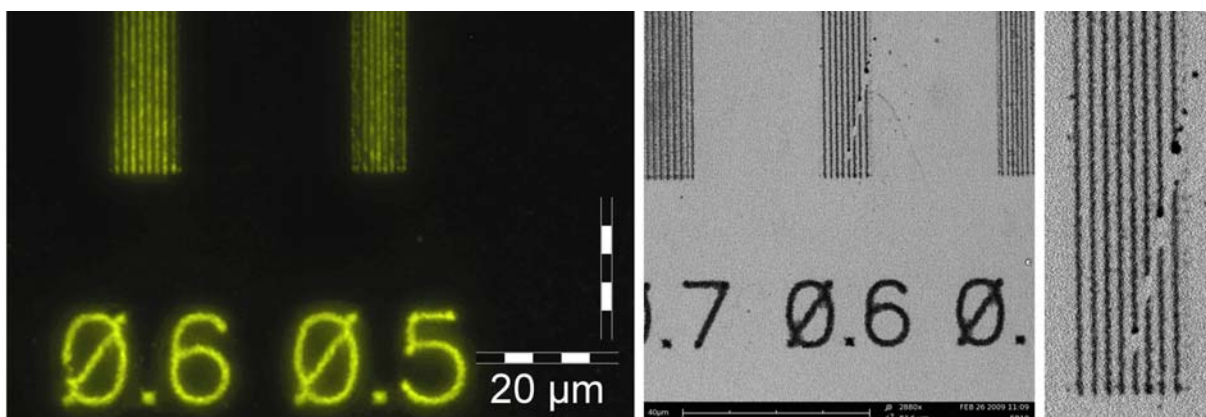
Figure 4-15. *Sub-micron scale patterns of **O2** observed under a fluorescence microscope (left) and SEM (right). The image on the far right shows a magnification of the 600 nm stripes of the SEM picture. Upon crosslinking the filter UG5 was used and the detailed conditions were: annealing at 50°C for 3 min, exposure at 60°C for 5.5 min. The numbers next to the stripes represent their width in µm.*

5 Statement

In the following, the contributions of the individual authors to the papers are specified.

Chapter 7

This work is published in *Macromolecular Symposia* (**2007**, *254*, 203) with the title:

"Synthesis and photopatterning of fluorene based reactive mesogens"
by **Esther Scheler**, Irene Bauer, Peter Strohriegl

I synthesized all monomers and oligomers with the help of the technician Irene Bauer. I characterized all compounds, performed the Maldi-ToF and photopatterning experiments. I took the fluorescence microscope images with the help of Werner Reichstein. The publication was written by me.
Peter Strohriegl supervised the project and corrected the manuscript.

Chapter 8

This work is published in the *Journal of Macromolecular Chemistry* (**2009**, *19*, 3207) with the title:

"Tailoring fluorene-based oligomers for fast photopatterning"
by **Esther Scheler**, Peter Strohriegl

I synthesized and characterized all compounds. I performed the photopatterning experiments and took the fluorescence microscope images. Florian Wieberger performed the scanning electron microscopy. I wrote the publication.
Peter Strohriegl supervised the project and corrected the manuscript.

Chapter 9

This work is submitted to *Chemistry of Materials* with the title:

"Three color random fluorene- based oligomers for fast micron scale photopatterning"
by **Esther Scheler**, Peter Strohriegl

I synthesized and characterized all compounds. I performed the photopatterning experiments and took the fluorescence microscope images. I performed the scanning electron microscopy and the energy level measurements. Klaus Kreger and Michael Rothmann were involved in the scientific discussion. I wrote the publication.
Peter Strohriegl supervised the project and corrected the manuscript.

Chapter 10

This work is intended for submission to *Macromolecular Chemistry and Physics* with the title:

"Synthesis and characterization of alternating fluorene-based oligomers for sub-micron photopatterning"
by **Esther Scheler**, Eva Betthausen, Peter Strohriegl

I synthesized and characterized all compounds with the help of Eva Betthausen who did her advanced lab course on that topic. I performed the photopatterning experiments and took the fluorescence microscope images. I performed the scanning electron microscopy and the energy level measurements. I wrote the publication.
Peter Strohriegl supervised the project and corrected the manuscript.

Chapter 11: Appendix

This work is published in *Liquid crystals* (**2007**, *34*, 667) with the title:

"Synthesis of oligofluorenes by endcapping"
by **Esther Scheler**, Peter Strohriegl

This work appears as appendix since I performed the synthesis and characterization of the oligofluorenes during my diploma thesis. The GPC calibration, the comparison of the thermal properties and the preparation of the manuscript were done afterwards in my PhD thesis. Klaus Kreger helped with the GPC calibration. Klaus Kreger and Heiko Thiem were involved in the scientific discussion. I wrote the publication.
Peter Strohriegl supervised the project and corrected the manuscript.

Chapter 12: Appendix

This work is published in *Applied Physics A: Materials Science and Processing* (**2009*, *95*, 61) with the title:

"Single molecule spectroscopy of oligofluorenes: how molecular length influences polymorphism"
by Enrico Da Como, **Esther Scheler**, Peter Strohriegl, John M. Lupton, Jochen Feldmann

This work appears as appendix since I performed the synthesis and characterization of the oligofluorenes during my diploma thesis. All other experiments were done afterwards in my phD thesis. Klaus Kreger helped with the GPC calibration. Enrico DaComo performed the single molecule spectroscopy experiments and wrote the publication. I was involved in the scientific discussion and corrected the manuscript.
Peter Strohriegl and Jochen Feldmann supervised the project and corrected the manuscript.

6   References

1   http://www.intel.com/

2   J. Huang, R. Xia, Y. Kim, X. Wang, J. Dane, O. Hofmann, A. Mosley, A.J. de Mello, J.C. de Mello, D.D.C. Bradley, *J. Mater. Chem.* **2007**, *17*, 1043.

3   A.J. Khandpur, S. Förster, F.S. Bates, I.W. Hamley, A.J. Ryan, W. Bras, K. Almdal, K. Mortensen, *Macromol.* **1995**, *28*, 87968806.

4   A.S. Edelstein, R.C. Cammarata, *Nanomaterials: Synthesis, Properties and Applications*, 1st edition, Institute of Physics Publishing **1998**, p. 497.

5   Hoechst High Chem Magazin 1/1986.

6   K. Ronse, *C. R. Physique* **2006**, *7*, 844.

7   D. Bratton, D. Yang, J. Dai, C.K. Ober, *Polym. Adv. Technol.* **2006**, *17*, 94.

8   http://www.amd.com/

9   A. Reiser, *Photoreactive Polymers*, Wiley-Interscience publication **1989**, p. 22.

10   B. Mortini, *C.R. Physique* **2006**, *7*, 924.

11   T.F Yeh, A. Reiser, R.R. Dammel, G. Pawlowski, H. Roeschert, *Pro. SPIE 1925* **1993**, 570.

12   A. De Silva, N.M. Felix, C.K. Ober, *Adv. Mater.* **2008**, *20*, 3355.

13   J. Dai, S.W. Chang, A. Hamad, A. Yang, N. Felix, C.K. Ober, *Chem. Mater.* **2006**, *18*, 3404.

14   C.K. Chiang, C. R. Fincher, Y.W. Park, A.J. Heeger, H. Shirakawa, E.J. Louis, S.C. Gau, A.G. Macdiarmid, *Phys. Rev. Lett.* **1977**, *39*, 1098.

15   http://nobelprize.org/nobel_prizes/chemistry/laureates/2000/chemadv.pdf.

16   T.W. Kelley, P.F. Baude, C. Gerlach, D.E. Ender, D. Muyres, M.A. Haase, D.E. Vodel, S.D. Theiss, *Chem. Mater.* **2004**, *16*, 4413.

17   C.W. Tang, S.A. VanSlyke, *Appl. Phys. Lett.* **1987**, *51*, 913.

18   C.J. Drury, C.M. Musaers, C.M. Hart, M. Matters, D.M. de Leeuw, *Appl. Phys. Lett.* **1998**, *73*, 108.

19   G. Horowitz, *Adv. Mater.* **1990**, *2*, 287.

20   C.W. Tang, *Appl. Phys. Lett.* **1986**, *48*, 183.

21   http://www.oled.at/

22   http://www.heise.de/

23   http://www.novaled.com/

24   http://www.eink.com/

25   http://www.businesswire.com/

26   http://www.rfidgazette.org/

27   W. Clemens, W. Fix, *Physik Journal* **2003**, *2*, 31.

28   http://www.polyic.de/

29   M. Pope, H.P. Kallmann, P. Magnante, *J. Chem. Phys.* **1963**, *38*, 2042.

30   W. Helfrich, W.G. Schneider, *Phys. Rev. Lett.* **1965**, *14*, 229.

31   D.D.C. Bradley, *Adv. Mater.* **1992**, *4*, 756.

32   L.J. Rothberg, A.J. Lovinger, *J. Mater. Res.* **1996**, *12*, 3174.

33   J.R. Sheats, H. Antoniadis, M. Hueschen, W. Leonard, J. Miller, R. Moon, D. Roitman, A. Stocking, *Science* **1996**, 273, 884.

34   G. Cheng, Y. Zhang, Y. Zhao, Y. Lin, C. Ruan, S. Liu, T. Fei, Y. Ma, Y. Cheng, *Appl. Phys. Lett.* **2006**, *89*, 043504.

35   Y. Shirota, *J. Mater. Chem.* **2000**, *10*, 1.

36   B.W. D`Andrade, S. Datta, S.R. Forrest, P. Djurovich, E. Polikarpov, M.E. Thompson, *Org. Electr.* **2005**, *6*, 11.

37   S.R. Forrest, P.E. Burrows, *Org. El. Mater. Dev.* **1997**, 415.

38   M. Deussen, H. Bässler, *Chiuz* **1997**, *31*, 76.

39   Y. Shirota, *Opt. Eng.* **2005**, *94*, 147.

40   Y. Shirota, *J. Mater. Chem.* **2005**, *15*, 75.

41   M. Thelakkat, H.-W. Schmidt, *Adv. Mater.* **1998**, *10*, 219.

42   A.P. Kulkarni, C.J. Tonzola, A. Babel, S.A. Jenekhe, *Chem. Mater.* **2004**, *16*, 4556.

43   Y. Kishigami, K. Tsubaki, Y. Kondo, J. Kido, *Synth. Met.* **2005**, *153*, 241.

44   R.A. Klenkler, H. Aziz, A. Tran, Z.D. Popovic, G. Xu, *Org. Electr.* **2008**, *9*, 285.

45   J.H. Burroughes, D.D.C. Bradley, A.R. Brown, R.N. Marks, K. MacKay, R.H. Friend, P.L. Burn, A.B. Holmes, *Nature* **1990**, *347*, 539.

46   A.J. Heeger, D. Brown, *J. Chem. Soc. Abstr.* **1993**, *118*, 157401.

47   H. Spreitzer, H. Becker, E. Kluge, W. Kreuder, H. Schenk, R. Demandt, H. Schoo, *Adv. Mater.* **1998**, *10*, 1340.

48   M.T. Bernius, M. Inbasekaran, J. O´Brien, W. Wu, *Adv. Mater.* **2000**, *23*, 1737.

49   M.A. Baldo, S. Lamansky, P.E. Burrows, M.E. Thompson, S.R. Forrest, *Appl. Phys. Lett.* **1999**, *75*, 4.

50   M.H. Tsai, H.W. Lin, H.C. Su, T.H. Ke, C.C. Wu, F.C. Fang, Y.L. Liao, K.T. Wong, C.I. Wu, *Adv. Mater.* **2006**, *18*, 1216.

51   E.J.W. List, R. Guentner, P. de Scanducci Freitas, U. Scherf, *Adv. Mater.* **2002**, *14*, 374.

52   J. Jo, C. Chi, S. Hoeger, G. Wegner, D.Y. Yoon, *Chem. Eur. J.* **2004**, *10*, 2681.

53   E. Scheler, P. Strohriegl, *Liq. Cryst.* **2007**, *34*, 667.

54   Grell, M., Bradley, D. D. C., Long, X., Chamberlain, T., Inbasekaran, M., Woo, E. P., Soliman, M., 1998, *Acta Polym.*, **49**, 439-444.

55   H. Thiem, M. Jandke, D. Hanft, P. Strohriegl, *Macromol. Chem. Phys.* **2006**, *207*, 370.

56   T. Yasuda, K. Namekawa, T. Iijima, T. Yamamoto, *Polymer* **2007**, *48*, 4375.

7 Synthesis and photopatterning of fluorene based reactive mesogens

Esther Scheler, Irene Bauer, Peter Strohriegl

Macromolecular Chemistry I, University of Bayreuth, Universitätsstr. 30, 95440 Bayreuth

peter.strohriegl@uni-bayreuth.de
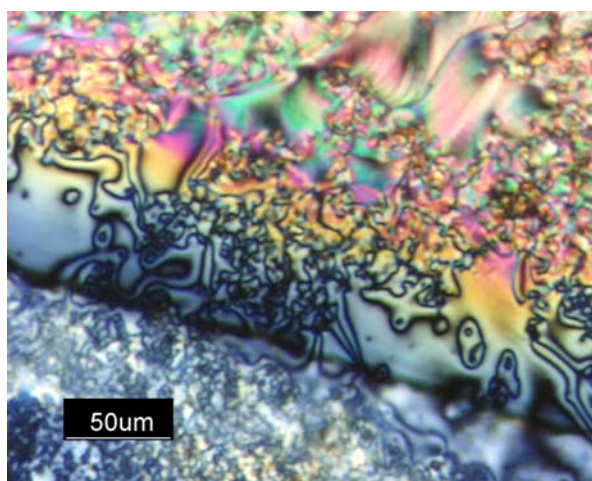
Summary

In this paper we report the synthesis, characterisation and photopatterning of polydisperse fluorene oligomers. The oligomers were synthesised using the Yamamoto coupling. The molecular weights of the oligomers and as a consequence the nematic-isotropic transition temperatures were tailored by an endcapping reaction. With the endcapping species we introduced reactive acrylate functionalities. Subsequent photocrosslinking through a test mask led to the formation of fluorescent microstructures with a resolution of 1 μm.

Keywords

Introduction

Semiconducting organic materials have gained interest in the last years due to their applications in displays, electronics or sensors. Especially organic light-emitting diodes (OLEDs) are currently emerging as promising technology for flat panel displays and large area lighting.[1,2] In view of the mentioned applications patterning techniques for the production of pixelated devices are of particular interest. Various cost-efficient printing techniques are used for structuring.[3] The accessible resolutions are sufficient for displays, but the main problem is the spatial separation of the red, green and blue droplets in the printing process. Thus pre-patterned substrates have to be used in many cases. An alternative method is the vapour deposition of small molecules using shadow masks, which is relatively expensive and shows a poor scalability to larger substrates.[4] Conventional photolithography techniques optimized for inorganic materials are difficult to apply to organic materials. It was shown that classic photoresist techniques can only be transferred to structure organic compounds with major modifications, e.g. as lift-off techniques [5], which limits their applicability in OLED manufacturing.

Thus an attractive approach is the direct photochemical crosslinking of the semiconducting material itself, for example by the introduction of photocrosslinkable moieties.[6,7] By light induced crosslinking the material becomes insoluble and can simultaneously be patterned, comparable to a negative photoresist. It is very important that during the crosslinking procedure the chemical structure of the material is not modified, which sometimes requires low processing temperatures and using inert atmospheres to avoid degradation processes.[8] In this study we report the synthesis of novel polydisperse oligofluorenes carrying photopolymerisable acrylate groups. The molecular weight of the oligofluorenes is tuned by using an endcapper, which terminates the reaction in a controlled way.[9,10] To obtain well

defined oligomers the endcapping process has to be quantitative, which was proven by Maldi-ToF and elemental analysis. Here, the acrylate groups are introduced directly with the endcapping species in a Yamamoto reaction. In many publications the acrylate functionalisation is performed after the polymerisation of a precursor monomer, which is more difficult particularly with regard to a desired full conversion of the OH- groups into acrylates.[11,12] Here we demonstrate, that the Yamamoto coupling tolerates acrylate moieties and the acrylates tolerate the reaction conditions without any side reactions. So well-defined oligomers were obtained directly and subsequent photopatterning using standard photoinitiators resulted in patterns with a minimum resolution of 1 μm.

Experimental part

Materials

All chemicals and reagents were purchased from Aldrich. Sec-BuLi was used as received from Acros. *N,N*-dimethylaniline, absolute toluene and dimethylformamide (DMF) were purchased from FLUKA. Ethanol (EtOH) and toluene were distilled and tetrahydrofuran (THF) was distilled over potassium prior to use. The photoinitiators were used as received from Ciba.

Synthesis of 2-Bromo-7-(6-(2-tetrahydropyranyloxy)-hexyl)-9,9-di-(2-ethylhexyl)-fluorene (2).

9.4 g (12.1 mmol) of compound **1** were dissolved in 250 ml absolute THF and cooled to -78°C. The solution was stirred for 5 min before 14.5 ml (18.9 mmol) sec-BuLi were added via a syringe. After stirring for 5 min 5 g (18.9 mmol) 2-(6-bromohexyloxy)tetrahydro-2*H*-

pyran were added dropwise. The solution was stirred and allowed to warm up over night. The product was extraced with ether and the organic phase was washed with water and dried with Na_2SO_4. The crude product was purified by column chromatography using hexane/ethylacetate 18:1 as eluent. A transparent oil with 43% yield was obtained.

^{1}H-NMR (250 MHz, $CDCl_3$). δ (ppm): 7.4-7.6 (m, 4H), 7.1-7.2 (m, 2H), 4.5 (d, 1H), 3.8 (m, 2H), 3.4 (m, 2H), 2.6 (t, 2H), 1.9 (d, 4H), 1.4 (m, 6H), 0.4-1.0 (m, 32H). IR (cm^{-1}): 2956, 2928, 2855 (CH stretch); 1454, 1378 (CH deformation); 1136, 1120 (CH_2-O); 813 (CH aromatic). m/z=654 (M^+).

Synthesis of 2-Bromo-7-(6-hydroxyhexyl)-9,9-di-(2-ethylhexyl)-fluorene (3).

A solution of 2.7 g (4.08 mmol) **2** and 0.1 g p-toluenesulfonic acid pyridinium salt (PPTS) in 200 ml EtOH was prepared. 5 drops HCl (conc.) were added and the mixture was heated to 60°C under stirring for 2 h. The EtOH was evaporated and 80 ml dichloromethane (CH_2Cl_2) and 80 ml water were added to the product mixture. After stirring for 5 min the phases were separated. The water phase was washed with CH_2Cl_2 and the combined organic phases were washed with water. Purification by column chromatography with hexane/THF 10:1 as eluent yielded 99% of **3** as transparent oil.

^{1}H-NMR (250 MHz, $CDCl_3$). δ (ppm): 7.4-7.6 (m, 4H), 7.1-7.2 (m, 2H), 3.6 (d, 2H), 2.6 (t, 2H), 1.9 (t, 4H), 0.4-1.0 (m, 38H). IR (cm^{-1}): 3355 (OH); 2957, 2928, 2855 (CH stretch); 1455, 1378 (CH deformation); 813 (CH aromatic). m/z=568 (M^+).

Synthesis of 2-Bromo-7-(6-acryloyloxy-hexyl)-9,9-di-(2-ethylhexyl)-fluorene (4).

A solution of 2.04 g (3.58 mmol) **3**, 0.035 g (0.16 mmol) 2,6-di-tert-butyl-p-cresol (BHT) and 0.5 ml (3.93 mmol) *N,N*-dimethylanilin in 150 ml toluene was prepared. 0.36 g (3.93 mmol)

acryloylchloride were added dropwise under argon and the mixture was stirred at 50°C for 14 h. The solvent was evaporated and the crude product was purified by column chromatography using hexane/ethylacetate 10:1 and medium pressure chromatography using hexane/ethylacetate 20:1 as eluents. A transparent oil was obtained in 65% yield.

^{1}H-NMR (250 MHz, CDCl$_3$). δ (ppm): 7.4-7.6 (m, 4H), 7.1-7.2 (m, 2H), 6.4 (d, 1H), 6.1 (dd, 1H), 5.8 (d, 1H), 4.1 (t, 2H), 2.6 (t, 2H), 1.9 (d, 4H), 1.4 (m 6H), 0.4-1.0 (m, 32H). IR (cm^{-1}): 2957, 2928, 2854 (CH stretch); 1725 (C=O); 1637 (C=C); 1455, 1378 (CH deformation); 1189 (C-O); 813 (CH aromatic); 753 (C-H double bond). m/z=624 (M$^+$). Anal. Calcd for C$_{38}$H$_{55}$BrO$_2$ (623.76): C, 73.17; H, 8.89; Br, 12.81; O, 5.13. Found: C, 73.26; H, 8.86; Br, 12.75; O, 5.05.

Synthesis of α,ω-Bis(6-acryloyloxy-hexyl)-oligo(9,9-di(ethylhexyl)-fluorene-2,7-diyl) (5a-e).

The synthesis of **5e** with a ratio of monomer **1** to endcapper **4** of 1:3 is described in detail:

A schlenk flask was charged with 0.8 g (2.91 mmol) nickeldicyclooctadiene, 0.36 ml (2.91 mmol) cyclooctadiene, 0.45 g (2.91 mmol) 2,2`-bipyridyl and 20 ml dry DMF under argon. The mixture was degassed by 3 freeze-thaw cycles before it was heated to 80°C for 30 min under stirring. 0.21 g (0.38 mmol) **1** and 0.71 g (1.14 mol) **4** were weighed into a separate flask under argon. 30 ml dry toluene were added and the mixture was degassed by 3 freeze-thaw cycles. Subsequently the monomer mixture was added to the catalyst mixture using a cannula. The reaction mixture was stirred at 80°C for 5 days in the dark. Afterwards it was poured into 140 ml methanol/HCl(conc.) 1:1 and stirred at room temperature for 2 hours. The organic phase was separated from the HCl phase which was then washed with Et$_2$O. The combined organic phases were washed with water and the solvent was evaporated. The crude

product was filtered over a small alumina (neutral) column using toluene as eluent, then washed with alkaline EDTA solution (5%), reprecipitated twice from THF into methanol and dried in vacuum yielding 0.22 g (40%) of **5e** as pale yellow oil.

^{1}H-NMR (250 MHz, CDCl$_3$). δ (ppm): 7.4-7.7 (m, 18H), 7.1-7.2 (m, 5H), 6.4 (d, 2H), 6.1 (dd, 2H), 5.8 (d, 2H), 4.1 (t, 4H), 2.7 (t, 4H), 2.5 (dd, 14H), 1.7 (m, 9H), 1.4 (m, 10H), 0.4-1.0 (m, 118H). IR (cm^{-1}): 2963, 2928, 2855 (CH stretch); 1726 (C=O); 1659 (C=C); 1470 (CH deformation); 1194 (C-O); 810 (CH aromatic); 742 (C-H double bond). M$_n$(GPC, polystyrene calibration)=1900 g/mol. Anal. Calcd for C$_{134}$H$_{190}$O$_4$ (1865.01): C, 86.30; H, 10.27; O, 3.43. Found: C, 85.17; H, 10.53; O, 3.10.

Table 1: *Molar amounts of dibromo compound **1** and endcapper **4** and the resulting yields.*

	ratio **1:4**	n$_1$ [mmol]	n$_4$ [mmol]	yield [%]
5a	2:1	0.32	0.16	55
5b	3:2	0.34	0.23	60
5c	1:1	0.24	0.24	50
5d	1:2	0.47	0.94	40
5e	1:3	0.38	1.14	40

Characterisation

^{1}H-NMR spectra were recorded on a Bruker AC 250 spectrometer in CDCl$_3$ at 250 MHz with tetramethylsilane as reference. The IR spectra were recorded using a Bio-Rad Digilab FTS-40. Mass spectra were obtained by a Finnigan MAT 8500 (70eV) with MAT 112S Varian. The molecular weights were determined by a Waters size exclusion chromatography system (GPC) for oligomers (analytical columns: crosslinked polystyrene gel, length 2 x 60 cm, width 0.8 cm, particle size 5 μm, pore size 100 Å, eluent THF (0.5 ml/min, 80 bar),

polystyrene calibration). The Maldi-ToF spectra were obtained by a Bruker Reflex III with highmass detector. The fluorescence spectra were recorded on a SHIMADZU RF-5301 PC spectrofluorometer with 90° detection. The emission spectra were obtained at ambient temperature from thin films spin coated (1000 rpm, 4 wt%) from xylene solutions on glass substrates. The liquid crystalline behaviour was examined by a polarisation microscope Nikon Diaphot 300 with a Mettler FP 90 hotstage from films that were obtained by drop casting from CH_2Cl_2 solutions. The irradiation experiments were performed using a Xe-Hg-mixgas lamp Ushio UXM 200H. The microstructures were examined with a fluorescence microscope Leica DMR-SP with selective filter systems (excitation 340-380 nm, dichromatic mirror 400 nm, suppression filter LP 420 nm).

Results and discussion

Synthesis

Compound **1** was synthesised by the alkylation of 2,7-dibromofluorene as described in literature.[13] The reactive endcapper **4** was synthesised in 3 steps. The first step is the selective alkylation of 9,9-di(2-ethylhexyl)-2,7-dibromofluorene **1** with 1 equivalent 2-(6-bromohexyloxy)tetrahydro-2H-pyran. The resulting THP-protected fluorene **2** is then deprotected using PPTS in EtOH which leads to the formation of the corresponding alcohol **3**. The last step is the esterification of compound **3** with acryloyl chloride to the acryloylfluorene **4** (see Scheme 1).
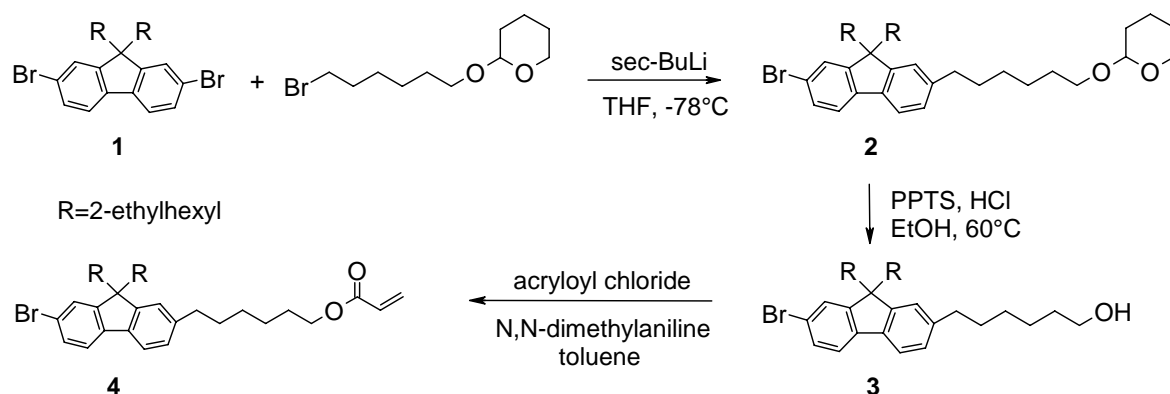
Scheme 1: *Synthesis of the reactive endcapper 2-Bromo-7-(6-acryloyloxy-hexyl)-9,9-di-(2-ethylhexyl)-fluorene **4**.*

The polydisperse reactive mesogens **5a-e** were obtained in a 1-step reaction shown in Scheme 2. The Yamamoto reaction of the bifunctional monomer **1** and the monofunctional endcapper **4** leads to the oligomeric mixtures **5a-e** with different molecular weights. The coupling was performed using Ni(COD)$_2$ and 2,2`-bipyridyl in a mixture of dry DMF and dry toluene.[14] The chemical structures and were validated by GPC, Maldi-ToF, ^{1}H-NMR and IR spectroscopy.
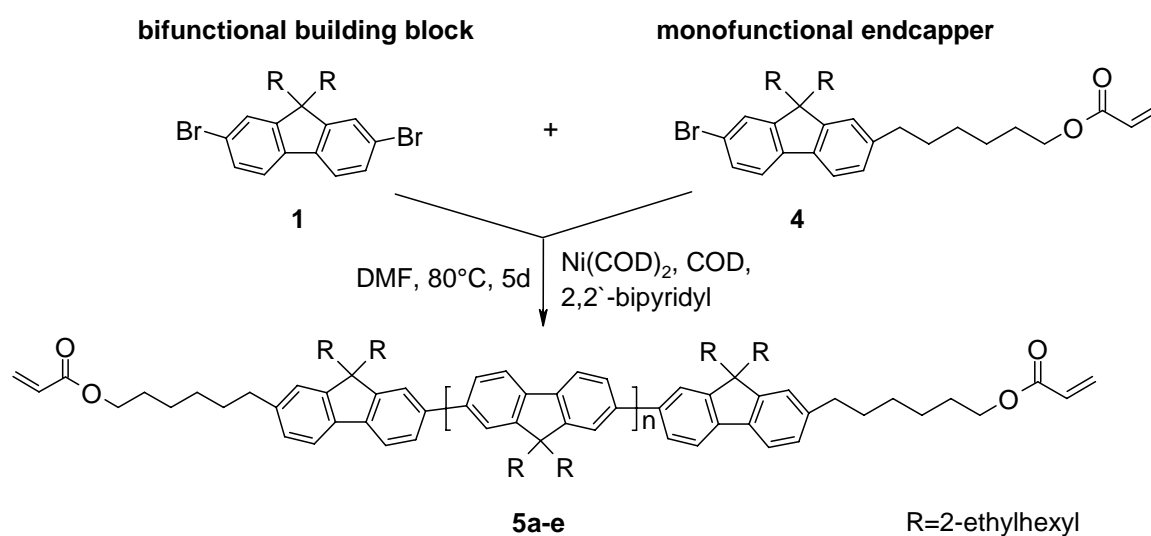
Scheme 2: *Synthesis of α,ω-Bis(6-acryloyloxy-hexyl)-oligo(9,9-di(ethylhexyl)-fluorene-2,7-diyl) **5a-e** via endcapping reaction.*

The molecular weights of the fluorene oligomers **5a-e** were determined by GPC and are shown in Table 2.

Table 2: *Molecular weights, degrees of polymerisation and isotropic-nematic transition temperatures $T_{i,n}$ of **5a-e**.*

	ratio 1^a:4^b	$M_n(GPC)^c$ [g/mol]	$M_w(GPC)^c$ [g/mol]	$P_n(GPC)$	$T_{i,n}$ [°C]^d
5a	2:1	4100	6500	9.7	-
5b	3:2	3800	5600	8.9	250
5c	1:1	3100	4400	7.1	190
5d	1:2	2000	2500	4.3	85
5e	1:3	1900	2200	4.1	65

^{a}Bifunctional building block; ^{b}endcapper; ^{c}Polystyrene calibration; ^{d}determined with polarisation microscopy.

Characterisation

The molecular weight of the oligomers decreases from 4100 g/mol to 1900 g/mol with increasing amounts of endcapper **4**. The molecular weight distributions of **5a-e** can be seen in Figure 1.
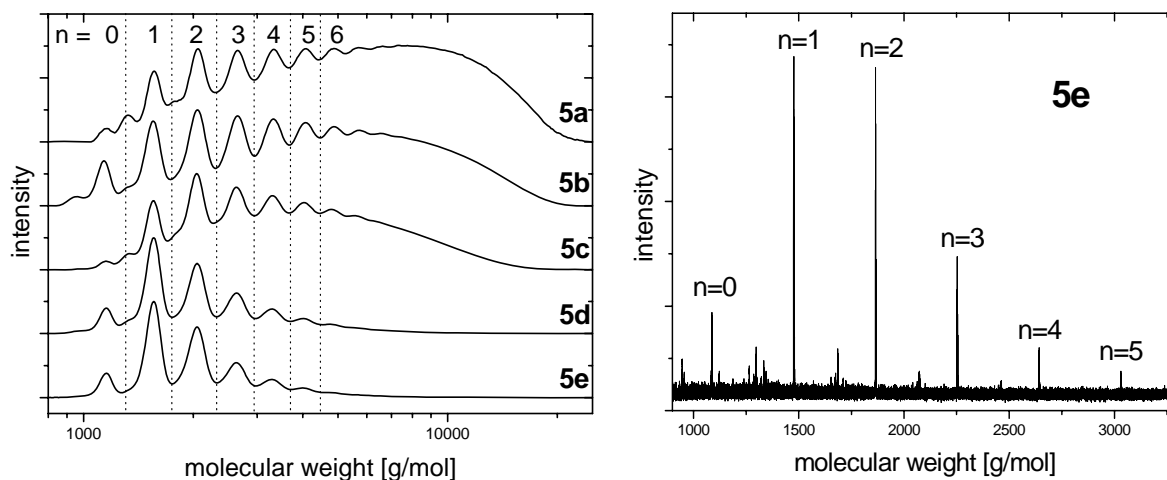
Figure 1: *left: GPC scans of the oligomers **5a-e** (polystyrene calibration), n refers to Scheme 2. right: Maldi-ToF spectrum of **5e**, recorded with 2,2'-p-phenylene-bis(5-phenyloxazole) (POPOP) as matrix material.*

The GPC scans in Figure 1 show one homologous series of oligomers. The lowest molecular weight compound in the mixtures is the dimeric species with a molecular weight of 1089 g/mol (n=0) and the resolution of the oligomer GPC goes up to the octamer (n=6). The lowest molecular weight mixture **5e** mainly consists of the trimeric species (n=1). With an increasing amount of bifunctional monomer **1** the intensity of the high molecular weight part increases and in mixture **5a** the polymeric part becomes dominant. Furthermore shoulders next to the oligomer signals appear from mixture **5c** on and the intensity of these shoulders increases with a decreasing amount of endcapper. Maldi-ToF spectra were recorded to investigate the completeness of the endcapping process (Figure 1). The Maldi-ToF spectrum in Figure 1 shows one homologous row of oligomers from the dimer on. Between the oligomer signals other small signals appear which can be assigned to decomposition products in the Maldi process. This was proven by Maldi-ToF experiments with purified monodisperse fluorene compounds. Maldi-ToF spectra of **5a-c** show additional signals which are assigned to the oligomers carrying only one acrylate group (Scheme 3). These one-arm compounds were only found in the high molecular weight mixtures from **5c** on which matches well with the results from GPC, where the one-arm compounds appear as small peaks in-between the main peaks of the oligomers. Thus the Maldi-ToF spectra reveal that the endcapping process is not complete, when the amount of endcapper **4** is reduced. The endcapping reaction is only complete if enough endcapper is provided. Compared to our results with the fluorene endcappers without acrylate groups [9] here the reactivity of the monobromo compound with alkylacrylate groups attached in position 7 is reduced drastically. The low reactivity of the endcapper is also reflected in the ratios of bifunctional building block to endcapper **(1:4)** and the resulting molecular weights. With the alkylacrylate endcapper a ratio of 3:2 gives a

molecular weight of 3800 g/mol, whereas with the non functionalised endcapper from

reference [9] the same molecular weight is obtained with a much higher ratio of 5:1.
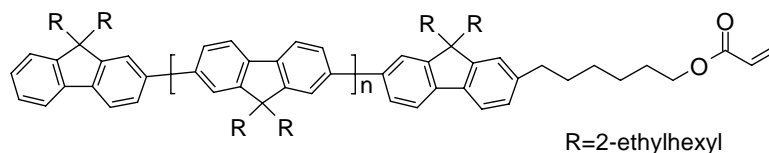
*Scheme 3: Mono-endcapped fluorene oligomers found in mixtures **5a-c**.*

Thermal Properties

All mixtures exhibit nematic mesophases and the transition temperatures strongly depend on

the molecular weights (Table 2). The clearing temperatures were determined with polarisation

microscopy and could be tuned in a broad temperature range from 250°C for **5b** to 65°C for

5e. $T_{i,n}$ of the highest molecular weight mixture **5a** could not be determined due to thermal

decomposition starting at 300°C. Upon cooling no crystallisation is observed and stable

nematic glasses are formed (Figure 2).
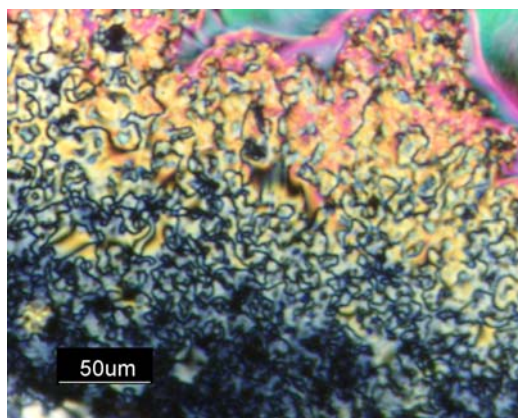
*Figure 2: Nematic Schlieren texture of **5b** observed upon cooling with 10°C/min between crossed polarisers; picture taken at 25°C.*

Photopolymerisation

The photopolymerisation experiments were carried out in the nematic phase of the reactive mesogens to achieve a high mobility of the acrylate groups in order to minimize the reaction time. Therefore the mixtures **5d** and **5e** seemed to be most suitable, because they contain only oligomers with two acrylate side arms and their nematic phases are at low temperatures to prevent a thermal polymerisation. Thin films of the photocrosslinkable bisacrylates **5d** and **5e** with 1wt% photoinitiator (Irgacure 819, Ciba Geigy) and 0.5wt% stabiliser (BHT) were prepared from xylene solutions (4wt%, thickness 40 nm). The films were heated into the nematic phase (25°C below $T_{i,n}$) and annealed for 20 min under inert atmosphere. Subsequently the crosslinking was achieved by exposure to UV light using a Xenon-mercury lamp where the photoinitiator gives rise to the formation of radicals. After that the films were developed in THF to wash away the residual monomer.

The exposure and development process were optimized to avoid oxidation processes and to obtain well resolved structures. 10-15 minutes were found to be the optimal irradiation time to get highly crosslinked films. Fluorescent oligofluorene microstructures were formed by irradiation through a μm size mask and subsequent development for 10s in THF (Figure 3). A minimum resolution of 1 μm could be obtained.
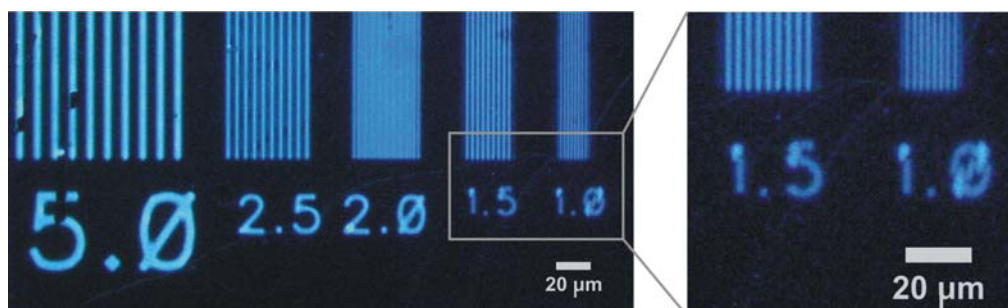
Figure 3: *Microstructures of a thin film of **5d** (+1wt% irgacure 819, 13 min exposure time at 60°C); picture taken under a fluorescence microscope.*

Conclusion

In this paper we presented the direct synthesis of novel photopolymerisable oligomeric fluorene oligomers. The conversion of bromine groups in the Yamamoto coupling is complete, if enough endcapper is provided and well defined oligomeric mixtures are obtained. The molecular weight decreases with an increasing amount of endcapper. All mixtures exhibit nematic mesophases, the transition temperatures strongly depend on the molecular weight and were tuned in the range of 65°C - 250°C. Subsequently photopolymerisation experiments were carried out and under optimised conditions irradiation through a μm-sized mask resulted in the formation of well resolved fluorescent 1 μm structures.

References

1   S. R. Forrest, *Nature* **2004**, *428*, 911.

2   A. Misra, P. Kumar, M. N. Kumalasanan, S. Chandra, *Semicond. Sci. Technol.* **2006**, *21*, R 35.

3   H. Sirringhaus, T. Kawase, R. H. Friend, T. Shimoda, M. Inbasekaran, W. Wu, E. P. Woo, *Science* **2000**, *290*, 2123.

4   M. Shtein, H. F. Gossenberger, J. B. Benzinger, S. R. Forrest, *J. Appl. Phys.* **2001**, *89*, 1470.

5   J. Huang, R. Xia, Y. Kim, X. Wang, J. Dane, O. Hofmann, A. Mosley, A. J. de Mello, J. C. de Mello, D. D. Bradley, *J. Mater. Chem.* **2007**, *17*, 1043.

6   C. D. Müller, A. Falcou, N. Reckefuss, M. Rojahn, V. Wiederhirn, P. Rudati, H. Frohne, O. Nyken, H. Becker, K. Meerholz, *Nature* **2003**, *421*, 829.

7   M. C. Gather, A. Köhnen, A. Falcou, H. Becker, K. Meerholz, *Adv. Func. Mater.* **2007**, *17*, 191.

8   L. Qiang, Z. Ma, Z. Zeng, R. Yin, W. Huang, *Macromol. Rapid Commun.* **2006**, *27*, 1779.

9   E. Scheler, P. Strohriegl, *Liquid Crystals* **2007**, *34*, 667.

10   H. Thiem, M. M. Rothmann, P. Strohriegl, *Designed Monomers and Polymers,* **2005**, *8*, 619.

11   H. Thiem, M. Jandke, D. Hanft, P. Strohriegl, *Macromol. Chem. Phys*. **2006**, *207*, 370.

12   G. Wu, C. Yang, B. Fan, B. Zhang, X. Chen, Y. Li, *J. Appl. Sci.* **2006**, *100*, 2336.

13   H. Thiem, P. Strohriegl, S. Setayesh, D. De Leeuw, *Synth. Met.* **2006,** *165*, 582.

14   M. Kreyenschmidt, G. Klaerner, T. Fuhrer, J. Ashnenhurst, S. Karg, W. D. Chen, V. Y. Lee, J. C. Scott, R. D. Miller, *Macromolecules* **1998**, *31*, 1099.

8 Tailoring fluorene-based oligomers for fast photopatterning

Esther Scheler, Peter Strohriegl

Macromolecular Chemistry I, University of Bayreuth, Universitätsstr. 30, 95440 Bayreuth

peter.strohriegl@uni-bayreuth.de
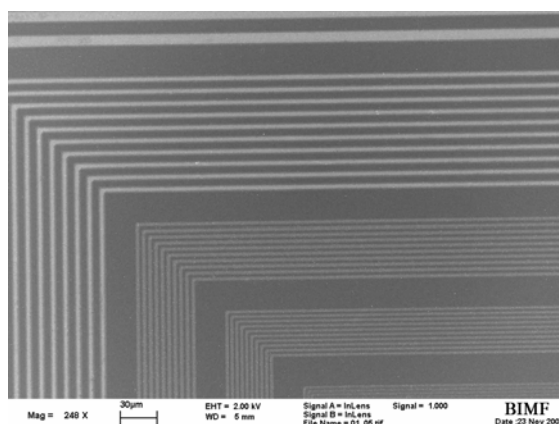
Abstract

In this publication we present a simple and efficient strategy for the synthesis of acrylate functionalized oligofluorenes. Within one single synthetic step photopatternable oligofluorenes with variable acrylate contents and molecular weights are formed. The Yamamoto condensation yields well defined oligomers by the direct polymerization of fluorene acrylates. The acrylate contents of the oligomers was varied from 10% to 100% by a statistical co-oligomerization. Photolithography experiments showed that for the species with highest acrylate content a crosslinking time of only 30 seconds leads to well resolved polyfluorene patterns. A minimum lateral resolution of 1 μm was achieved.

Introduction

Semiconducting organic materials have gained interest in the last years due to their applications in displays, electronics and sensors. One critical feature in the manufacturing of such devices is the spatial patterning of the organic material.[1] Furthermore, in view of the ongoing miniaturization in the electronic world, the semiconducting materials must have very small feature sizes.

In general there are two different approaches which lead to spatial patterns of organic materials: additive and subtractive techniques. Additive techniques include printing processes, like inkjet printing and screen printing, as well as thermal vacuum deposition of small molecules via shadow masks.[2] However these techniques bear some major drawbacks, such as limited resolution (>10 μm) in the case of printing and poor scalability to large substrate sizes in the case of the thermal deposition. To achieve adequate resolutions of 5-10 μm via inkjet printing prepatterned substrates are used. For example patterned polyimide lines prepared by photolithography have been made to define a channel length of 5 μm in an organic field effect transistor.[3] The use of such substrates add considerable complexity to the production process. However printing is a high throughput technique, what makes it very attractive for the mass production of electronic devices.

Subtractive techniques include lithographic methods, like photolithography or electron beam lithography. Here, a chemical modification of the organic material is induced by light or an electron beam, which leads to different solubilities of the exposed and non-exposed areas. With lithographic techniques, very small feature sizes of less than 100 nm are attainable. To realize these small feature sizes ultra precise equipment and cleanroom conditions are neccessary, which makes the process expensive. For feature sizes in the range of 1-10 μm the cost argument is less pronounced. In a recent publication, a

combination of additive and subtractive techniques was presented. D. Broer et al. showed that a reactive liquid crystalline material can be structured by printing and subsequent crosslinking.[4]

Conventional photoresists are optimized for inorganic semiconductor manufacturing and are not applicable to organic materials. It was shown that classic photoresist techniques can only be used to pattern organic compounds with major modifications, such as lift-off techniques, which limits their applicability in organic light emitting diode (OLED) manufacturing.[2] Thus the direct photochemical crosslinking of the semiconducting material itself, for example by the introduction of photocrosslinkable moieties, is a promising approach to patternable organic materials.[5,6,7] With light-induced crosslinking, the material becomes insoluble and can simultaneously be patterned, which means that the material works as a negative photoresist. It was shown that oxetane-substituted light-emitting polymers can be directly patterned with lithographic techniques under mild conditions, and resolutions of 2 μm were obtained under optimized conditions.[8,9] Photocrosslinkable functional compounds based on acrylates are also well known[10,11,12] where the focus is mainly on the multilayer capability of the crosslinked films in OLEDs or in preserving a liquid crystalline long range order for polarized luminescence.[13,14,15] In the case of the low-molecular-weight liquid crystalline materials, the irradiation is performed at elevated temperatures in the liquid crystalline (LC) state where the molecules have high mobility.[16] In polymeric acrylate systems, long exposure times of up to 15 minutes are often necessary in order to complete the network formation.[11]

It is very important that, during the crosslinking procedure, the chemical structure of the material is not altered.[17] However, photocrosslinking often causes a substantial degree of photochemical degradation. To avoid this, the processing conditions have to be very mild in terms of temperature and exposure time. In a previous publication we showed that

acrylate containing fluorene oligomers can be lithographically patterned at low temperatures and a spatial resolution of 1 μm was achieved.[18] The major drawback of these compounds turned out to be the long irradiation time of 15 minutes due to the low number of photopolymerizable groups per oligomer. Therefore we focused on the development of fluorene oligomers containing more acrylate sites in order to reduce the irradiation time and increase the crosslinking density of the resulting polymer network. In the present publication we report the development of tailored fluorene oligomers bearing different amounts of acrylate units. Using mixtures of an acrylate containing fluorene monomer and a fluorene monomer without crosslinkable units, the acrylate content in the resulting oligomers can be tuned from 10% to 100% in a 1-step synthesis. By adding monofunctional endcapper, which terminates the polymerization reaction in a controlled way, the molecular weight of the reactive fluorene oligomers was limited to 5000 g/mol. The subsequent photopolymerization of thin films leads to the formation of well resolved 1 μm-sized structures.

Results and discussion

Synthesis and characterization

Scheme 1 shows the overall reaction pathway to the acrylate containing monomers **A** and **C**. At position 9 of the fluorene backbone (see Scheme 1 top left for numbering) an asymmetric substitution of alkyl chains was chosen due to solubility reasons. Surprisingly we found that the fluorene bisacrylate 9,9-bis-(6-acryloyloxy-hexyl)fluorene showed poor solubility in the solvents used in the Yamamoto coupling. Since it is important that the

acrylate functionalized monomers are incorporated into the oligomers in a statistical manner we have chosen an asymmetrical substitution with one 6-acrylolyloxy-hexyl unit and an additional branched 2-ethylhexyl substituent in 9-position. This substitution pattern also ensures that the resulting oligomers are easily processible from common organic solvents.

In the first synthetic step (i) a 1:1 mixture of 2-(6-bromohexyloxy)-tetrahydro-2H-pyran and 2-ethylhexylbromide was used to alkylate the 9-position. Due to reaction statistics three different substitution products are formed (stereoisomers not considered) the one with one tetrahydropyran (THP) group being the desired product. The products were not separated after the alkylation reaction (i) because of their very similar polarity and solubility. The first purification was performed after the removal of the tetrahydropyran protective group (ii). The products carry free hydroxy groups and show different
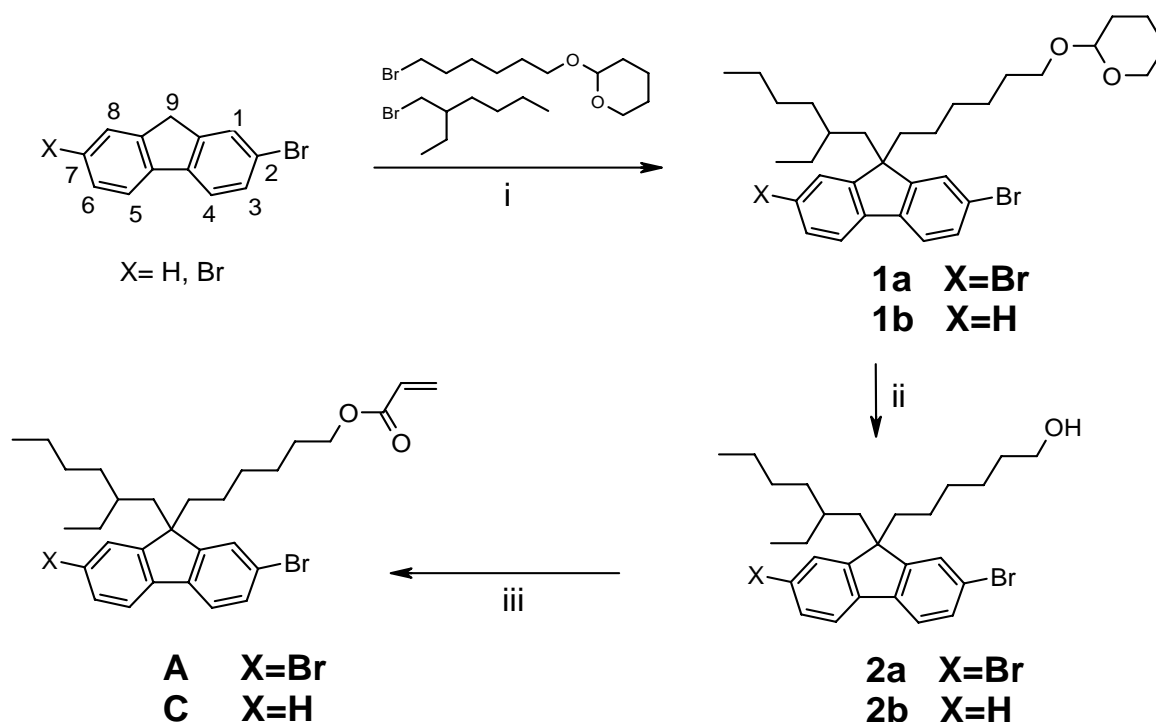
Scheme 1. *Synthesis of the monomers A and C. i) 50% NaOH, DMSO, 100°C; ii) PPTS, EtOH, 65°C; iii) acryloyl chloride, N,N-dimethylaniline, toluene, BHT, 65°C. The small numbers top left next to the carbon atoms indicate the fluorene backbone numbering.*

polarities. The yields were 40% for **2a** and 43% for **2b**. The hydroxy compounds **2** were then converted into the acrylate monomers **A** and **C** by an esterification with acryloyl chloride. This synthetic strategy comprises two major advantages compared to literature reports.[11] It uses an easily removable THP protecting group and the number of synthetic and purification steps is reduced, which remarkably lowers the overall synthesic effort. Scheme 2 presents the synthesis of the acrylate- functionalized fluorene oligomers **D** via

Scheme 2. *Endcapping approach for the fluorene oligomers* **D** *with variable acrylate content from n=0 to n=100%. The average degree of polymerization (n+m+2) was ~ 13 for a series of oligomers* **D**. *i) Ni(COD)$_2$, COD, 2,2′-bipyridyl, DMF, toluene, BHT, 80°C. Bottom: Structure of the photoinitiator Irgacure 784, used here.*

endcapping reaction. In a previous publication we showed that the endcapping approach for the formation of oligomeric mixtures is a simple way to tune the properties of the compounds in a 1-step synthesis.[18,19] Furthermore the formation of residual bromine endgroups is avoided.[19] We showed that the thermal properties of the oligomeric mixtures, e. g. the glass transition temperatures and clearing points, correlate very well with those of monodisperse fluorene oligomers with a similar molecular weight.[20] The most important advantage of this strategy compared to the multistep synthesis of monodisperse fluorene model compounds is that large quantities of the material become easily available.

Here the classic Yamamoto condensation using $Ni(COD)_2$ was applied. Since Ni(0) is not regained in the catalytic cycle $Ni(COD)_2$ has to be used in stoichometric amounts (see experimental section for details). It is also possible to carry out Yamamoto reactions with only catalytic amounts of Nickel. Here Ni(0) is generated in situ with Zn as reducing agent and is fully regained during the catalytic cycle.[21]

The synthetic route shown in Scheme 2 combines the endcapping approach with the variation of the acrylate content by co-oligomerization of the acrylate containing dibromofluorene **A** with the non-functionalized 2,7-dibromo-9,9-di(2-ethylhexyl)-fluorene **B**. The synthesis of compound **B** is described elsewhere.[22] We synthesized six different oligomeric mixtures with overall acrylate contents of 100%, 80%, 60%, 44%, 28% and 11% by the variation of the ratio **A** to **B** (see Tab. 1 for details). We found that the acrylate feeds correlate well with the acrylate contents found in the products and we assume that the condensation reaction between all monomers proceeds in a statistical manner. A ratio of 6:1 of the bifunctional monomers **A** and **B** compared to the mono- functional endcapper **C** was chosen to compromise on relatively low molecular weights while having enough acrylate moieties for a fast photopolymerization. By that

Table 1. *Acrylate feeds and molecular weights of **D10-100**.*

sample	feed A [%]	feed B [%]	A found in polymer* [%]	M_n**[g/mol]	P_n	average number of acrylates per chain
D 100	100	0	100	5100	12	12
D 80	83	17	80	5900	14	11
D 60	55	45	60	5200	13	8
D 40	48	52	44	5300	13	6
D 20	30	70	28	4700	12	3
D 10	14	86	11	4900	13	1

* determined by NMR spectroscopy; ** Polymer GPC, oligofluorene calibration.

procedure the molecular weights were limited to ~ 5000 g/mol (see Tab. 1), which corresponds to an average degree of polymerization P_n of ~13. The molecular weights of the six fluorene oligomers with different acrylate contents were all in the same range, which shows that the monomers **A** and **B** and the endcapper **C** have a comparable reactivity in the Yamamoto coupling. The endcapping process of monomer **C** is very
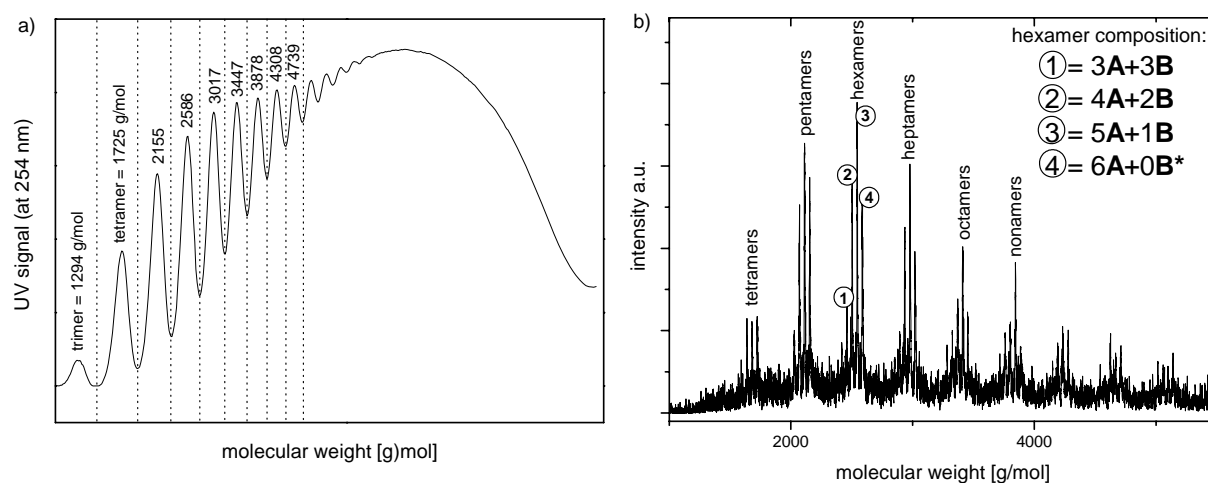
Figure 1. *(a) Oligomer GPC of **D100**. In the low molecular weight region the single oligomers (trimer, tetramer ...) are well resolved and the exact molecular weights can be assigned by MALDI-TOF spectrometry. (b) MALDI-TOF spectrum of **D80** (recorded in the linear mode with POPOP as matrix). The inlet top right shows the composition of the different hexamers. *refers to Scheme 2.*

efficient, which can be seen in the oligomer GPC (gel permeation chromatography) scan of **D100** in Fig. 1a. In the low-molecular-weight region the oligomer signals are well resolved without any shoulders. The exact molecular weights were determined using MALDI-TOF spectrometry and can be assigned to the GPC peaks as shown in Fig. 1a. Fig. 1b shows a MALDI-TOF spectrum of the oligomer **D80** with both acrylate and non-acrylate repeat units. For each oligomer (tetramer, pentamer ...) different signals appear. For the hexamer at around 2500 g/mol four main peaks are found. The lowest molecular weight peak at 2460 g/mol is assigned to the oligomer having three repeat units of monomer **A** and three of monomer **B**. The signal at highest molecular weight of 2585.9 g/mol is assigned to the oligomer having six repeat units of **A**. No residual bromine endgroups are found. Here we note that the molecular weight distribution (MWD) in the MALDI-TOF is shifted to lower values compared to GPC. In the MALDI-TOF experiment shorter chains are much easier desorbed from the target than longer chains. This leads to a shift of the MWD to lower values. Thus MALDI-TOF can only be used here to determine the composition of distinct oligomers.

Furthermore our results show that the Yamamoto coupling tolerates acrylate functionalities in contrast to the Suzuki coupling.[16,18] In the Suzuki coupling Pd(0) is the active species and therefore the acrylates can undergo a Heck coupling and various unwanted side products are formed. The NMR analysis of **D10-100** shows that the acrylates are quantitatively preserved in the Yamamoto coupling. Thus we avoid a polymeranalogous conversion of protected hydroxy groups into acrylates as often described.[11,23]

Photolithography

We have developed a procedure for the photopatterning of the fluorene oligomers **D** (Fig. 2). Thin films of oligofluorenes were spin coated from toluene solution together with 1 wt% of the commercial radical photoinitiator Irgacure 784 (see Scheme 2). After drying, the films were exposed to UV light using a Hg/Xe lamp and a long pass filter cutting off wavelengths below 400 nm. In the case of classic photoresists the irradiation procedure takes place at room temperature and ambient atmosphere.[24] Minimal damage to the chemical structure of the resist material can usually be tolerated since a photoresist is only used during one processing step in semiconductor manufacturing and is afterwards removed. In contrast the fluorene oligomers described here serve as organic semiconductors in a device and thus no damage during processing can be tolerated. It was shown that if polyfluorenes are exposed to UV light or annealed for an extended time at ambient conditions, an oxidation reaction in the 9-position takes place and the fluorescence is shifted to longer wavelengths due to the formation of fluorenone units.[25] Hence for the UV-induced crosslinking of fluorenes, the processing steps have to be slightly modified compared to classic resists as shown in Fig. 2. The films were protected from oxidation by putting them in a vacuum chamber with a quartz glass cover (Fig. 2b). During UV exposure the radical photoinitiator decomposes into radicals and the photocrosslinking starts. High acrylate mobility is crucial in order to complete the network formation. There are two ways to provide this mobility: the sample is heated either during the exposure or after the exposure step. Here, 60°C was found to be a suitable temperature for sufficient crosslinking in both cases. Both methods lead to the formation of well resolved microstructures. In the case of **D100**, irradiation for 30 s at
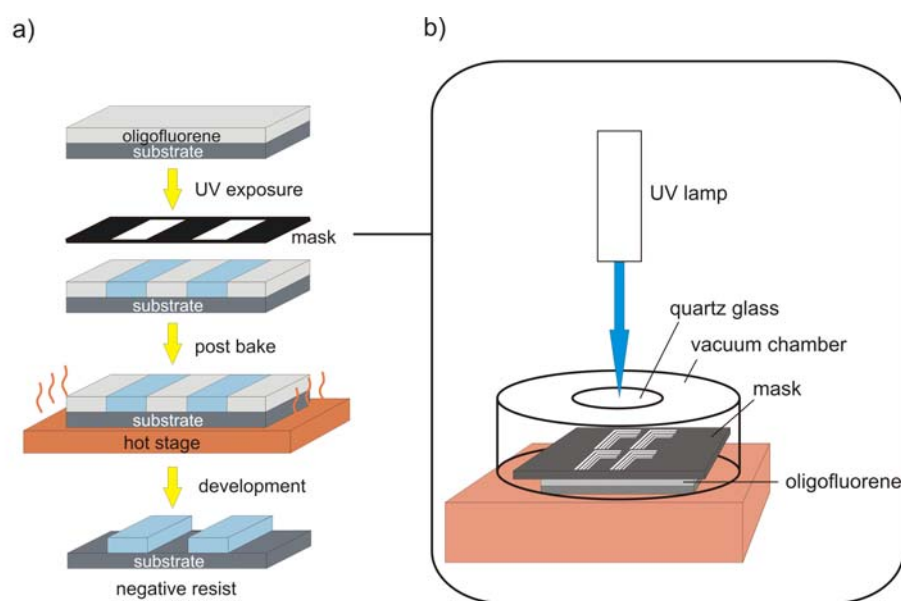
Figure 2. *Processing steps for the lithographic pattern formation: (a) Photolithographic process for a polyfluorene resist system. The first step is the spin coating of the oligofluorene followed by the irradiation with UV light through a mask (shown in detail in (b)). The UV exposure can be carried out at 60°C or at RT. If the sample is illuminated at RT a post-bake step at 60°C is necessary. In the last step the lithographic pattern is developed by dissolving the non-exposed parts in THF. (b) Experimental setup of the UV exposure step. The film is irradiated in a closed chamber in vacuum through a μm-sized mask.*

60°C leads to the formation of 1 μm-sized lines. An irradiation at room temperature (RT) for 60 s followed by a post-bake step for 2 minutes at 60°C, we are currently able to create 2 μm-sized patterns. Compared to our prior results[18,23] and to literature reports[11] the conditions of the photocrosslinking, e.g. the irradiation time, are improved significantly. The possibility to irradiate the reactive oligofluorenes at RT allows the use of commercial lithography equipment as long as the sample is kept in an inert atmosphere.

The last lithographic step is the development of the patterns, which is achieved by dissolving the non-irradiated areas in THF for 10 s. During the whole process the strong blue fluorescence of the oligofluorenes was preserved, which was checked by fluorescence spectroscopy.

The quality of the patterns was investigated with a fluorescence microscope and by scanning electron microscopy (SEM, see Fig. 3). In the fluorescence microscope the excitation wavelength was 340-380 nm. Strong blue fluorescent micrometer-sized stripes are observed (Fig. 3 left). The glass substrate appears black, which indicates a removal of the polyfluorene in the non-exposed areas. The full resolution cannot be seen in the fluorescence microscope picture due to a probable slight overexposure in the fluorescence microscope during the recording of the picture. The main purpose for showing this picture is to prove that the fluorene is not oxidized and the strong blue fluorescence of the oligofluorene is preserved in the patterning procedure. The lithographic resolution is best observed by SEM (Fig. 3 right). Here the dark grey stripes correspond to the crosslinked polyfluorene film and the white areas represent the glass substrate. Well resolved 1 µm-sized lines are observed.
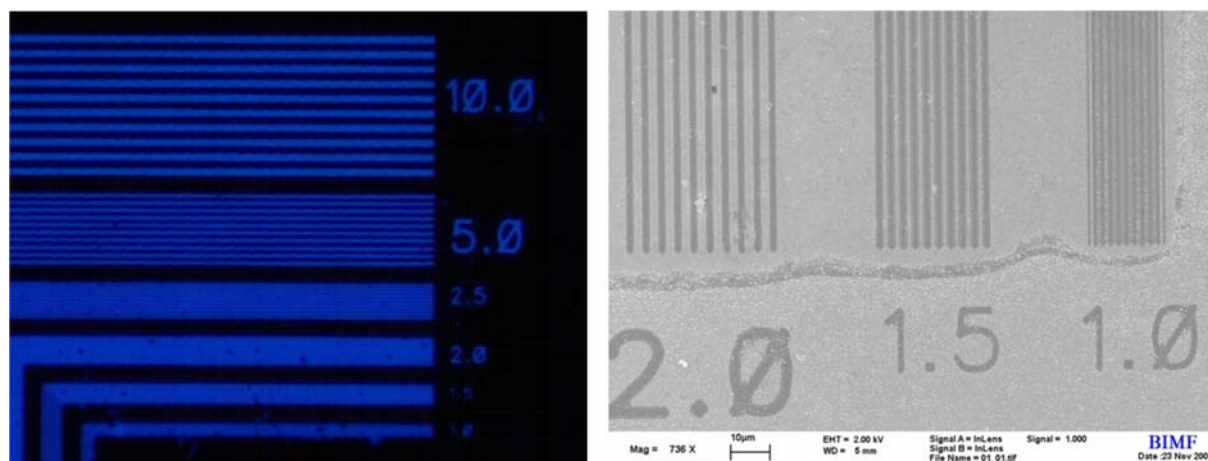
Figure 3. Left: Fluorescence microscope picture of the micro-structured oligofluorene **D100**. The thin film was irradiated for 30 s at 60°C under vacuum and subsequently developed in THF. Right: Corresponding SEM picture. The dark lines represent the crosslinked polyfluorene film, the white surrounding area the glass substrate. In both images the numbers next to the stripes represent their width in µm.

Conclusion

In conclusion we present an efficient synthetic strategy for photopatternable oligofluorenes. In one single step, both the amount of acrylate units and the molecular weight can be varied by using different ratios of the two monomers **A** and **B** and the endcapper **C**. Both acrylate and non-acrylate monomers show a similar reactivity in the Yamamoto coupling and a statistical co-oligomerization takes place. The endcapping process is efficient and the molecular weights were adjusted to ~5000 g/mol in each case. Photopatterning of the oligofluorenes was successfully carried out using normal photoresist processing. The exposure and post-bake step both have to be carried out under inert conditions. The films can be irradiated either at 60°C or at RT. If the irradiation is performed at RT a post-bake step at 60°C is necessary. In both cases highly resolved patterns with a minimum feature size of 1 micron are obtained. Under these mild processing conditions degradation was not observed.

Experimental

Synthesis

2,7-dibromo-9-(2-ethylhexyl)-9-(6-(2-tetrahydropyranyl-oxy)-hexyl)-fluorene 1a.
2.73 g (8.43 mmol) of 2,7-dibromofluorene were dissolved in 100 mL DMSO under argon. Under stirring 20 mL of 50% NaOH were added dropwise. 0.14 g of benzyltriethylammonium chloride : tetrabutylammonium chloride (1:1) as phase transfer catalysts were added. After that 3.35 g (12.64 mmol) 2-(6-bromohexyloxy)tetrahydro-2H-pyran and 2.44 g (12.64 mmol) 2-ethylhexylbromide were added dropwise. The solution

was heated to 100°C and stirred over night. The product was poured into 200 mL ice water and extracted with diethyl ether. The ether phase was washed with water and then the solvent was removed. The crude product was used in the next step without purification.

2,7-dibromo-9-(2-ethylhexyl)-9-(6-hydroxyhexyl)-fluorene 2a.

A solution of 12.64 mmol of the crude product **1a** and 0.635 g (2.53 mmol) p-toluenesulfonic acid pyridinium salt (PPTS) in 300 ml EtOH was prepared. 10 drops HCl (conc.) were added and the mixture was heated to 65°C and stirred for 4h. Then the solvent was evaporated and 100 mL dichloromethane and 100 mL water were added to the product mixture. After stirring for 5 min the phases were separated. The water phase was washed with dichloromethane and the combined organic phases were washed with water. Purification by column chromatography with hexane/ethylacetate 5:1 as eluents yielded in 40% of 2a as a transparent oil.

δ (250 MHz, CDCl$_3$, Me$_4$Si) 7.43-7.54 (6 H, m, Ar H), 3.53 (2 H, t, CH$_2$-OH), 1.94 (4 H, m, CH), 0.6-1.5 (17 H, m, alkyl H), 0.53 (6 H, t, CH$_3$). m/z 536 (M+, 75%), 323 (35).

2,7-dibromo-9-(2-ethylhexyl)-9-(6-acryloyloxy-hexyl)-fluorene A.

A solution of 1.7 g (3.16 mmol) **2a**, 0.061 g (0.28 mmol) 2,6-di-tert-butyl-p-cresol (BHT) and 0.48 mL (3.8 mmol) N,N-dimethylanilin in 160 mL toluene was prepared. 0.31 mL (3.8 mmol) of acryloyl chloride were added dropwise under argon and the mixture was stirred at 65°C over night. The solvent was evaporated and the crude product was purified by column chromatography using hexane/ethylacetate 10:1 and subsequent medium pressure chromatography using hexane/THF 30:1 as eluents. After drying white crystals were obtained with 60% yield.

δ (250 MHz, CDCl₃, Me₄Si) 7.43-7.54 (6 H, m, Ar H), 6.35 (1 H, d, =CH₂), 6.05 (1 H, d, =CH), 5.78 (1 H, d, =CH₂), 4.04 (2 H, t, CH₂), 1.93 (4 H, m, CH₂), 0.6-1.2 (17 H, m, Alkyl H), 0.54 (6 H, t, CH₃). m/z 590 (M+, 70%), 323 (35%).

The preparation of the 2-bromofluorene compounds **1b**, **2b** and **C** were perfomed in an analogous way. The yields were 43% for 2b and 66% for compound **C**.

Synthesis of oligo(9-(2-ethylhexyl)-9-((6-acryloyloxy)-hexyl)-fluorene-2,7-diyl) D100.

A schlenk flask was charged with nickeldicyclooctadiene (Ni(COD)₂, 1.0 g, 3.64 mmol), cyclooctadiene (COD, 0.4 g, 3.64 mmol), 2,2`-bipyridyl (0.56 g, 3.64 mmol) and 25 mL dry DMF under argon. The mixture was degassed by three freeze-thaw cycles before it was heated to 80°C for 30 min while stirring. Appropriate amounts of monomer **A** (0.64 g, 1.09 mmol) and the endcapper **C** (0.09 g, 0.18 mmol) were weighed into a separate flask under argon. A trace of BHT and 50 mL of dry toluene were added and the mixture was degassed by three freeze-thaw cycles. Subsequently the monomer mixture was added to the catalyst mixture using a cannula. The reaction mixture was stirred at 80°C for five days in the dark. Afterwards it was poured into methanol/HCl(conc.) 1:1 and stirred at room temperature for two hours. The organic layer was separated from the HCl layer which was then washed with Et₂O. The combined organic layers were washed with water and the solvent was evaporated. The crude product was filtered over a short neutral alumina column using toluene as eluent, then washed with alkaline EDTA solution (5%), reprecipitated twice from THF into methanol and dried under vacuum, yielding 0.282 g (51%) of **D100** as a pale yellow powder.

δ (250 MHz, CDCl₃, Me₄Si) 7.55-7.85 (6.4 H, m, Ar H), 6.33 (1 H, d, =CH₂), 6.05 (1 H, d, =CH), 5.74 (1 H, d, =CH₂), 4.01 (2 H, m, CH₂), 2.12 (4 H, m, CH₂), 0.66-1.3 (23 H, m, Alkyl H). λ_max (60 nm film)/nm 375 (optical density 0.4). MALDI-TOF (POPOP matrix,

linear mode): 1294 [M^+ trimer], 1724.5 [M^+ tetramer], 2155.2 [M^+ pentamer], 2585.8 [M^+ hexamer] 3016.5 [M^+ heptamer], 3447.1 [M^+ octamer], 3877.7 [M^+ nonamer], 4308.4 [M^+ decamer], 4739.0 [M^+ undecamer]. M_n(GPC, oligofluorene calibration)=5100 g/mol.

The oligofluorenes **D10 - D80** were prepared in an analogous manner.

Film preparation and irradiation

For the formation of thin films, the oligofluorene and 1wt% of photoinitiator Irgacure 784 (Ciba Geigy) were mixed. From this mixture 4wt% solutions in toluene were prepared and spin coated onto cleaned glass substrates at 1000 rpm for 60 sec. For the spin coating and development procedure purified solvents were used. The film thicknesses were 60 nm. The irradiation was performed with a Hg/Xe lamp Ushio UXM 200H with an intensity of 70mW/cm^2 and a long pass filter (Schott GG 400) cutting off wavelengths below 400 nm.

Analytical instruments

The molecular weights were determined by a Waters gel permeation chromatography system (GPC) for oligomers (analytical columns: crosslinked polystyrene gel, length 2 x 60 cm, width 0.8 cm, particle size 5 μm, pore size 100 Å, eluent THF (0.5 ml/min, 80 bar), oligofluorene calibration) and polymers (2 analytical columns: crosslinked polystyrene gel, length 2 x 30 cm, width 0.8 cm, particle size 5 μm, eluent THF (0.5 ml/min), oligofluorene calibration).

The MALDI-TOF spectra were recorded with a Bruker Reflex III with a high-mass detector in the linear mode using POPOP (1,4-Bis(5-phenyl-2-oxazolyl)benzene) as

matrix. For high resolution scanning electron microscopy, a LEO 1530 FESEM with field emission cathode was used. The NMR spectra were recorded with a Bruker AC 250. A Finnigan Mat 8500 Mat 112 S Varian with EI inization was used for the mass spectra. The fluorescence microscope used was a Leica DMR-SP with selective filter systems (here: dichromatic mirror 400 nm, suppression filter LP 420 nm).

Acknowledgement

References

1   S. Holdcroft, *Adv. Mater.,* 2001, **13**, 1753.

2   J. Huang, R. Xia, Y. Kim, X. Wang, J. Dane, O. Hofmann, A. Mosley, A.J. de Mello, J.C. de Mello, D.D.C. Bradley, *J. Mater. Chem.,* 2007, **17**, 1043.

3   H. Sirringhaus, T. Kawase, R.H. Friend, T. Shimoda, M. Inbasekaran, W. Wu, E.P. Woo, *Science*, 2000, **290**, 2123.

4   C. Sanchez, F. Verbakel, M.JC.W.M. Bastiaansen, D. J. Broer, *Adv. Mater.,* 2008, **20**, 74.

5   X.C. Li, T.M. Yong, J. Grüner, A.B. Holmes, S.C. Moratti, F. Cacialli, R.H. Friend, *Synth. Metals,* 1997**, 84**, 437.

6   A. Bacher, C.H. Erdelen, W. Paulus, H. Ringsdorf, H.W. Schmidt, P. Schuhmacher, *Macromolecules,* 1999, **32**, 4551.

7   M.S. Bayerl, T. Braig, O. Nuyken, C.D. Mueller, M. Gross, K. Meerholz, *Macromol. Rapid Commun.,* 1999, **20**, 224.

8   C.D. Müller, A. Falcou, N. Reckefuss, M. Rojahn, V. Wiederhirn, P. Rudati, H. Frohne, O. Nyken, H. Becker, K. Meerholz, *Nature,* 2003, **421**, 829.

9   M.C. Gather, A. Köhnen, A. Falcou, H. Becker, K. Meerholz, *Adv. Func. Mater.,* 2007, **17**, 191.

10   E. Peeters, J. Lub, J.A.M. Steenbakkers, D.J. Broer, *Adv. Mater.,* 2006, **18**, 2412.

11   G. Wu, C. Yang, B. Fan, B. Zang, X. Chen, Y. Li, *J. Appl. Polym. Sci.,* 2006, **100**, 2336.

12   R. Penterman, S.I. Klink, H.de Koning, G. Nisato, D.J. Broer, *Nature,* 2002, **417**, 55.

13   Y.-H. Yao, L.-R. Kung, S.-W. Chang, C.-S. Hsu, *Liq. Cryst.,* 2006, **33**, 33.

14   M.P. Aldred, A.J. Eastwood, S.M. Kelly, P. Vlachos, *Chem. Mater.,* 2004, **16**, 4928.

15   M. Jandke, D. Hanft, P. Strohriegl, K. Whitehead, M. Grell, D.D.C. Bradley, *Proceedings of SPIE,* 2001, **4105**, 338.

16   H. Thiem, P. Strohriegl, *Macromol. Chem. Phys.,* 2005, **206**, 2153.

17   L. Qiang, Z. Ma, Z. Zeng, R. Yin, W. Huang, *Macromol. Rapid Commun.,* 2006, **27**, 1779.

18   E. Scheler, I. Bauer, P. Strohriegl, *Macromol. Symp.,* 2007, **254**, 203.

19   E. Scheler, P. Strohriegl, *Liq. Cryst.,* 2007, **34**, 667.

20   J. Jo, C. Chi, S. Höger, G. Wegner, D.Y. Yoon, *Chem. Eur. J.,* 2004, **10**, 2681.

21   *WO Pat.*, 05184, 1997.

22   H. Thiem, P. Strohriegl, S. Setayesh, D. De Leeuw, *Synth. Met.* 2006**, 165**, 582.

23   H. Thiem, M. Jandke, D. Hanft, P. Strohriegl, *Macromol. Chem. Phys.,* 2006, **207**, 3

70.

24   J. Dai, S.W. Chang, A. Hamad, D. Yang, N. Felix, C.K. Ober, *Chem. Mater.,* 2006,

18, 3404.

25   E.J.W. List, R. Guentner, P. Scanducci de Freitas, U. Scherf, *Adv. Mater.,* 2002, **14**,

374.

9 Three color random fluorene-based oligomers for fast micron-scale photopatterning

Esther Scheler, Peter Strohriegl

Macromolecular Chemistry I, University of Bayreuth, Universitätsstr. 30, 95440 Bayreuth, Germany

peter.strohriegl@uni-bayreuth.de
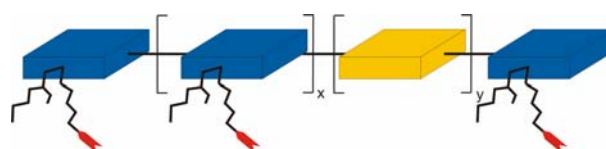
Abstract

In this contribution we show that random fluorene cooligomers with photo reactive acrylate units can be prepared in a simple 1-step Yamamoto synthesis. The acrylate functionalities are preserved quantitatively under Yamamoto conditions. NMR and Maldi-ToF measurements point to an almost statistical incorporation of the comonomers into the oligomer chain. Maldi-ToF analyses give a further insight into the chain compositions and we found fluorene-only oligomers to be present in low quantities. Thin films of the aromatic amine containing cooligomer show a blue fluorescence, the benzothiadiazole oligomer shows yellow photoluminescence and the bithiophene oligomer emits orange-red light upon excitation. Compared to pure fluorene oligomers with a HOMO of 5.7 eV the HOMO levels of the TPD and bithiophene derivatives are increased to 5.25 and 5.31 eV respectively, whereas the HOMO level of the benzothiadiazole oligomer is decrased to 5.85 eV. Photolithography experiments reveal that a careful optimization of the conditions, e.g. the choice of the photoinitiator, temperature and irradiation wavelength, leads to well resolved micrometer sized patterns. A minimum feature size of 1 micron was obtained. Thus we showed that with a simple 1-step Yamamoto coupling oligomers with photocrosslinkable acrylate groups are accessible. UV irradiation leads to densely crosslinked, insoluble networks. Thus these materials are ideal candidates for multilayer as well as patterned semiconducting devices.

Introduction

Conjugated organic materials have been in the focus of research for more than 20 years due to their various applications in organic light emitting devices (OLEDs) or organic field effect transistors (OFETs). The first commercially available products based on semiconducting organic molecules were launched in the late 1990s and since then constant research and development has opened up many more applications. A critical feature in the manufacturing of such devices often is the spatial patterning of the organic material.[1] Furthermore in view of the ongoing miniaturization in the electronic world it can be expected that the feature sizes of patterns from organic semiconductors will become smaller in the future.

In general there are two different approaches for lateral patterning: additive and subtractive techniques. Additive methods include vacuum deposition using shadow masks and printing techniques. The vacuum deposition technique is only suitable for small molecules needs expensive equipment and the scalability to larger substrate sizes is difficult. In contrast printing techniques allow a roll-to-roll production process and are therefore most suitable for the production of low cost and large area devices. A critical feature in the printing process is the spatial resolution. The single droplets must not mix on the substrate, which is difficult to achieve when it comes to very small pattern sizes. Thus to obtain a reasonable separation in the range of ≤ 10 μm pre-patterned substrates are often used.[2] This adds considerable complexity and costs to the production process.

Subtractive techniques include lithographic methods, like photolithography or electron beam lithography. Here, a chemical modification of the organic material is induced by light or an electron beam, which leads to different solubilities of the exposed and non-exposed areas. With lithographic techniques, very small feature sizes of less than 100 nm are attainable. To

realize these small feature sizes ultra precise equipment and cleanroom conditions are necessary, which makes the process expensive. For feature sizes in the range of 1-10 μm the cost argument is less pronounced. However conventional photolithography is not well suited to pattern conjugated organic semiconductors.[3] A very promising approach is the use of conjugated organic polymers with pendant photocrosslinkable groups. Such materials can be processed exactly like negative photoresists. Thus the direct formation of single pixels or patterns of arbitrary size and shape becomes possible. A second advantage of such compounds is their multilayer capability. Upon crosslinking the organic semiconductor becomes insoluble and allows the successive spincoating of a second layer.

It was shown that oxetane-substituted light-emitting polymers can be directly patterned with lithographic techniques under mild conditions, and resolutions of 2 μm were obtained.[4,5] Photocrosslinkable acrylates for passive optical elements like polarizers are also described in the literature.[6,7,8,9,10] Further on fluorene based polymers were intensively studied due to their strong blue fluorescence properties and are frequently used as emitting materials in OLEDs.[11,12]

In recent papers we have described the synthesis and photopatterning of acrylate functionalized oligofluorenes.[13,14] Fluorene copolymers with electron donating or withdrawing comonomers have become increasingly important in organic electronics. Copolymers incorporating aromatic amines like TPD (*N,N`*-bis(3-methylphenyl)-*N,N`*-bis(phenyl)-benzidine) are used as hole conductors[15] and bithiophene copolymers such as F8T2 (poly(9,9`-dioctylfluorene-co-bithiophene)) are known to exhibit high mobilities in organic field effect transistors.[16]

We have now extended our studies on photopatternable fluorene acrylates to cooligomers with TPD, benzothiadiazole and bithiophene units. In this paper we describe the synthesis, photophysical characterization and photopatterning of three novel crosslinkable fluorene cooligomers.

Experimental Section

Measurements

The molecular weights were determined by a Waters gel permeation chromatography system (GPC) for polymers (2 analytical columns: crosslinked polystyrene gel, length 2 x 30 cm, width 0.8 cm, particle size 5 μm, eluent THF (0.5 ml/min), oligofluorene calibration). The Maldi-ToF spectra were recorded with a Bruker Reflex III with a high-mass detector in the linear mode using POPOP (1,4-Bis(5-phenyl-2-oxazolyl)benzene) as matrix. The differential scanning calorimetry (DSC) analyses were performed on a Perkin Elmer DSC7 at a heating rate of 40K/min. The thermogravimetric analyses (TGA) were performed on a Netsch Simultane Thermoanalysis apparatus STR 409 C with a heating rate of 10 K/min under N_2. The abosrption spectra were recorded with a Hitachi U-3000 spectrophotometer and the photoluminescence spectra were measured with a Shimadzu RF-5301 PC spectrofluorometer. For the solution measurements distilled chloroform was used. The HOMO energy values were measured using a Riken Keiki AC-2 apparatus. For scanning electron microscopy (SEM) a Phenom™ from Fei Company was used. The ^{1}H NMR spectra were obtained in CDCl$_3$ with a Bruker AC 250. A Finnigan Mat 8500 Mat 112 S Varian with EI iniziation was used for the

mass spectra. The fluorescence microscope used was a Leica DMR-SP with selective filter systems (here: dichromatic mirror 400 nm, suppression filter LP 420 nm).

Film preparation and irradiation

For the formation of thin films, the oligomers and 1wt% of photoinitiator Irgacure 784 (Ciba Geigy) were mixed. From this mixture 4wt% solutions in toluene were prepared and spin coated onto cleaned silicon wafers at 1000 rpm for 60 sec. For the spin coating and development procedure purified solvents were used. The film thicknesses were approximately 100 nm. The irradiation was performed with a Hg/Xe lamp Ushio UXM 200H with an intensity of 70mW/cm^2 and selective filters GG400 and UG5 (Schott).

Materials

The Yamamoto and Suzuki reagents Ni(COD)$_2$, COD, bipyridyl, Pd(OAc)$_2$, P(o-tol)$_3$ and aliquat were used as received from Aldrich. CCl$_4$, dry DMF and dry toluene were used as received from Fluka. Na-$tert$-butylat, N-Bromosuccinimide (NBS), 5,5`-dibromo-2,2`-bithiophene and tri-$tert$-butylphosphin were used as obtained from Aldrich. CuBr$_2$-Al$_2$O$_3$[17], 2-(4,4,5,5-tetramethyl-1,3,2-dioxaborolane-2-yl)-9,9-dihexylfluorene[18] and 4,7-dibromo-2,1,3-benzothiadiazole[19] were prepared according to literature methods. The acrylate monomers **F** and **E** were synthesized as described elsewhere.[14]

N,N`-bis(4-methylphenyl)-N,N`-diphenyl-benzidine (1).

A schlenk flask was charged with 4 g (12 mmol) *N,N`*-diphenylbenzidine, 6.1 g (36 mmol) 4-bromotoluene, 0.08 g (0.34 mmol) Pd(OAc)$_2$ and 3.05 g (31 mmol) sodium-*tert*-butylat under

argon. 75 mL dry freshly distilled THF were added. 7.8 g (1 mmol) tri-*tert*-butylphosphin were added and the solution was heated to 80°C upon stirring. After 3 hours the solution was filtered over neutral alumina and washed with THF. The solvent was removed and compound **1** precipitated into MeOH. After drying 4.6 g (75%) of **1** were obtained as light brown powder. ^{1}H NMR (CDCl$_3$): δ 7.4 (s, 5H), 7.07 (s, 21 H), 2.32 (s, 6H). m/z 515 (M+, 100%), 258 (M2+, 80%)

N,N`*-bis(4-methylphenyl)-*N,N`-bis(4-bromophenyl)-benzidine (C1).

2.5 g (5 mmol) of compound **1** and 1.72 g (10 mmol) NBS were weighed into a flask. 25 mL of chloroform were added and the solution was stirred at room temperature (RT) for 1 h. 12.5 mL of acetic acid were added and the solution was stirred for further 6.5 h at RT. The product was extracted with diethyl ether and the solvent was removed. The crude product was purified by column chromatography using hexane/toluene 5:1 as eluent. After drying 2.35 g (75%) of **C2** were obtained as pale yellow needles. ^{1}H NMR (CDCl$_3$): δ 7.36 (m, 8H), 7.23 (m, 2H), 7.11 (m, 14H), 2.34 (s, 6H). m/z 672 (M+, 100%), 336 (25%)

4,7-bis(9,9`-dihexylfluorene-2-yl)-2,1,3-benzothiadiazole (2).

0.22 g (0.75 mmol) 4,7-dibromo-2,1,3-benzothiadiazole and 0.69 g (1.5 mmol) 2-4,4,5,5-tetramethyl-1,3,2-dioxaborolane-2-yl)-9,9-dihexylfluorene were weighed into a schlenk flask under argon. 30 mL toluene, 15 mL 2M K$_2$CO$_3$ and one drop of aliquat were added. The mixture was degassed by three freeze-thaw cycles before it was heated to 65°C for 12 h. The product was extracted with diethyl ether and the solvent was removed. The crude product was purified by column chromatography using hexane/toluene 2:1 as eluent. 0.416 g (70%) of **2**

were obtained as yellow crystalline material. ^{1}H NMR (CDCl$_3$): δ 8.1 (m, 2H), 7.95 (s, 2H), 7.88 (m, 4H), 7.77 (m, 2H), 7.36 (d, 6H), 2.03 (m, 8H), 1.08 (s, 24H), 0.77 (t, 20H). m/z 800 (M+, 100%).

4,7-bis[2,7-dibromo-(9,9`-dihexylfluorene-2-yl)]-2,1,3-benzothiadiazole (C2).

A flask was charged with 0.219 g (0.27 mmol) **2** and 0.91 g CuBr$_2$-Al$_2$O$_3$. 30 mL CCl$_4$ were added and the suspension was stirred at 70°C for two weeks. The CuBr$_2$-Al$_2$O$_3$ was filtered off and washed with CH$_2$Cl$_2$. The crude product was purified by recrystallization from hexane. 70 mg (30%) of **C2** as yellow crystals were obtained. ^{1}H NMR (CDCl$_3$): δ 8.1 (m, 2H), 7.95 (s, 2H), 7.88 (m, 4H), 7.64 (m, 2H), 7.50 (d, 4H), 2.00 (m, 8H), 1.10 (s, 24H), 0.77 (t, 20H). m/z 958 (M+, 100%).

Oligo[(9-(2-ethylhexyl)-9-((6-acryloyloxy)-hexyl)-fluorene-2,7-diyl)-_co_-2,2`-bithiophene] (O3).

A schlenk flask was charged with nickeldicyclooctadiene (Ni(COD)$_2$, 0.45 g, 1.64 mmol), cyclooctadiene (COD, 0.17 g, 1.64 mmol), 2,2`-bipyridyl (0.25 g, 1.64 mmol) and 20 mL dry DMF under argon. The mixture was degassed by three freeze-thaw cycles before it was heated to 80°C for 30 min while stirring. Appropriate amounts of monomer **F** (0.203 g, 0.34 mmol), the endcapper **E** (0.04 g, 0.08 mmol) and **C3** (0.048 g, 0.147 mmol) were weighed into a separate flask under argon. A trace of BHT (2,6-di-tert-butyl-p-cresol) and 40 mL of dry toluene were added and the mixture was degassed by three freeze-thaw cycles. Subsequently the monomer mixture was added to the catalyst mixture using a cannula. The reaction mixture was stirred at 80°C for five days in the dark. Afterwards it was poured into

methanol/HCl(conc.) 1:1 and stirred at room temperature for two hours. The organic layer was separated from the HCl layer which was then washed with Et_2O. The combined organic layers were washed with water and the solvent was evaporated. The crude product was washed with alkaline EDTA solution (5%) then filtered over a short neutral alumina column using toluene as eluent. It was reprecipitated twice from THF into methanol and dried under vacuum, yielding 0.130 g (50%) of **O3** as a red powder. ^{1}H NMR ($CDCl_3$): δ 7.72 (m, 7.9H), 6.3 (d, 1H), 6.06 (m, 1H), 5.74 (d, 1H), 4.01 (s, 2.6H), 2.05 (s, 5.6H), 0.887 (m, 36.7H). M_n (GPC, oligofluorene calibration) 5500 g/mol.

The oligomers **O1** and **O2** were prepared in an analogous manner, but the workup of **O1** was slightly changed. The crude product mixture of **O1** was directly extracted with Et_2O without pouring it into MeOH/HCl(conc.) before.

Data for **O1**: ^{1}H NMR ($CDCl_3$): δ 7.63 (m, 10.9H), 7.14 (m, 8.9H), 6.28 (d, 1H), 6.04 (m, 1H), 5.73 (d, 1H), 4.00 (s, 2.1H), 2.35 (s, 2.6H), 2.05 (s, 4.7H), 0.887 (m, 27.8H). M_n (GPC, oligoluorene calibration) 5200 g/mol, yield 84%.

Data for **O2**: ^{1}H NMR ($CDCl_3$): δ 7.72 (m, 9.7H), 7.34 (m, 1.2H), 6.33 (d, 1H), 6.04 (m, 1H), 5.74 (d, 1H), 4.01 (m, 2.6H), 2.08 (s, 6.7H), 0.887 (m, 42.6H). M_n (GPC, oligofluorene calibration) 5800 g/mol, yield 30%.

Results and discussion

Oligomer Synthesis

Scheme 1 shows the overall reaction pathway to the acrylate functionalized fluorene cooligomers **O1-3**. The preparation of the comonomers **C1** and **C2** is described in Scheme 2.

The TPD-comonomer **C1** was prepared in a two-step synthesis. In the first step diphenylbenzidine and p-bromo-toluene were coupled using palladium acetate as catalyst. The resulting TPD derivative **1** was brominated in its two vacant para-positions using NBS. The overall yield was 56%. The benzothiadiazole trimer **C2** had to be designed because we found that the strong electron withdrawing 4,7-dibromo-2,1,3-benzothiadiazole was not incorporated into the polyfluorene chains in the Yamamoto polymerization. The trimer **2** was prepared from a fluorene borolane and 4,7-dibromo-2,1,3-benzothiadiazole in a Suzuki coupling with 70% yield Scheme 2 *right*). Compound **2** was then selectively brominated in the two terminal positions of the fluorene rings using activated $CuBr_2$ on alumina to yield in 30% **C2**.[20] The bithiophene comonomer **C3** is commercially available. The Yamamoto condensation was chosen as aryl-aryl coupling method, because acrylates are tolerated and the coupling reaction can be carried out without any protecting groups.[13,14]
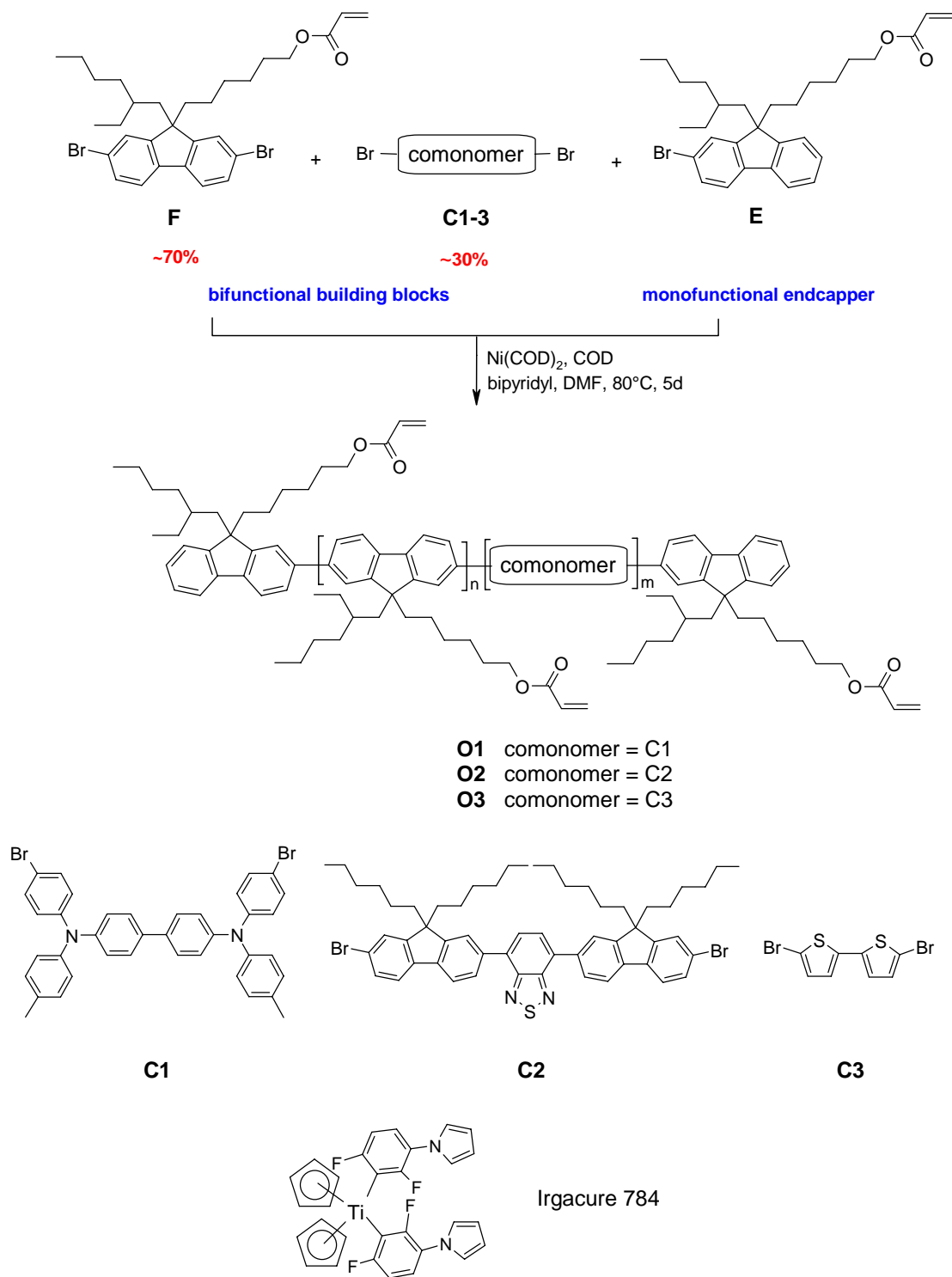
Scheme 1. *Synthetic route for the preparation of the acrylate containing fluorene cooligomers **O1-3**. The photoinitiator Irgacure 784 is displayed below.*
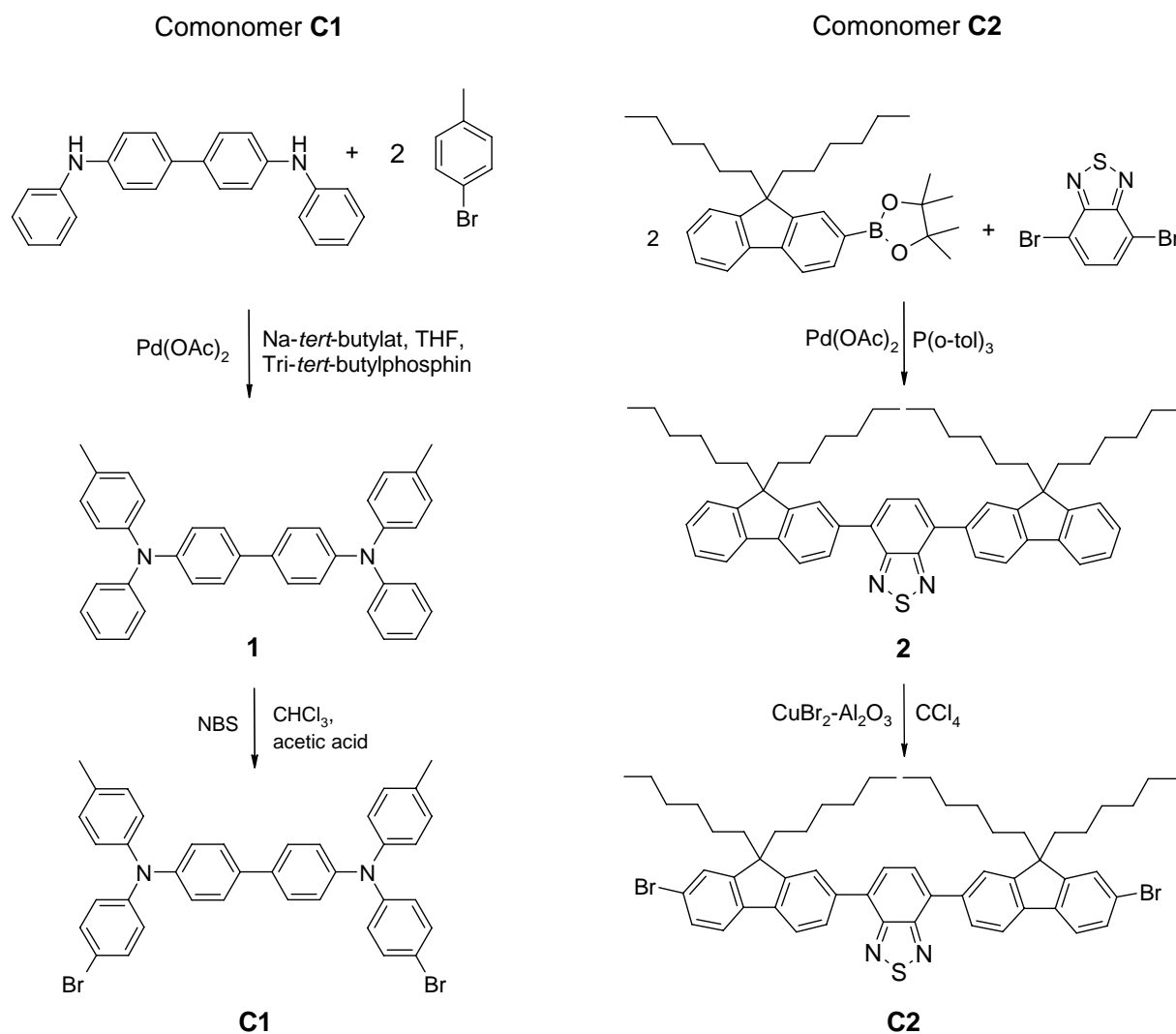
Scheme 2. *Synthesis of the comonomers **C1** and **C2***.

Conjugated polymers often suffer from their low solubility. In the fluorene cooligomers described here the comonomers do not contain any solubilizing substituents. To ensure a good solubility and processability of the cooligomers we have limited the molecular weights by the addition of a monofunctional endcapper **E** during the polymerization. The endcapper terminates the chain growth in a controlled way and residual bromine endgroups are avoided.[14] Further on decreased molecular weights also lead to lower glass transition

temperatures as we have shown previously.[21] Low glass transition temperatures allow low processing temperatures during photolithography and photodegradation upon UV illumination is prevented. From our experience on fluorene oligomers we chose a ratio of 6:1 of dibromo monomers (**F+C**) to the monobrominated endcapper **E** for oligomers **O1** and **O3**. In the case of the comonomer **C2** with higher molecular weight a ratio (**F+C2**)/**E** of 4:1 was applied. For the cooligomerization ~70mol% of the fluorene compound **F** and ~30mol% of the comonomers **C1-3** were used to ensure a good solubility of the oligomers and to introduce enough acrylate functionalities for a fast photocrosslinking reaction.

The molecular weights of **O1-3** were determined by gel permeation chromatography (GPC) and were in the range of 5200-5800 g/mol (oligofluorene calibration, see Table 1 for details). That points to an efficient and controlled termination with the endcapper **E**. NMR analysis shows that the comonomer feeds **C1-3** correlate well with the comonomer contents in the oligomers.

Table 1. *Composition, molecular weights and thermal analyses of **O1-3**.*

oligomer	co-monomer	ratio (F+C): E	feed C1-3 [mol%]	found C1-3 [mol%]^a	M_n [g/mol]^b	M_w [g/mol]^b	T_g [°C]^c	$T_{d,onset}$ [°C]^d
O1	**C1**	**6:1**	30	30.5	5200	7900	119	340
O2	**C2**	**4:1**	20	25	5800	7400	50	355
O3	**C3**	**6:1**	30	33	5500	6100	58	350

^{a} Comonomer content determined by NMR. ^{b} Values determined by GPC, oligofluorene calibration. ^{c} Measured with DSC upon heating with a rate of 40 K/min. ^{d} Onset of decomposition determined by thermogravimetry with a heating rate of 10 K/min under N_2.

Thermal properties

All oligomers were characterized by both differential scanning calorimetry (DSC) and thermogravimetric analysis (TGA) and the results are summarized in Table 1. The decomposition temperatures are all in the range of 350°C. The DSC scans of the oligomers showed no signs of melting or recrystallization. The glass transition temperatures (T_gs) were 50°C and 58°C °C for **O2** and **O3** respectively and 119°C for **O1**. The transition enthalpies were very small and only detectable using a heating rate of 40 K/min. They were determined upon heating and due to the high heating rate the values are expected to be slightly overestimated. The value of 119°C measured for **O1** is in the range of the reported value for TPD containing polyfluorenes.[15,22] For an efficient photopolymerization the acrylate units have to be mobile. Thus photocrosslinking experiments with organic semiconductors are usually carried out at elevated temperatures to provide an appropriate mobility of the reactive groups. Here the low T_gs of **O2** and **O3** allow low processing temperatures, which helps to avoid photodegradation during UV exposure.

Due to the limited molecular weights of the oligomers Maldi-ToF measurements could be performed and the Maldi-ToF spectrum of **O1** is shown in Figure 1. Oligomer **O1** is well suited for Maldi-ToF investigations since aromatic amines are known to form stable molecular ions. The spectrum was recorded in the linear mode with POPOP (1,4-Bis(5-phenyl-2-oxazolyl)benzene) as matrix. The signals are well resolved in the range of 1000 to 4500 g/mol. A magnification of the spectrum between 2100 and 3400 g/mol is also shown in Figure 1 *right*. Every single peak can be assigned to an oligomer with a distinct composition of **TPD** and **F** (=fluorene) units and a detailed assignment is included in Figure 1. In general

all expected products are found and different `series` can be observed. Consequently the reactivities of fluorene monomers **F** and **E** in the Yamamoto condensation seem to be similar to those of **C1-3**. In the range of 2100 to 2500 g/mol all pentamers, between 2600 and 2900 g/mol all hexamers and from 3000 to 3400 g/mol all heptamers are found. In the case of the hexamers five different signals are observed. The signal at lowest molecular weight corresponds to a pure fluorene hexamer named F_6 and with increasing molecular weight the number of incorporated **TPD** units increases. The highest molecular weight hexamer consists of two fluorene units **F** and four **TPD** units (named F_2TPD_4). The occurrence of fluorene-only oligomers is not unexpected if mathematical probability considerations are performed. The probability of adding a fluorene monomer **F** to a growing chain end is 70% according to the monomer feed. If now the two endcapping molecules **E** are fixed at both ends of the chain, the probability of a (hexamer)-chain consisting of six fluorene units is 24%, assuming an equal reactivity of **F** and **TPD**.
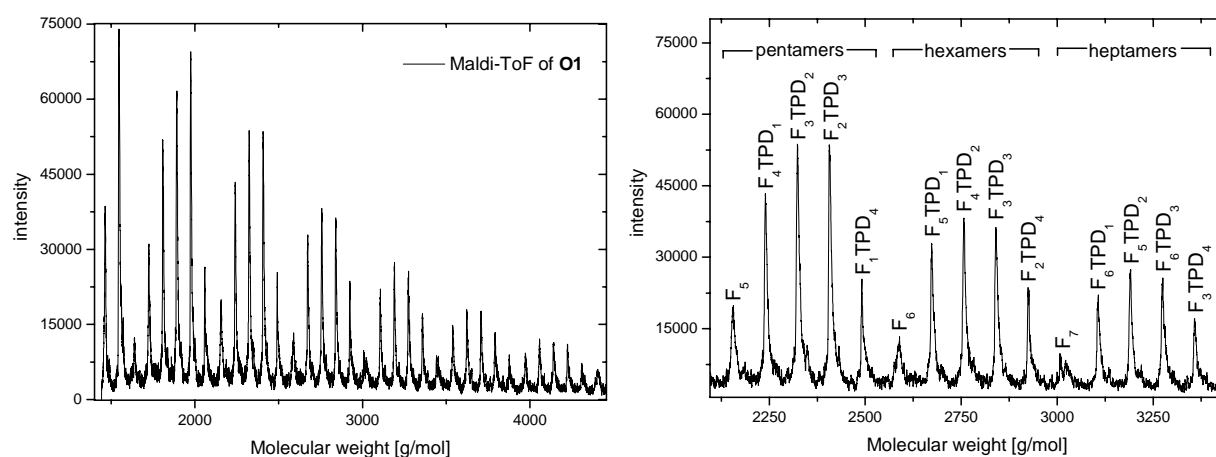
Figure 1. *Left: Maldi-ToF spectrum of **O1**. Right: Magnification and assignment of the signals between 2100 and 3400 g/mol. The spectrum was recorded in the linear mode using POPOP as matrix. **F** corresponds to a fluorene and **TPD** to a **C1** unit according to Scheme 1. **F_4TPD_2** e.g. is an oligomer consisting of four fluorene and two **TPD** repeat units.*

Within the pentamers and heptamers pure fluorene oligomers, named F_5 and F_7 respectively, are also found. However the probability for the formation of fluorene-only compounds decreases with increasing chain lengths according to reaction statistics.

The existence of these pure fluorene oligomers has major consequences on the spectroscopic properties in solution as described later on. In the case of the pentamers in addition to the expected oligomers a peak corresponding to a mono-endcapped pentamer (F_1TPD_4) is observed. For higher molecular weight oligomers mono-endcapped species are not found. Oligomers with bromine endgroups are not present.

Optical properties

The absorption and emission spectra of **O1-3** were measured in chloroform solution and thin film and are shown in Figure 2. The solution spectra are displayed left and the film spectra right. The results are summarized in Table 2.

Table 2. *Optical properties of chloroform solutions and thin films of **O1-3**.*

	solution		films	
	UV	PL	UV	PL
O1	375	439 (375)[a]	375	442 (375)[a]
O2	373, 430	415, 437, 537 (373)[a]	375, 440	534 (375, 440)[a]
O3	373, 430	413, 438, 477, 520 (373)[a]	375, 440	568 (375, 440)[a]

[a] The values in brackets give the corresponding excitation wavelength in nm.

In solution the TPD containing oligomer **O1** exhibits one absorption maximum at 375 nm. Upon excitation at 375 nm one photoluminescence maximum at 439 nm is observed. The film spectra of **O1** are similar to the solution spectra, an absorption maximum at 375 nm and an emission maximum at 442 nm are found. In the case of **O2** the solution absorption spectrum shows two maxima, a dominant maximum at 373 nm and a small maximum at 430 nm (Figure 2c). Upon excitation at 373 nm a PL spectrum with three maxima is obtained. The first two maxima at 415 and 437 nm correspond to the typical oligfluorene emission pattern and result from the fluorene-only oligomers present in the mixture. The third maximum at 537 nm originates from the benzothiadiazole containing cooligomers. If the excitation wavelength is 430 nm the fluorene-only emission is suppressed and only the benzothiadiazole oligomers emit light with a maximum at 540 nm.[23] The film spectra of **O2** are displayed in Figure 2d. Here the absorption also shows two maxima, one dominant maximum at 375 nm and a weak one at 440 nm. An excitation at 375 and 440 nm lead to the same PL maxima at 534 nm. This demonstrates that in thin films an intermolecular energy transfer between different oligomer chains becomes possible. The energy is transferred from the fluorene-only compounds to the benzothiadiazole oligomers and a pure yellow emission color independent from excitation is obtained. The solution absorption spectrum of **O3** (Figure 2e) also exhibits two maxima, one at 373 nm and one at 430 nm. An excitation at 373 nm leads to a complex PL spectrum with four maxima. The first two maxima at 413 and 438 nm display the emission pattern of the pure oligofluorenes present in the mixture. The other maxima at 477 and 520 nm originate from the bithiophene cooligomers. However an excitation at 430 nm leads to a simpler PL spectrum with one dominant maximum at 521 nm. Here only the bithiophene cooligomers are excited and emit light, the fluorene-only emission is suppressed. The thin film spectra of **O3**

are shown in Figure 2f. The absorption spectrum again exhibits two maxima, a dominant one at 375 nm and a weak one at 440 nm. Upon excitation at both wavelengths (375 and 440 nm) the same PL spectrum with a maximum at 568 nm is obtained. Thus an intermolecular energy transfer from the fluorene-only oligomers to the bithiophene oligomers takes place and pure emission colors independent from the excitation wavelength are obtained. Here we note that for **O3** the PL maximum in solution is blue shifted (47 nm) compared to the film spectrum. This may be due to well-known packing phenomena described for thiophene compounds.[24]

In general the typical fluorene emission pattern found for solutions of **O2** and **O3** also indicate that pure-fluorene compounds are present in the mixtures, which confirms the Maldi-ToF results. However for practical applications as emitters in yellow and red OLEDs, the oligomers are well suited since the blue oligofluorene fluorescence is not present in thin films.
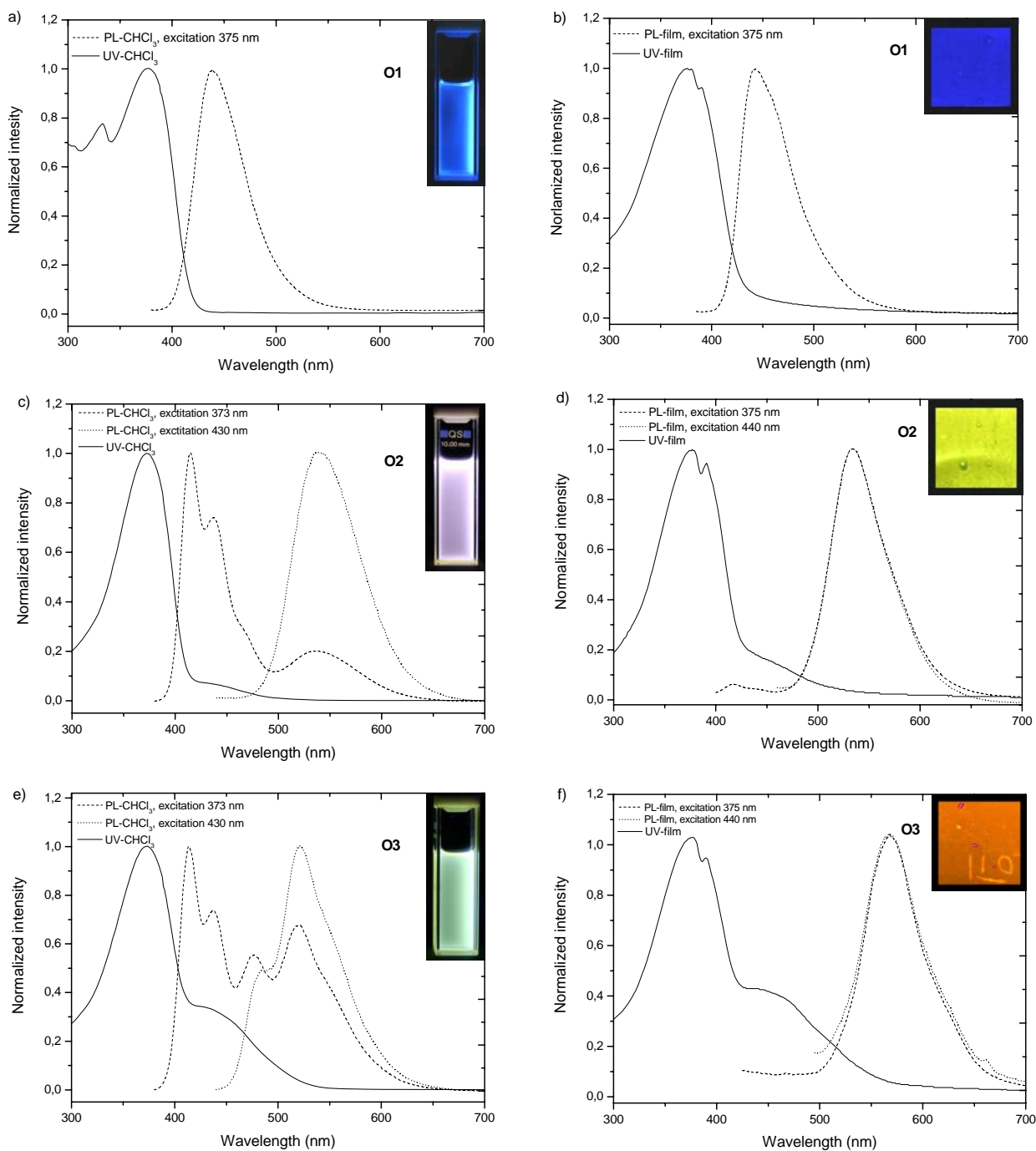
Figure 2. *Normalized absorption and emission spectra of **O1-3** (a-f) in chloroform solutions and as thin films. The photographical insets show the chloroform solutions and thin films upon excitation at 366 nm.*

The HOMO levels were measured by photoelectron spectrometry (Riken Keiki AC-2) from thin films. From the optical bandgaps, determined as intersection of the UV/VIS and photoluminescence spectra, the LUMO values were calculated. All data are listed in Table 3. The oligomers **O1** and **O3** with electron donating units have HOMO energies of 5.25 eV and 5.31 eV respectively. In comparison to a fluorene-only oligomer, whose data are also displayed in Table 3, the HOMO values are increased. For the oligomer **O2** with an electron withdrawing comonomer we find a slight decrease of the HOMO level from 5.70 to 5.85 eV and a LUMO energy level of 3.29 eV, which is 0.59 eV lower than for a fluorene-only oligomer. Both **O2** and **O3** have smaller bandgaps (2.56 and 2.40 eV respectively) and decreased LUMO energy values compared to a pure fluorene oligomer.

Table 3. *Energy levels and optical bandgaps of **O1-3**.*

	HOMO [eV][a]	LUMO [eV][b]	optical bandgap [eV][c]
O1	5.25	2.30	2.95
O2	5.85	3.29	2.56
O3	5.31	2.91	2.40
Oligofluorene[d]	5.70	2.73	2.97

[a] Measured with photoelectron spectrometry. [b] Calculated from the HOMO and optical bandgap values. [c] Determined as intersection of absorption and emission spectra (film spectra) [d] Oligofluorene with an average degree of polymerization of 13 from ref. [14].

Photolithography

With regard to the use of **O1-3** as photopatternable materials the photocrosslinking conditions were thoroughly investigated. Concerning the use of the patterned oligomers as semiconductors it is very important that, during the crosslinking procedure, the chemical structure of the material is not altered.[25] However, photocrosslinking often causes a substantial degree of photochemical degradation. To avoid this, the processing conditions have to be very mild in terms of temperature and exposure time. The new materials **O1-3** are well suited due to their large number of acrylate functionalities and their low glass transition temperatures. To exclude any oxygen we put the samples into a vacuum chamber during the exposure procedure (Figure 3b).
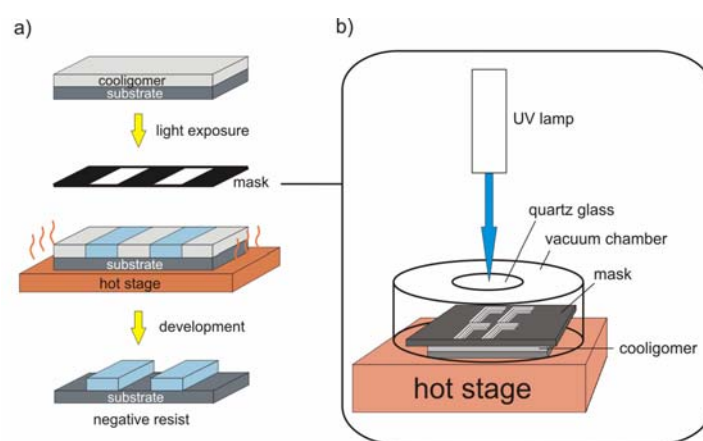
Figure 3. *(a) Photolithographic process for a (negative) fluorene resist system. The first step is the spin coating of the oligofluorene followed by the irradiation with light through a mask (shown in detail in (b)). The exposure is carried out on a hot stage. In the last step the lithographic pattern is developed by dissolving the non-exposed parts in THF. (b) Experimental setup of the exposure step. The film is irradiated in a closed chamber in vacuum to avoid degradation processes.*

The first processing step is the spin coating of the oligomer onto cleaned silicon wafers (see Figure 3). For this purpose solutions of **O1-3** in toluene with concentrations of 4wt% were

prepared. 1wt% (refers to the amount of oligomer) photoinitiator Irgacure 784 was added. The spin coating was performed at 1000 rpm for 60s. After that the films were dried at 115°C for one minute under inert atmosphere. The thickness of all films was about 100 nm. The second step is the UV-exposure. The samples were put in a vacuum chamber as shown in Figure 3b, annealed at a certain temperature for several minutes in the chamber and then irradiated using a Hg-Xe lamp while keeping the temperature. The heating during irradiation is essential because the chains have to be mobile to polymerize. The last lithographic step is the development of the patterns, which is achieved by dissolving the non-irradiated areas in THF for 30 s.

Our previous experiments with photopolymerizable oligofluorenes showed that the use of an additional filter during exposure is helpful.[14] In that case we used the long pass filter GG400 (Schott) to cut off wavelengths below 400 nm, which avoids the excitation of the fluorene backbone. Thus most of the energy is absorbed by the initiator Irgacure 784 and a very fast crosslinking can be achieved. Here we note that the initiator Irgacure 784 shows absorption below 360 nm and above 400 nm. Its chemical structure is presented in Scheme 1. For **O1-3** we also tested the filter GG400, but the irradiation times needed appeared to be very long (up to 15 minutes). We attribute that to the absorption of **O1-3** above 400 nm. Irgacure 784 is not able to decompose into radicals, because most of the light energy is absorbed by the oligomers. Therefore we decided to irradiate using wavelengths below 300 nm. We utilized the Schott filter UG5, which transmits light between 230 and 400 nm and blocks shorter and longer wavelengths. Here we find much faster photocrosslinking. For **O1** an exposure of 2 minutes at 40°C was sufficient enough for the formation of well resolved patterns. In the case of **O2** the films had to be exposed for 6 minutes at 50°C and for **O3** an irradiation at

50°C for 4.5 minutes were found to be most suitable. In each case minimum resolutions of 1-

2 µm were achieved.
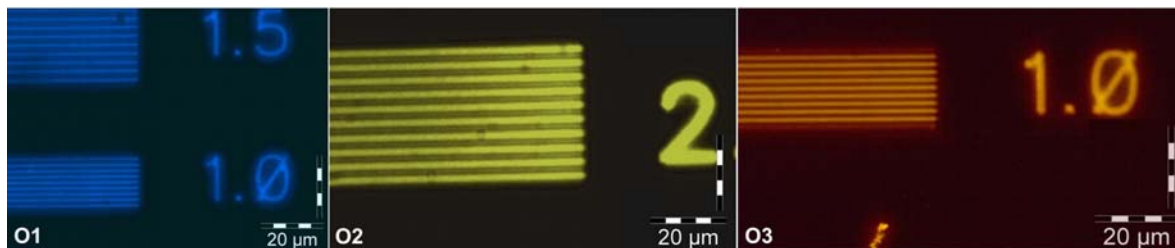
*Figure 4. Fluorescent microstructures of **O1-3** observed under a fluorescence microscope with an excitation wavelength of 340-380nm. Upon crosslinking the filter UG5 was used and the detailed conditions were: **O1**: exposure at 40°C for 2 min; **O2**: exposure at 50°C for 6 min; **O3**: exposure at 50°C for 4.5 min. The corresponding SEM images are found in Figure 5. The numbers next to the stripes represent their width in µm.*

Photooxidation was not observed, during the whole process the fluorescence colors of the

oligomers were preserved, which was checked by fluorescence spectroscopy and microscopy.

The quality of the patterns was investigated with fluorescence microscopy and scanning

electron microscopy (SEM). In the fluorescence microscope the excitation wavelength was

340-380 nm. Strong blue, yellow-green and red fluorescent micrometer-sized stripes are

observed (see Figure 4). That indicates the preservation of the chemical structure and thus the

opto-electronic properties of the oligomers during irradiation. The silicon wafers appear

black, which indicates a complete removal of the polyfluorene in the non-exposed areas. The

resolution goes down to 1 µm for **O1** and **O3** and 2 µm for **O2**. From the same samples SEM

images were taken and are displayed in Figure 5. Here the same resolutions are found as

observed with fluorescence microscopy. For **O1** and **O2** a slight overexposure is observed

because the micrometer sized lines are slightly broader than given by the mask. In the case of

O3 the line width corresponds well to the given width, which points to ideal photolithographic conditions.
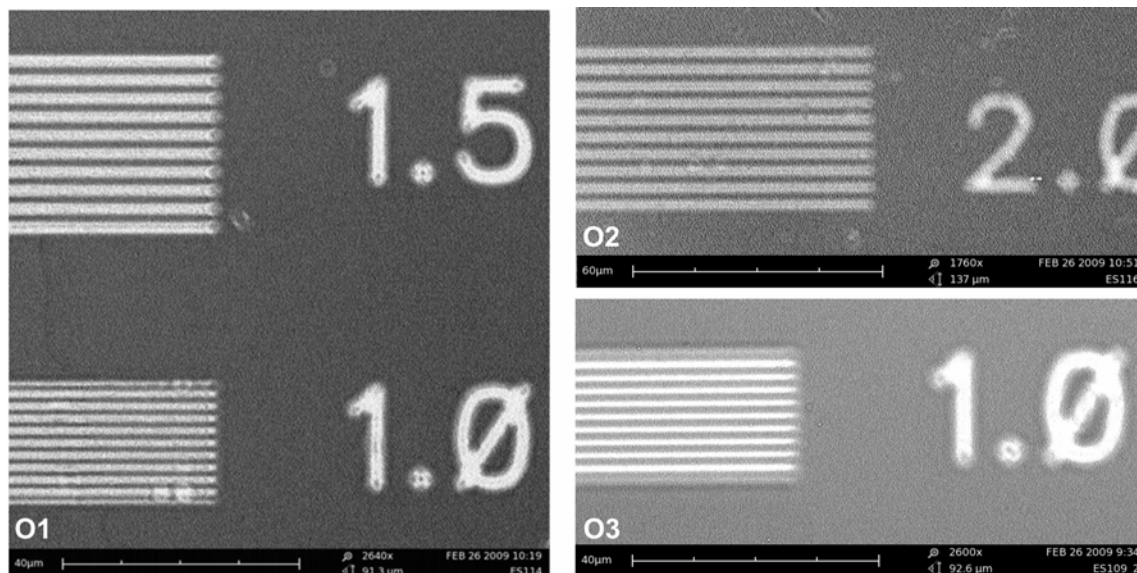
Figure 5. *SEM images of microstructured oligomers **O1-3**. White corresponds to the crosslinked material, black and dark grey represent the wafer. For the SEM pictures the same samples were used as for the fluorescence microscopy images from Figure 4. The numbers next to the stripes represent their width in μm.*

Conclusion

In this publication we show that random fluorene cooligomers with photo reactive acrylate units can be prepared in a simple 1-step Yamamoto synthesis. The acrylate functionalities are preserved quantitatively under Yamamoto conditions. NMR and Maldi-ToF measurements point to an almost statistical incorporation of the comonomers into the oligomer chain. Maldi-ToF analyses give a further insight into the chain compositions and we found fluorene-only oligomers to be present in low quantities. Thin films of the aromatic amine containing cooligomer show a blue fluorescence, the benzothiadiazole oligomer shows yellow photoluminescence and the bithiophene oligomer emits orange-red light upon excitation.

Compared to pure fluorene oligomers with a HOMO of 5.7 eV the HOMO levels of the TPD and bithiophene derivatives are increased to 5.25 and 5.31 eV respectively, whereas the HOMO level of the benzothiadiazole oligomer is decrased to 5.85 eV. Photolithography experiments reveal that a careful optimization of the conditions, e.g. the choice of the photoinitiator, temperature and irradiation wavelength, leads to well resolved micrometer sized patterns. A minimum feature size of 1 micron was obtained. Thus we showed that with a simple 1-step Yamamoto coupling oligomers with photocrosslinkable acrylate groups are accessible. UV irradiation leads to densely crosslinked, insoluble networks. Thus these materials are ideal candidates for multilayer as well as patterned semiconducting devices.

Acknowledgement

References

1   Holdcroft, S. *Adv. Mater.* **2001**, *13*, 1753.

2   Sirringhaus, H.; Kawase, T.; Friend R. H.; Shimoda T.; Inbasekaran, M.; Wu, W.; Woo, E. P. *Science*, 2000, **290**, 2123.

3   Huang, J.; Xia, R.; Kim, Y.; Wang, X.; Dane, J.; Hofmann, O.; Mosley, A.; de Mello, A. J.; de Mello, J.C.; Bradley, D. D. C. *J. Mater. Chem.,* **2007,** *17*, 1043.

4   Müller, C. D.; Falcou, A.; Reckefuss, N.; Rojahn, M.; Wiederhirn, V.; Rudati, P.;

     Frohne, H.; Nyken, O.; Becker, H.; Meerholz, K. *Nature,* **2003**, *421*, 829.

5   Gather, M. C.; Köhnen, A.; Falcou, A.; Becker, H.; Meerholz, K. *Adv. Func. Mater.,*

     2007, *17*, 191.

6   Wu, G.; Yang, C.; Fan, B.; Zang, B.; Chen, X.; Li, Y. *J. Appl. Polym. Sci.,* **2006**, *100*,

     2336.

7   Yao, Y.-H.; Kung, L.-R.; Chang, S.-W.; Hsu, C.-S. *Liq. Cryst.,* **2006**, *33*, 33.

8   Jandke, M.; Hanft, D.; Strohriegl, P.; Whitehead, K.; Grell, M.; Bradley, D. D. C.

     Proceedings of SPIE, **2001**, *4105*, 338.

9   Broer, D. J.; Boven, J.; Mol, G. N.; Challa, G. *Makromol. Chem.* **1989**, *190*, 2255.

10   Broer, D. J.; Lub, J.; Mol, G. N. *Nature* **1995**, *378*, 467.

11   Grell, M.; Knoll, W.; Lupo, D.; Meisel, A.; Miteva, T.; Neher, D.; Nothofer, H.-G.;

     Scherf, U.; Yasuda, A. *Adv. Mater.* **1999**, *11*, 671.

12   Whitehead, K. S.; Grell, M.; Bradley, D. D. C.; Jandke, M.; Strohriegl, P. *Appl. Phys.*

     Lett. **2000**, *76*, 2946.

13   Scheler, E.; Bauer, I.; Strohriegl, P. *Macromol. Symp.,* **2007**, *254*, 203.

14   Scheler, E.; Strohriegl, P. *J. Mater. Chem.* **2009**, *19*, 3207.

15   Redecker, M.; Bradley, D. D. C.; Inbasekaran, M.; Wu, W. W.; Woo, E. P. *Adv. Mater.*
      1999, *11*, 241.

16   Sirringhaus, H.; Wilson, R. J.; Friend, R. H.; Inbasekaran, M.; Wu, W.; Woo, E. P.;
      Grell, M.; Bradley, D. D. C. *Appl. Phys. Lett.* **2000**, *77*, 406.

17   Kodomari, M.; Satoh, H.; Yshitomi, S. *J. Org. Chem.* **1988**, *53*, 2093.

18   Thiem, H.; Jandke, M.; Hanft, D.; Strohriegl, P. *Macromol. Chem. Phys.* **2006**, *207*,
      370.

19   Mancilha, F.S.; Da Silveira Neto, B.A.; Lopes, A.S.; Moreira, P.F.Jr.; Quina, F.H.;
      Goncalves, R.S.; Dupont, J. *Eur. J. Org. Chem.* **2006**, *21*, 4924.

20   Kodomari, M.; Satoh, H.; Yoshitomi, S. *J. Org. Chem.* **1988**, *53*, 2093.

21   Scheler, E., Strohriegl, P. *Liq. Cryst.* **2007**, *34*, 667.

22   Sato, H.; Ogino, K.; Hirai, H. *Macromol. Symp.* **2001**, *175*, 159.

23   Chuang, C.-Y.; Shih, P.-I.; Chien, C.-H.; Wu, F.-I.; Shu, C.-F. *Macromolecules* **2007**,
      40, 247.

24   Yasuda, T.; Namekawa, K.; Iijima, T.; Yamamoto, T. *Polymer* **2007**, *48*, 4375.

25   Qiang, L.; Ma, Z.; Zeng, Z.; Yin, R.; Huang, W. *Macromol. Rapid Commun.,* **2006**, *27*,
      1779.

10 Synthesis and properties of alternating fluorene-based oligomers for sub-micron photopatterning

Esther Scheler, Eva Betthausen, Peter Strohriegl

Macromolecular Chemistry 1, University of Bayreuth, Universitätsstr. 30, 95440 Bayreuth,

Germany

peter.strohriegl@uni-bayreuth.de
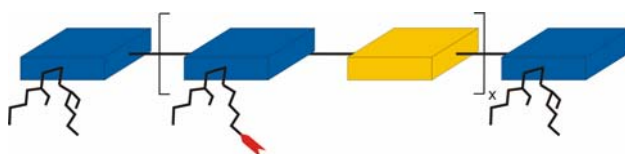
Abstract

In this publication we present the synthesis of alternating photocrosslinkable cooligomers via Suzuki coupling. Since the Suzuki reaction does not tolerate acrylate functionalities fluorene monomers carrying OH-groups were synthesized. During polymerization the OH-groups had to be protected by THP groups. After the Suzuki coupling two polymeranalogous conversions were performed, the removal of the THP group and the esterification with acryloyl chloride. The molecular weights of the oligomers were limited using a monofunctionalized endcapper. We analyzed the cooligomers with NMR, GPC and Maldi-ToF, which gives a detailed insight into the chain compositions. Three different series of oligomers are present in the product, carrying either two, one or no endcapping molecules.

The thermal properties were investigated and the oligomers show low T_gs of 53-63°C and are thermally stable up to ~300°C. The optical properties were analyzed in thin films and solutions. We obtained a blue emitting oligomer in the case of the TPD comonomer, a yellow fluorescent material for the benzothiadiazole and a red (film) and yellow-green (solution) emitting material for the bithiophene. The energy levels were determined by photoelectron spectrometry and are very similar to those of randomly linked oligomers. The photocrosslinking behavior was studied and under optimized conditions a lateral resolution of 600 nm was obtained.

Introduction

The potential of organic material for the fabrication of flat panel displays or integrated circuits has been in the focus of recent research in the field of organic light emitting diodes (OLEDs) and of organic field effect transistors (OFETs). A critical feature in the manufacturing of such devices is the spatial patterning of the organic material.[1] Spatial patterning can be achieved either by additive techniques, such as printing or vacuum deposition or by subtractive methods, such as lithography.

In the case of lithography feature sizes of less than 100 nm are accessible and routinely used in the manufacturing of integrated circuits, but ultra precise equipment and cleanroom conditions are necessary, which makes the process expensive. For larger feature sizes in the range of 0.5-10 μm the cost argument is much less pronounced. However conventional photolithography is not well suited to pattern conjugated organic semiconductors.[2] Therefore a very promising approach is the use of conjugated organic polymers with pendant photocrosslinkable groups. Such materials can be processed exactly like negative photoresists. Thus the direct formation of single pixels or patterns of arbitrary size and shape becomes possible. A second advantage of such compounds is their multilayer capability. Upon crosslinking the organic semiconductor becomes completely insoluble and allows the successive spincoating of a second layer. It was shown that oxetane-substituted light-emitting polymers can be directly patterned with this technique and resolutions of 2 μm were obtained.[3,4] Photocrosslinkable acrylates for example for passive optical elements like polarizers are also described in the literature. [5,6,7,8,9,10,11,12]

In recent papers we have described the tailoring and photopatterning of acrylate functionalized oligofluorenes.[13,14] Feature sizes of 1 μm are easily accessible under very mild processing conditions. The focus of our ongoing research is to optimize not only the photocrosslinking behavior, but also to prepare fluorene cooligomers with improved hole and

electron conductivity. This has become increasingly important in organic electronics in view of all-organic flexible devices. Copolymers incorporating aromatic amines like TPD (*N,N`*-bis(3-methylphenyl)-*N,N`*-bis(phenyl)-benzidine) are frequently used as hole conductors in polymer OLEDs[15] and bithiophene copolymers such as F8T2 (poly(9,9`-dioctylfluorene-co-bithiophene)) are well known to exhibit high mobilities in organic field effect transistors.[16] For this purpose we extended our studies on patternable fluorene oligomers to cooligomers containing TPD, benzothiadiazole and bithiophene units. In a recent paper we described the direct Yamamoto coupling of fluorene acrylates with several comonomers.[17] We found that the fluorene acrylates and comonomers were incorporated almost statistically. The Yamamoto condensation uses bromine functionalities in both monomers and due to reaction statistics fluorene-only oligomers are formed in low quantities.

Since the Yamamoto coupling results in statistical cooligomers we now apply the Suzuki coupling to obtain strictly alternating compounds. We introduced TPD, benzothiadiazole and bithiophene units applying the Suzuki reaction, which is described in this contribution. Here a cross coupling between boronic compounds and bromine functionalities ensures an alternating incorporation of the comonomers. Photolithography experiments show that under optimized conditions sub-micron resolutions of 600 nm are attainable.

Experimental Part

Instruments

^{1}H-NMR spectra were recorded on a Bruker AC 250 spectrometer in CDCl$_3$ at 250 MHz with tetramethylsilane as the reference. Mass spectra were obtained by a Finnigan MAT 8500 (70 eV). The MALDI-TOF spectra were obtained by a Bruker Reflex III with high-mass detector. The oligomer GPCs were performed with a WATERS model 515 HPLC PUMP with UV detector (WATERS 486, 254 nm) and RI detector (WATERS 410) equipped with two MESOPORE columns (particle size: 3 μm, length: 30 cm, eluent: THF, flow rate: 0.5 mL·min^{-1}, calibration with polystyrene and oligofluorene standards). For DSC measurements a Perkin-Elmer DSC-7 apparatus was used (heating/cooling rate: 40 K·min^{-1}). TGA measurements were performed on a NETSCH Simultane Thermoanalyses Apparatus STR 409C at a standard heating rate of 10 K·min^{-1} under N$_2$. UV-Vis absorption spectra were recorded on a HITACHI U-3000 spectrophotometer and the fluorescence spectra on a SHIMADZU RF-5301 PC spectrofluorometer with 90° detection. The absorption and emission spectra were obtained at ambient temperature from thin films spin coated at 1000 rpm from toluene solutions on glass substrates using a B 0574 Spin-Coater form HAMATECH GmbH. The HOMO energy values were measured with the surface analyzer AC2 from Riken (Japan). The irradiation experiments were performed using a Hg-Xe lamp Ushio UXM 200H with a UV band pass filter (UG 5, Schott). The fluorescence microscope used was a Leica DMR-SP with selective filter systems.

Materials

All chemicals were used as received from Aldrich. All solvents were purified by distillation prior to use. Dry THF was distilled over potassium prior to use. The photoinitiator Irgacure 784 was purchased from Ciba and used as received.

Synthesis

2,7-Dibromo-9-(2-ethylhexyl)-9-(6-hydroxyhexyl)fluorene (1).

4.07 g (12.57 mmol) of 2,7-dibromofluorene and 0.20 g of a mixture of the phase transfer catalysts benzyltriethylammonium chloride and tetrabutylammonium chloride (1:1) were dissolved in 300 mL of DMSO under vigorous stirring. To remove dissolved oxygen argon was bubbled through the solution for 30 min. 30 mL of NaOH solution (50 %) were added resulting in an immediate color change to dark red. A mixture of 3.35 mL (18.85 mmol) 2-ethylhexyl bromide and 4.13 mL (18.85 mmol) 2-(6-bromohexyloxy)tetrahydro-2H-pyran was added dropwise and the mixture was heated to 100 °C under reflux over night. The solution was poured into ice water and extracted with diethyl ether. The combined organic phases were washed with water, dried over Na_2SO_4 and the solvent was evaporated. Afterwards to the crude mixture 947 mg (3.77 mmol) pyridinium p-toluenesulfonate (PPTS) and 500 mL EtOH were added. 30 drops of HCl (conc.) were added and the mixture was heated to 60 °C and stirred over night. The reaction mixture was poured into water and stirred for 5 min. The phases were separated and the aqueous phase was extracted with diethylether. The combined organic phases were washed with water, dried over Na_2SO_4 and the solvent was evaporated. The crude product was purified by column chromatography using n-hexane/ethyl acetate 5:1 as the eluent yielding 2.25 g (4.19 mmol, 22 %) of **1** as a transparent oil.

^{1}H-NMR (CDCl$_3$): δ = 7.43 - 7.54 (m, 6H, fluorene H), 3.52 (t, 2H, CH$_2$-OH), 1.88 - 1.95 (m, 4H, CH$_2$), 0.51 - 1.40 (m, 23H, alkyl H).

MS (70 eV): m/z = 536 (M$^+$).

2,7-Dibromo-9-(2-ethylhexyl)-9-(6-(2-tetrahydropyranyloxy)hexyl)fluorene (2).

A solution of 2.25 g (4.19 mmol) of **1** and 0.46 ml (5.03 mmol) of 3,4-dihydro-2H-pyran in 70 mL of CH$_2$Cl$_2$ was prepared. 92 mg (0.37 mmol) of PPTS dissolved in 5 mL of CH$_2$Cl$_2$ were added and the solution was stirred for 16 h at RT. The reaction mixture was washed with water, dried over Na$_2$SO$_4$ and the solvent was evaporated. Purification by column chromatography with n-hexane/ethyl acetate 5:1 as the eluent and subsequent freeze-drying in benzene yielded 1.36 g (2.19 mmol, 52 %) of **2** as a white solid.

^{1}H-NMR (CDCl$_3$): δ = 7.43 - 7.54 (m, 6H, fluorene H), 4.51 (t, 1H, CH), 3.75 - 3.90 (m, 1H, CH$_2$-O), 3.55 - 3.70 (m, 1H, CH$_2$-O), 3.40 - 3.55 (m, 1H, CH$_2$-O), 3.20 - 3.35 (m, 1H, CH$_2$-O), 1.87 - 1.94 (m, 4H, CH$_2$), 1.49 - 1.81 (m, 6H, CH$_2$), 0.51 - 1.44 (m, 23H, alkyl H).

MS (70 eV): m/z = 620 (M$^+$).

2,7-Bis(4,4,5,5-tetramethyl-1,3,2-dioxaborolane-2-yl)-9-(2-ethylhexyl)-9-(6-(2-tetrahydropyranyloxy)hexyl)fluorene (F).

1.34 g (2.16 mmol) of compound **2** were dissolved in 20 mL absolute THF under argon and cooled to -78 °C. 3.24 mL (5.18 mmol) n-butyllithium (1.6 M in hexane) were added dropwise via a syringe while keeping the temperature at -78 °C. After stirring for 5 min 1.06 mL (5.18 mmol) 2-isopropoxy-4,4,5,5-tetramethyl-1,3,2-dioxaborolane were added. The solution was stirred and allowed to warm up over night. The reaction mixture was poured into water, the phases were separated and the aqueous phase was extracted with diethylether. The combined organic phases were washed with water, dried over Na$_2$SO$_4$ and the solvent was

evaporated. The crude product was purified by column chromatography with n-hexane/ethyl acetate 10:1 as eluent. After drying in vacuum 641 mg (0.897 mmol, 42 %) of **F** were obtained as a white solid.

^{1}H-NMR (CDCl$_3$): δ = 7.69 - 7.80 (m, 6H, fluorene H), 4.48 (t, 1H, CH), 3.70 - 3.90 (m, 1H, CH$_2$-O), 3.50 - 3.65 (m, 1H, CH$_2$-O), 3.35 - 3.50 (m, 1H, CH$_2$-O), 3.15 - 3.30 (m, 1H, CH$_2$-O), 1.98 - 2.04 (m, 4H, CH$_2$), 1.49 - 1.79 (m, 6H, CH$_2$), 0.48 - 1.42 (m, 23H, alkyl H), 1.37 (s, 24H, CH$_3$).

MS (70 eV): m/z = 715 (M$^+$).

Oligo[(9-(2-ethylhexyl)-9-(6-(2-tetrahydropyranyloxy)hexyl-fluorene-2,7-diyl)-*alt*-2,1,3-benzothiadiazole] (O2(THP)).

A schlenk flask was charged with 206 mg (0.288 mmol) of **F**, 83.0 mg (0.282 mmol) of 4,7-dibromobenzo[1,2,5]-thiadiazole (**C2**) and 26.5 mg (0.057 mmol) of **E**. 1 spatula of the phase transfer catalyst Aliquat 336, 20 mL toluene and 10 mL K$_2$CO$_3$ solution (2 M) were added. The mixture was degassed by two freeze-thaw cycles. Afterwards 1.3 mg (5.65*10^{-6} mol) of Pd(OAc)$_2$ and 5.1 mg (1.69E-5 mol) of P(*o*-tol)$_3$ were added under argon followed by another freeze-thaw cycle. The mixture was then stirred at 60 °C under argon atmosphere over night. The organic and aqueous phases were separated and the aqueous phase was washed with diethylether. The combined organic phases were washed with water, dried over Na$_2$SO$_4$ and the solvent was evaporated. The residue was dissolved in THF and the polymer was precipitated into 200 mL MeOH with 1 drop of HCl (conc.). It was kept in the freezer over night, filtered off and washed with MeOH. After drying in vacuum 184 mg (97 %) of **O2(THP)** were obtained as a bright yellow powder.

^{1}H-NMR (CDCl$_3$): δ = 7.70 - 8.11 (m, 7H, fluorene H), 7.64 (s, 0.7H, Ar H), 4.47 (t, 1H, CH), 3.70 - 3.85 (m, 1H, CH$_2$-O), 3.55 - 3.70 (m, 1H, CH$_2$-O), 3.35 - 3.50 (m, 1H, CH$_2$-O), 3.20 - 3.35 (m, 1H, CH$_2$-O), 2.00 - 2.28 (m, 4.6H, CH$_2$), 0.54 - 1.74 (m, 34H, alkyl H).

GPC (THF): M$_n$ = 4000 g/mol, M$_w$ = 4900 g/mol, PDI = 1.23 (oligofluorene calibration).

The THP-protected oligomers **O1(THP)** and **O3(THP)** were synthesized in an analogous manner.

Data for **O1(THP)**: ^{1}H-NMR (CDCl$_3$): δ = 7.68 - 7.80 (m, 2.79H, Ar H), 7.40 - 7.65 (m, 12.16H, Ar H), 7.07 - 7.20 (m, 14.7H, Ar H), 4.47 (t, 1H, CH), 3.70 - 3.85 (m, 1H, CH$_2$-O), 3.50 - 3.65 (m, 1H, CH$_2$-O), 3.35 - 3.50 (m, 1H, CH$_2$-O), 3.15 - 3.30 (m, 1H, CH$_2$-O), 2.35 (s, 4.8H, CH$_3$-TPD), 1.95 - 2.08 (m, 5.5H, CH$_2$), 1.47 - 1.76 (m, 6H, CH$_2$), 0.53 - 1.42 (m, 34H, alkyl H).

GPC (THF): M$_n$ = 3500 g/mol, M$_w$ = 4000 g/mol, PDI = 1.14 (OF calibration). yield: 240 mg, 80%.

Data for **O3(THP)**: ^{1}H-NMR (CDCl$_3$): δ = 7.59 - 7.76 (m, 6.7H, fluorene H), 7.14 - 7.32 (m, 4H, Ar H), 4.48 (t, 1H, CH), 3.70 - 3.85 (m, 1H, CH$_2$-O), 3.50 - 3.70 (m, 1H, CH$_2$-O), 3.35 - 3.50 (m, 1H, CH$_2$-O), 3.20 - 3.35 (m, 1H, CH$_2$-O), 1.97 - 2.18 (m, 4.4H, CH$_2$), 0.53 - 1.75 (m, 32H, alkyl H).

GPC (THF): M$_n$ = 5800 g/mol, M$_w$ = 7200 g/mol, PDI = 1.24 (OF calibration). yield: 200 mg, 100%.

Oligo[(9-(2-ethylhexyl)-9-(6-hydroxyhexyl-fluorene-2,7-diyl)-*alt*-2,1,3-benzothiadiazole] (O2(OH)).

170 mg of **O2(THP)** and 14 mg (0.056 mmol) of PPTS were dissolved in 50 mL of THF. 150 mL EtOH as well as 30 drops of conc. HCl were added and the mixture was heated to 80 °C under stirring over night. The polymer was precipitated into 200 mL of water with 1

drop of HCl (conc.). It was kept in the freezer over night, filtered off and washed with H_2O.

After drying in vacuum 145 mg (97 %) of **O2(OH)** were obtained as bright yellow powder.

^{1}H-NMR (CDCl$_3$): δ = 7.72 - 8.10 (m, 7H, fluorene H), 7.64 (s, 0.7H, Ar H), 3.51 (t, 2H, CH$_2$-OH), 2.00 - 2.30 (m, 4.6H, CH$_2$), 0.54 - 1.40 (m, 28H, alkyl H).

GPC (THF): M_n = 4200 g/mol, M_w = 5000 g/mol, PDI = 1.19 (OF calibration).

O1(OH) and **O3(OH)** were synthesized in an analogous way.

Data for **O1(OH)**: ^{1}H-NMR (CDCl$_3$): δ = 7.70 - 7.80 (m, 2.47H, Ar H), 7.45 − 7.62 (m, 10.88H, Ar H), 7.07 − 7.22 (m, 12.68H, Ar H), 3.48 (t, 2H, CH$_2$-OH), 2.35 (s, 4.4H, CH$_3$-TPD), 1.95 - 2.10 (m, 4.90H, CH$_2$), 1.05 - 1.20 (m, 8H, CH$_2$), 0.50 − 0.95 (m, 42H, alkyl H).

GPC (THF): M_n = 3500 g/mol, M_w = 3900 g/mol, PDI = 1.11 (OF calibration). yield: 200 mg, 90%.

Data for **O3(OH)**: ^{1}H-NMR (CDCl$_3$): δ = 7.60 - 7.72 (m, 6.7H, fluorene H), 7.13 - 7.32 (m, 4H, Ar H), 3.51 (t, 2H, CH$_2$-OH), 1.98 - 2.15 (m, 4.4H, CH$_2$), 0.55 - 1.36 (m, 26H, alkyl H).

GPC (THF): M_n = 5900 g/mol, M_w = 7000 g/mol, PDI = 1.19 (OF calibrarion). yield: 138 mg, 84%.

Oligo[(9-(2-ethylhexyl)- 9-(6-acryloyloxy)-hexyl)- fluorene-2,7-diyl)-*alt*-2,1,3-benzothiadiazole] (O2).

A double-necked flask was charged with 127 mg of **O2(OH)**, a small amount of 2,6-di-*tert*-butyl-4-methylphenol (BHT) and 80 mL of CH$_2$Cl$_2$. To remove dissolved oxygen argon was bubbled through the solution for 30 min. 0.02 mL (0.246 mmol) of acryloyl chloride and 0.03 mL (0.246 mmol) of *N,N*-dimethylaniline were added and the mixture was heated to 50 °C while stirring. After 5h another 0.02 mL (0.246 mmol) of acryloyl chloride were added. The mixture was heated to 50°C and stirred over night. The reaction mixture was poured into water and stirred for 5 min. The organic and aqueous phases were separated and the aqueous

phase was washed with diethylether. The combined organic phases were washed with water, dried over Na_2SO_4 and the solvent was evaporated. The residue was dissolved in THF and the polymer was precipitated into 200 mL of MeOH with 1 drop of HCl (conc.). It was kept in the freezer over night, filtered off and washed with MeOH. After drying in vacuum 107 mg (78 %) of **O2** were obtained as a bright yellow powder.

^{1}H-NMR (CDCl$_3$): δ = 7.73 - 8.10 (m, 7H, fluorene H), 7.64 (s, 0.7H, Ar H), 6.32 (d, 1H, =CH$_2$), 6.04 (dd, 1H, =CH), 5.74 (d, 1H, =CH$_2$), 4.03 (t, 2H, CH$_2$-O), 2.03 - 2.30 (m, 4.6H, CH$_2$), 0.55 - 1.51 (m, 28H, alkyl H).

GPC (THF): M_n = 4200 g/mol, M_w = 5100 g/mol, PDI = 1.21 (OF calibration).

The acrylate-oligomer **O1** was synthesized in an analogous manner. For **O3** the esterification with acryloyl chloride was performed three times to get 100% conversion.

Data for **O1**: ^{1}H-NMR (CDCl$_3$): δ = 7.45 - 7.80 (m, 16H, Ar H), 7.09 - 7.20 (m, 14.6H, Ar H), 6.28 – 6.34 (d, 1H, =CH$_2$), 5.98 – 6.10 (dd, 1H, =CH), 5.71 – 5.75 (d, 1H =CH$_2$), 3.99 (t, 2.21H, CH$_2$-O), 2.35 (s, 4.8H, CH$_3$-TPD), 1.95 - 2.10 (m, 5.5H, CH$_2$), 1.05 - 1.15 (m, 4.8H, CH$_2$), 0.51 - 1.00 (m, 32H, alkyl H). yield: 190 mg, 90%.

GPC (THF): M_n = 3600 g/mol, M_w = 4000 g/mol, PDI = 1.11 (OF calibration).

Data for **O3**: ^{1}H-NMR (CDCl$_3$): δ = 7.55 - 7.80 (m, 9.7H, fluorene H), 7.28 - 7.40 (m, 3.55H, Ar H), 6.28 – 6.37 (d, 1H, =CH$_2$), 5.95 – 6.12 (dd, 1H, =CH), 5.70 – 5.80 (d, 1H, =CH$_2$), 4.03 (t, 2.7H, CH$_2$-O), 2.05 – 2.10 (m, 10.8H, CH$_2$), 1.05 - 1.20 (m, 8.35H, alkyl H), 0.5 - 1.0 (m, 38.3H, alkyl H).

GPC (THF): M_n = 6150 g/mol, M_w = 8400 g/mol, PDI = 1.41 (OF calibration). yield: 80 mg, 56%.

Results and Discussion

Synthesis of the monomers and oligomers

Scheme 1 shows the overall reaction pathway to acrylate functionalized oligomers **O1-3** via Suzuki coupling. The Suzuki reaction is a cross coupling between halides and borolanes, which ensures an alternating sequence of monomers. Here the fluorene **F** with two borolane units and the dibromo compounds **C1-3** are coupled. The bisborolane monomer **F** is synthesized in a three step synthesis as depicted in Scheme 2. Here the first step is the asymmetric alkylation of the commercially available 2,7-dibromofluorene in 9-position with 2-ethylhexylbromide and 2-(6-bromohexyloxy)-tetrahydro-2*H*-pyran. A 1:1 mixture of the alkyl bromides is applied. Due to statistics three different products are formed the asymmetric one being the desired product. The polarity and solubility of the three products is very similar and their separation becomes very difficult. Therefore the THP-protecting groups are removed and the corresponding hydroxy fluorenes are formed. Now a separation of the three different products with none, one or two hydroxy groups is possible by column chromatography and the asymmetrically substituted compound **1** is obtained with 22% yield.[14] The hydroxy group of **1** is then protected by a THP-group because the Suzuki coupling does not tolerate hydroxy functionalities.[18] The THP-protected compound **2** is obtained in 52% yield. The last step is the formation of the bisborolane fluorene **F** with 2-isopropoxy-4,4,5,5-tetramethyl-1,3,2-dioxaborolane. Now the monomer **F** can be applied in the Suzuki reaction (Scheme 1). The syntheses of **E**[19] and **C1**[17] are described elsewhere. **C2** and **C3** are commercially available. We know, that low molecular weights lead to low glass transition temperatures as we have shown previously.[20] Low glass transition temperatures allow low processing temperatures during photolithography and photo degradation upon illumination is prevented.[14] Therefore we added a monobromo-fluorene endcapper **E**, which limits the molecular weights by
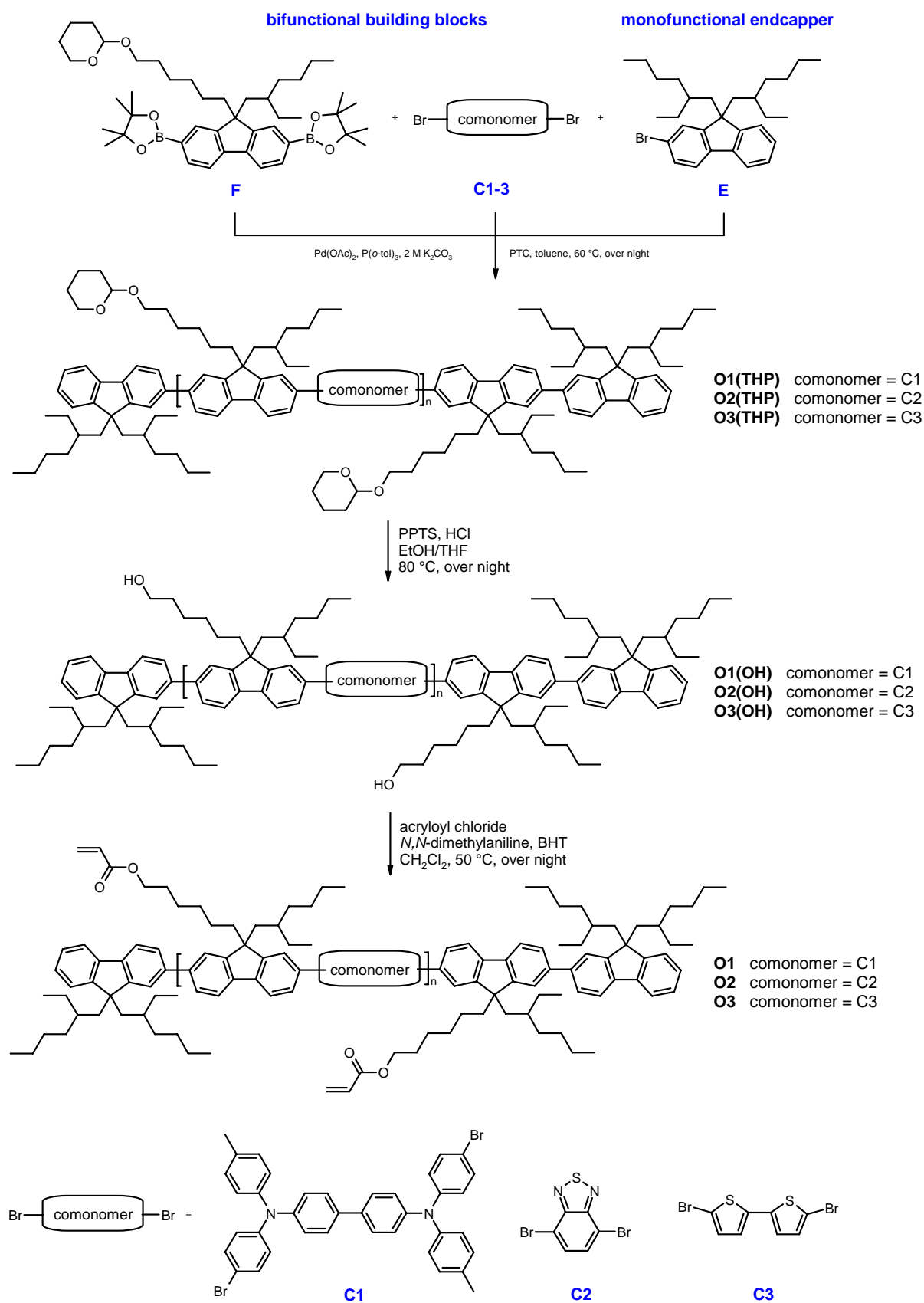
Scheme 1. *Overall reaction pathway to acrylate functionalized oligomers* **O1-3**.

terminating the chain growth in a controlled way. In addition residual bromine endgroups are avoided.[14] The ratio of bifunctional compounds to endcapper now determines the molecular weight and a ratio **F:E** of **5:1** was chosen for **C2-3** and **3:1** for **C1** due to the high molecular weight of **C1**. The ratio of the bisborolane **F** to the comonomers **C1-3** was 1:1. The Suzuki coupling was performed with palladium acetate at 60°C and the THP-protected oligomers **O1-3(THP)** were formed, which were characterized by NMR and GPC (see experimental section for details). The next step is the cleavage of the THP-groups using p-toluenesulfonic acid pyridinium salt (PPTS) and HCl. The THP-groups were quantitatively removed under mild conditions and the hydroxy oligomers **O1-3(OH)** were formed. The last step to acrylate oligomers **O1-3** was the esterification with acryloyl chloride. The oligomers **O1-2(OH)** were readily soluble in CH_2Cl_2 and the esterification proceeded well at 40°C over night with a conversion of 100%. The polymeranalogous esterification became difficult for **O3(OH)** due to its insufficient solubility. The resulting acrylate oligomers **O1-3** were characterized with NMR, GPC and Maldi-ToF and the detailed data are given in Table 1. The molecular weights range from 3600 – 6150 g/mol (GPC, oligofluorene calibration).

Table 1. *Molecular weights, degrees of polymerization and thermal analyses of* **O1-3**.

	ratio F:E	M_n [g·mol^{-1}][b]	M_w [g·mol^{-1}][b]	n (GPC)[c]	T_g [°C][d]	$T_{d,onset}$ [°C][e]
O1	3:1[a]	3600	4000	3.0	-	-
O2	5:1	4200	5100	5.3	63	340
O3	5:1	6150	8700	9.0	53	300

[a] A lower ratio F:E was chosen due to the high molecular weight of C1. [b] Determined with GPC, oligofluorene calibration. [c] Estimated from GPC values: $M_n(GPC)=(M_{FA}+M_C) \cdot n + M_{FA} + 2 \cdot M_E$; M= molecular weights of the monomers F_A, C and E; n corresponds to Scheme 1 [d] Determined with DSC upon heating with a rate of 40 K·min^{-1}. [e] Onset of decomposition determined by thermogravimetry with a heating rate of 10 K·min^{-1} under N_2.
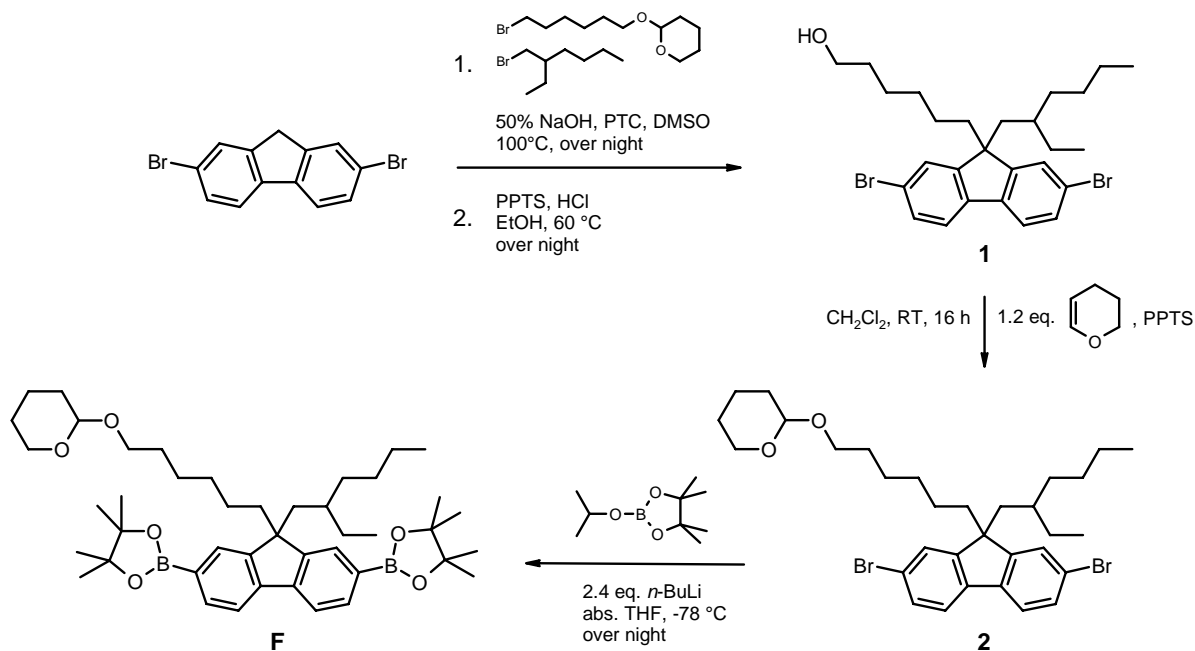
Scheme 2. *Three-step reaction to the THP-protected bisborolane fluorene F.*

To get a deeper insight into the chain compositions we performed Maldi-ToF experiments and the Maldi-ToF spectrum of **O2** is shown in Figure 1. The magnification between 1500 and 4000 g/mol in Figure 1 *right* shows the assignment of the peaks in detail. In general we found three different series of signals. The first series named **a** in Figure 1 consists of the desired oligomers with two endcapper molecules **E** (named E–[F_A–C2]$_n$–F_A–E with E=endcapper, F_A=fluorene acrylate unit, C2=comonomer 2 unit, n=degree of polymerization). The second series **b** can be assigned to mono-endcapped species (named E–[F_A–C2]$_n$–F_A) and in the third series **c** the oligomers do not carry endcapper molecules at all (named [F_A–C2]$_n$–F_A). Here we note that the signals of series **b** have the highest intensity and those of series **c** the lowest. We attribute this to a loss of borolane groups during Suzuki coupling, which has been observed and described before.[21] Nevertheless borolane or bromine endgroups were not found in the Maldi-ToF.
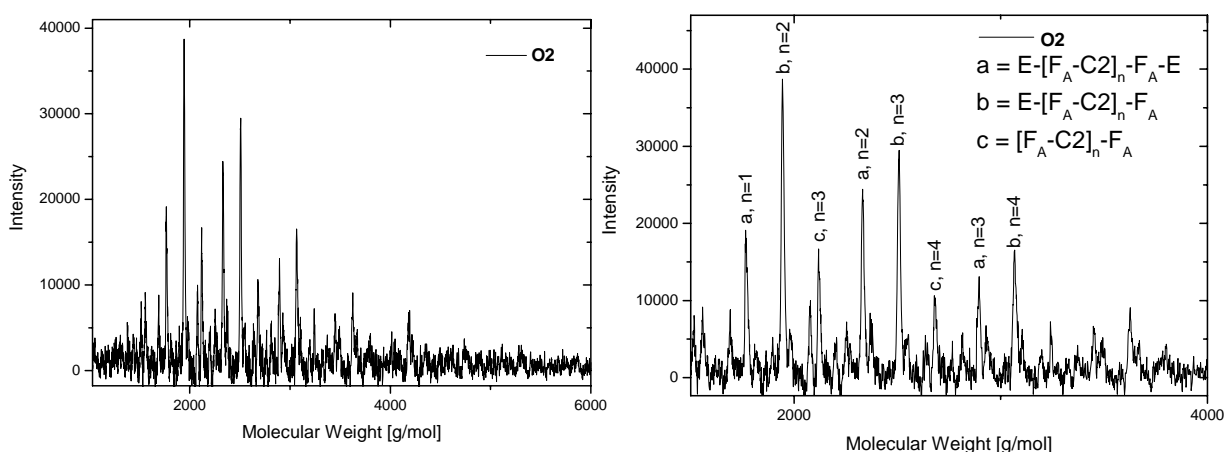
Figure 1. *Left: Maldi-ToF spectrum of **O2**. Right: Magnification and assignment of the signals between 1500 and 4000 g/mol. The spectrum was recorded in the linear mode using POPOP as matrix. The assignment of the peaks is named as follows: E=Endcapper, F_A=Fluorene acrylate unit, C2=C2 monomer, n=degree of polymerization.*

Thermal Properties

All oligomers were characterized by both differential scanning calorimetry (DSC) and thermogravimetric analysis (TGA) and the results are summarized in Table 1. The decomposition temperatures were all in the same range of around 300 - 340°C. None of the oligomers showed no melting or recrystallization in the DSC. The glass transition temperatures (T_gs) were 63°C for **O2** and 53°C for **O3.** In the case of **O1** a glass transition was not detectable. The transition enthalpies were very small and only detectable using a heating rate of 40 K·min^{-1}. The T_gs were determined upon heating and due to the high heating rate the values are expected to be slightly overestimated. For an efficient photopolymerization the acrylate units have to be mobile. Thus crosslinking experiments with organic semiconductors are usually carried out at elevated temperatures to provide an appropriate mobility of reactive groups. Here the low T_gs of **O2** and **O3** allow low processing temperatures, which helps to prevent degradation during photocrosslinking.

Optical Properties

The optical properties of **O1-3** were determined in chloroform solutions and thin films (see Figure 2). The details are given in Table 2. For the TPD containing oligomer **O1** similar spectra were obtained in solution and thin films. In solution the absorption maximum is 380 nm and excitation at 380 nm leads to an emission maximum in the blue at 435 nm. In thin films the absorption maximum is 384 nm and the emission maximum is 442 nm. In the case of **O2** with benzothiadiazole units the absorption spectra exhibit two maxima at 320 nm and 446 nm (CHCl$_3$ solution) and 335 nm and 455 nm (film) respectively. The fluorescence spectra are rather simple. For the CHCl$_3$ solution excitations at 320 and 446 nm lead to a yellow-green emission at 529 nm. In thin films excitation both at 335 and 455 nm lead to a yellow emission maximum of 540 nm. For **O3** the solution spectra differ from the film spectra. In solution the absorption maximum is 446 nm and excitation at 446 nm leads to a green emission at 525 nm. The absorption maximum in thin films is 451 nm and the PL maximum is 565 nm. We attribute this 40 nm red-shift of the PL film spectrum to well known packing phenomena for thiophene compounds.[22] Thus the film shows red fluorescence, whereas the solution appears green upon excitation (see Figure 2 e,f).

*Table 2. Optical properties of chloroform solutions and thin films of **O1-3.***

	solution		films	
	absorption λ_{max} [nm]	PL $\lambda_{em.}$ [nm]	absorption λ_{max} [nm]	PL $\lambda_{em.}$ [nm]
O1	380	435 (380)[a]	384	442 (384)[a]
O2	320, 446	529 (320)[a] 529 (446)[a]	335, 455	540 (335)[a] 540 (455)[a]
O3	446	525 (446)[a]	451	565 (451)[a]

[a] The values in brackets give the corresponding excitation wavelength in nm.

The HOMO levels were measured by photoelectron spectrometry (Riken Keiki AC-2) from thin films. From the optical bandgaps, determined as intersection of the UV/VIS and photoluminescence spectra, the LUMO values were calculated. All data are listed in Table 3. The oligomers **O1** and **O3** with electron donating comonomes have HOMO energies of 5.25 eV and 5.46 eV respectively. In comparison to a fluorene-only oligomer, whose data are also displayed in *Table 3*, the HOMO values are increased. For the oligomer **O2** with an electron withdrawing benzothiadiazole unit instead we find a slight decrease of the HOMO level from 5.70 to 5.80 eV and a LUMO energy level of 3.27 eV, which is 0.57 eV lower than for a fluorene-only oligomer. Both **O2** and **O3** have smaller bandgaps (2.53 and 2.39 eV respectively) and decreased LUMO energy values compared to a pure fluorene oligomer.
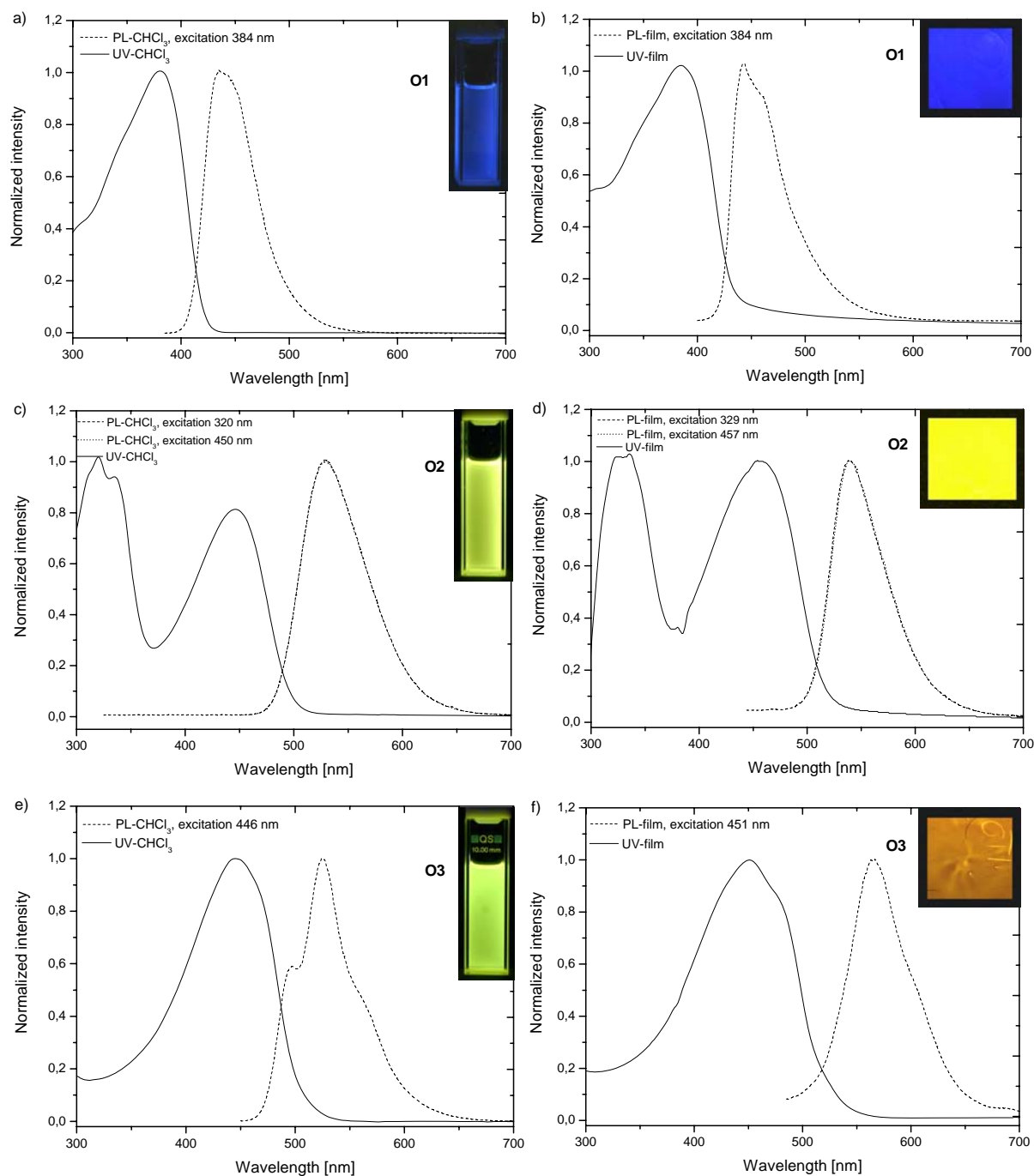
*Figure 2. Normalized absorption and emission spectra of **O1-3** (a-f) in chloroform solutions and as thin films. The photographical insets show the chloroform solutions and thin films upon excitation at 366 nm.*

Table 3. *Energy levels and optical bandgaps of O1-3.*

	HOMO [eV][a]	LUMO [eV][b]	optical band gap [eV][c]
O1	5.25	2.30	2.96
O2	5.80	3.27	2.53
O3	5.46	3.07	2.39
Oligofluorene[d]	5.70	2.73	2.97

[a] Measured with photoelectron spectrometry (Riken Keiki AC-2). [b] Calculated from the HOMO and optical bandgap values. [c] Determined as intersection of absorption and emission spectra (film spectra). [d] Oligofluorene with an average degree of polymerization of 13 from ref. [14].

Figure 3 shows a graphical summary of the energy levels of both, alternating and random oligomers (from ref [17]). The HOMO and LUMO values of the TPD and benzothiadiazole containing oligomers **O1** and **O2** are identical and for the bithiophene cooligomer **O3** we find a small difference. This is due to packing phenomena described for bithiophene compounds[22], which are strongly governed by the chain compositions (random or alternating).
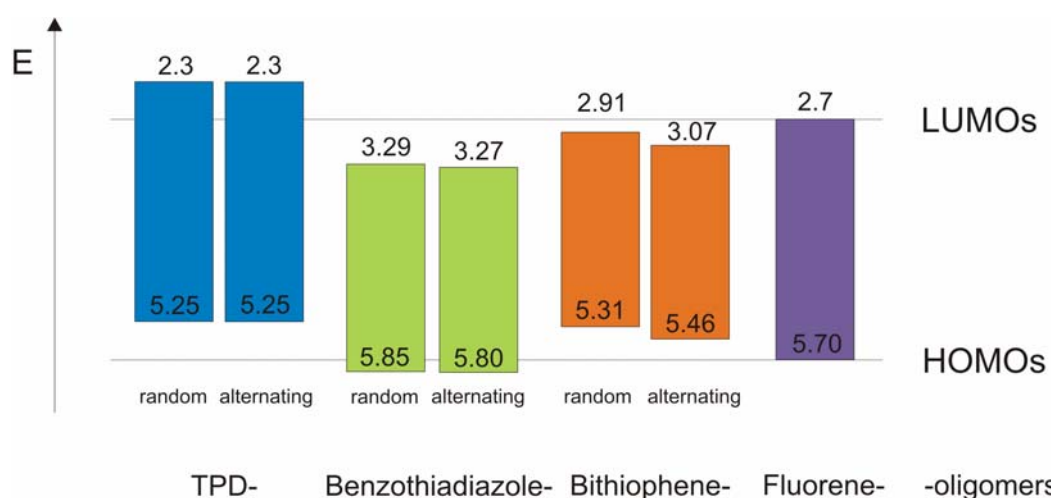
Figure 3. *Energy levels of the oligomers O1-3 and their randomly linked counterparts from ref. [17]. Additionally the energy levels of a pure fluorene oligomer with a similar molecular weight are displayed on the right (from ref. [14]). The energy levels were measured with photoelectron spectrometry (Riken Keiki AC-2) from thin films.*

Photopatterning

With regard to the use of **O1-3** as patternable materials the photocrosslinking conditions were investigated. We optimized the photocrosslinking and the development steps particularly to maximize the lateral resolution.

We followed the patterning procedure as described and displayed in refs [14] and [17]. The first processing step is the spin coating of the oligomer onto cleaned silicon wafers. For this purpose solutions of the oligomers in toluene with concentrations of 4wt.-% were prepared. 1wt.-% (refers to the amount of oligomer) of photoinitiator Irgacure 784 was added. The spin coating was performed at 1000 rpm for 60 s. After that the films were dried at 115°C for one minute under inert atmosphere. The thickness of all films was in the range of 100 nm. The second step is the UV-exposure. The samples were put in a vacuum chamber, annealed at a certain temperature in the chamber and then irradiated using a Hg-Xe lamp while keeping the temperature. The last lithographic step is the development of the patterns, which is achieved by dissolving the non-irradiated areas in THF for 30 s.

During irradiation we used a filter as described in ref [17]. The filter UG5 (Schott) transmits light between 230 and 400 nm and blocks shorter and longer wavelengths. Thus we irradiate in the absorption maximum of the photoinitiator Irgacure 784 at 250 nm. We find a very fast polymerization of the acrylate units. An irradiation for just 2-5 minutes was sufficient enough to form sub-micron sized fluorescent patterns. Photooxidation was not observed. During the whole process the fluorescence colors of the oligomers were preserved, which was checked by fluorescence microscopy.

The quality of the patterns was investigated with fluorescence microscopy and scanning electron microscopy (SEM, see Figure 4). The fluorescence microscope is equipped with different filter systems, which allow a selective excitation and detection of the fluorescence of the samples. Upon excitation of the cooligomers in their absorption maxima strongly

fluorescent stripes are observed. That indicates the preservation of the chemical structure and thus the opto-electronic properties of the oligomers during irradiation. The silicon wafer appears black, which indicates a complete removal of the oligomer in the non-exposed areas. For **O2** sub-micron sized structures of 600 nm were obtained, which can be seen in both, fluorescence microscopy and SEM. A magnification of the SEM image (Figure 4 *right*) shows that the 600 nm stripes are well resolved.
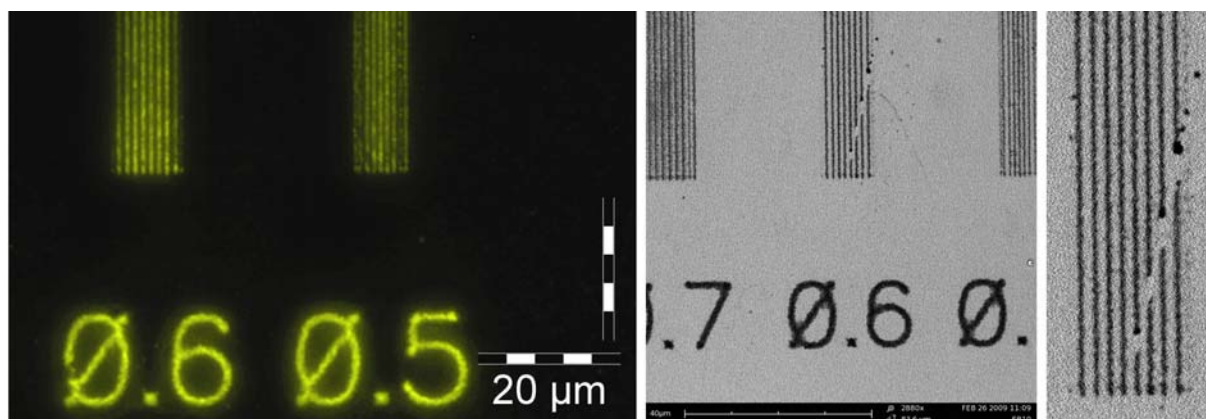
Figure 4. *Sub-micron scale patterns of **O2** observed under a fluorescence microscope (left) and SEM (right). The image on the far right shows a magnification of the 600 nm stripes of the SEM picture. Upon crosslinking the filter UG5 was used and the detailed conditions were: annealing at 50°C for 3 min, exposure at 60°C for 5.5 min. The numbers next to the stripes represent their width in μm.*

Conclusion

In this publication we have presented the synthesis of alternating photocrosslinkable cooligomers via Suzuki coupling. Since the Suzuki reaction does not tolerate acrylate functionalities fluorene monomers carrying OH-groups were synthesized. During polymerization the OH-groups had to be protected by THP groups. After the Suzuki coupling polymeranalogous conversions were performed, the removal of the THP group and the esterification with acryloyl chloride. The molecular weights of the oligomers were limited using a monofunctionalized endcapper. We analyzed the cooligomers with NMR, GPC and

Maldi-ToF, which gives a detailed insight into the chain compositions. Three different series of oligomers are present in the product, carrying either two, one or no endcapping molecules. The thermal properties were investigated and the oligomers show low T_gs of 53-63°C and are thermally stable up to ~300°C. The optical properties were analyzed in thin films and solutions. We obtained a blue emitting oligomer in the case of the TPD comonomer, a yellow fluorescent material for the benzothiadiazole and a red (film) and yellow-green (solution) emitting material for the bithiophene. The energy levels were determined by photoelectron spectrometry and are very similar to those of randomly linked oligomers. The photocrosslinking behavior was studied and under optimized conditions a lateral resolution of 600 nm was obtained.

In a preceding paper we have described the preparation of photocrosslinkable fluorene cooligomers by Yamamoto coupling. Comparing both methods we conclude, that for electron donating monomers like TPD or bithiophene the Yamamoto coupling is easier to perform, since it tolerates acrylate groups during polymerization. Suzuki cross coupling is only necessary if a strictly alternating monomer sequence is needed.

The Yamamoto coupling is more difficult if electron withdrawing comonomers like benzothiadiazole are involved. In this case the Suzuki reaction ensures an alternating incorporation of the benzothiadiazole units in the oligomer. Due to a good solubility of the benzothiadiazole oligomers the polymeranalogous conversions after the coupling are performed without any problems and lead to almost complete conversion.

In principle both, Yamamoto and Suzuki coupling, are suited for the preparation of acrylate functionalized cooligomers. For electron donating comonomers the Yamamoto reaction and for electron withdrawing comonomers the Suzuki reaction is preferred.

Acknowledgement

References

1   S. Holdcroft, *Adv. Mater.* **2001**, *13*, 1753.

2   J. Huang, R. Xia, Y. Kim, X. Wang, J. Dane, O. Hofmann, A. Mosley, A. J. de Mello, J. C. de Mello, D. D. C. Bradley, *J. Mater. Chem.* **2007,** *17*, 1043.

3   C. D. Müller, A. Falcou, N. Reckefuss, M. Rojahn, V. Wiederhirn, P. Rudati, H. Frohne, O. Nyken, H. Becker, K. Meerholz, *Nature* **2003**, *421*, 829.

4   M. C. Gather, A. Köhnen, A. Falcou, H. Becker, K. Meerholz, *Adv. Func. Mater.* **2007**, *17*, 191.

5   E. Peeters, J. Lub, J. A. M. Steenbakkers, D. J. Broer, *Adv. Mater.* **2006**, *18*, 2412.

6   G. Wu, C. Yang, B. Fan, B. Zang, X. Chen, Y. Li, *J. Appl. Polym. Sci.* **2006**, *100*, 2336.

7   R. Penterman, S. I. Klink, H. de Koning, G. Nisato, D. J. Broer, *Nature* **2002**, *417*, 55.

8   Y.-H. Yao, L.-R. Kung, S.-W. Chang, C.-S. Hsu, *Liq. Cryst.* **2006**, *33*, 33.

9   M. P. Aldred, A. J. Eastwood, S. M. Kelly, P. Vlachos, *Chem. Mater.* **2004**, *16*, 4928.

10   M. Jandke, D. Hanft, P. Strohriegl, K. Whitehead, M. Grell, D. D. C. Bradley, *Proceedings of SPIE* **2001**, *4105*, 338.

11   D. J. Broer, J. Boven, G. N. Mol, G. Challa *Makromol. Chem.* **1989**, *190*, 2255.

12   D. J. Broer, J. Lub, G. N. Mol *Nature* **1995**, *378*, 467.

13   E. Scheler, I. Bauer, P. Strohriegl, *Macromol. Symp.* **2007**, *254*, 203.

14   E. Scheler, P. Strohriegl, *J. Mater. Chem.* **2009**, *19*, 3207.

15   M. Redecker, D. D. C. Bradley, M. Inbasekaran, W. Wu, E. P. Woo, *Adv. Mater.* **1999**, *11*, 241.

16   H. Sirringhaus, R. J. Wilson, R. H. Friend, M. Inbasekaran, W. Wu, E. P. Woo, M. Grell, D. D. C. Bradley, *Appl. Phys. Lett.* **2000**, *77*, 406.

17   E. Scheler, P. Strohriegl, *Chem. Mater.* submitted.

18   A. D. Schlüter, *J. Polym. Sci. Part A: Polym. Chem.* **2001**, *39*, 1533.

19   H. Thiem, M. M. Rothmann, P. Strohriegl, *Designed Monomers and Polymers* **2005**, *8*, 619.

20   E. Scheler, P. Strohriegl, *Liq. Cryst.* **2007**, *34*, 667.

21   H. Thiem, M. Jandke, D. Hanft, P. Strohriegl, *Macromol. Chem. Phys.* **2006**, *207*, 370.

22   T. Yasuda, K. Namekawa, T. Iijima, T. Yamamoto, *Polymer* **2007**, *48*, 4375.

11 Appendix:

Synthesis of oligofluorenes by endcapping

Esther Scheler, Peter Strohriegl

Macromolecular Chemistry I, University of Bayreuth, 95440 Bayreuth, Germany

peter.strohriegl@uni-bayreuth.de
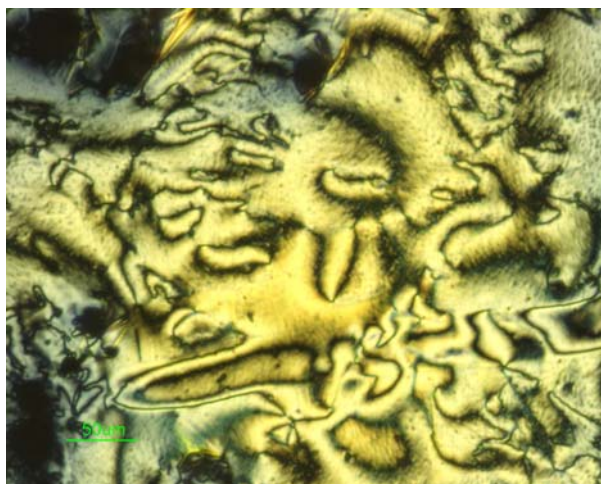
Abstract

An efficient 1-step synthesis of 9,9-di(2-ethylhexyl)-2,7-fluorene oligomers via endcapping reaction is reported. Controlled endcapping demands a full conversion of functional groups and thus the Yamamoto reaction was chosen as aryl-aryl coupling method. SEC analysis showed that the endcapping is complete. The molecular weights were adjusted in the range from 1300 g/mol to 3800 g/mol by different amounts of endcapper. The mixtures exhibit broad mesophases and the transition temperatures strongly increase with the molecular weight. In the series of oligomers reported here, clearing temperatures between 57°C and more than 360°C could be realised.

Keywords

Introduction

Among conjugated polymers known today poly(9,9-dialkylfluorenes) have achieved much attention as efficient blue light emitting materials [1, 2]. Besides the strong blue emission, polyfluorenes exhibit a thermotropic liquid crystalline phase which allows a facile orientation of the polymer into large monodomains [3]. Such a parallel orientation of the polyfluorene chains directly leads to the emission of polarised light in organic light emitting diodes (OLEDs) [4, 5, 6]. In addition to polyfluorene homopolymers the orientation of polyfluorene copolymers like poly(9,9-dioctylfluorene-alt-bithiophene) (F8T2) has been carefully investigated and used to increase the carrier mobility in organic field effect transistors (OFETs) [7].

One major problem concerning the orientation of polyfluorenes are the high temperatures necessary for the orientation in the LC phase. Poly[9,9-di(2-ethylhexyl)fluorene] (PF2/6) exhibits a nematic phase only at temperatures above 169°C. The clearing temperature (T_c) can not be detected due to the decomposition of the material [2]. Thus orientation experiments at such high temperatures have to be carried out under carefully controlled inert conditions since the polyfluorenes are sensitive towards oxidation to the corresponding fluorenones in 9-position, which leads to an undesirable green shift of the fluorescence [2, 8, 9, 10]. It was proven by several experiments that this green shift results from intra- or intermolecular energy transfers from the fluorene to the fluorenone moieties [11].

In addition to high molecular weight polyfluorenes low molecular mass fluorene model compounds with up to 12 fluorene units have been described [12, 13, 14]. In a series of fluorene model compounds with 2-ethylhexyl substituents the glass transition temperatures (T_g) rise from 22°C for the tetramer to 42°C for the heptamer [15]. Above T_g a nematic phase is observed for all model compounds from the tetramer on. The clearing temperatures rise from 64°C for the tetramer to 246°C for the heptamer. Cyclic voltammetry was used to

investigate the electrochemical properties of this homologous series and it was demonstrated that an increasing number of fluorene units leads to an increase of reversibly accessible oxidation states [16]. Furthermore the optical properties of the model compounds were studied in detail and extrapolated to an ideal polymer chain [17, 18]. A lot of insight into the physical properties of fluorene polymers comes from the investigation of a homologous series of model compounds and it could be shown that the nematic phase of the tetramer, pentamer and hexamer are below 200°C and allow a facile orientation in the LC- phase without the risk of oxidation reactions. Nevertheless the synthesis of these monodisperse compounds is a time consuming procedure, which comprises a large number of synthetic steps [15].

For the limitation of the molecular weight of a growing polymer chain endcapping with a monofunctional monomer is a well known method. As a consequence well defined endgroups can be introduced and the number of ill defined groups at the chain end (e.g. bromine) can be reduced drastically.

PF2/6 endcapped with triphenylamine moieties was already described in literature [19]. The molecular weight of PF2/6 varied from 122000 g/mol to 12000 g/mol by increasing amounts of triphenylamine endcapper. The liquid crystalline phases of the polyfluorene are not altered by the endcapper in this molecular weight range [19].

Another study deals with the influence of the molecular weight of PF2/6 on its thermotropic alignment [20, 21]. Low molecular weight materials with $M_n< 10000$ g/mol were found to exhibit only a nematic mesophase whereas high molecular weight compounds ($M_n> 10000$ g/mol) showed nematic as well as hexagonal phases. These two LC phases were investigated by x-ray scattering and the orientation of the different PF2/6s on polyimide was described in detail.

In this paper we describe the synthesis and characterisation of polydisperse oligo[9,9-di(2-ethylhexyl)fluorene-2,7-diyl]s in the low molecular weight range between 1300 and

3800 g/mol. The Yamamoto reaction was chosen as aryl-aryl coupling method. By this simple synthetic strategy large amounts of well defined oligomers can be made in a single step. The resulting oligomers exhibit nematic phases at moderate temperature, which allows a controlled alignment without decomposition processes taking place. Both T_g and T_c were determined and compared with monodisperse model compounds from literature [15].

Results and Discussion

Synthesis

The polydisperse oligofluorenes **3a-e** were obtained in a 1-step reaction shown in Scheme 1. The monomers **1** and **2** were synthesised by alkylation of 2,7-dibromofluorene and 2-bromofluorene respectively as described in literature [22]. The Yamamoto reaction of the bifunctional monomer **1** and the monofunctional endcapper **2** leads to the oligomeric mixtures **3a-e** with different molecular weights. The coupling was performed using Ni(COD)$_2$ and 2,2`-bipyridyl in a mixture of dry DMF and dry toluene [23]. The chemical structure was validated by ^{1}H NMR and ^{13}C NMR spectroscopy.
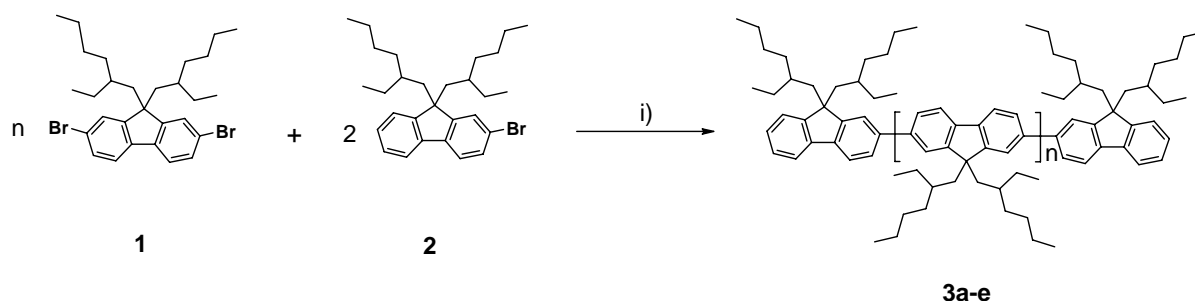
Scheme 1. *Synthesis of oligo[9,9-di(2-ethylhexyl)fluorene-2,7-diyl] via endcapping reaction; (i) dry DMF/dry toluene/2,2`-bipyridyl/COD/Ni(COD)$_2$*

The molecular weights of the fluorene oligomers **3a-e** were determined by SEC and are shown in Table 1.

**Table 1.** Molecular weights and degrees of polymerisation of **3a-e.**

	ratio **1/2**	$M_n(SEC)^a$ [g/mol]	$M_w(SEC)^a$ [g/mol]	$P_n(SEC)$
3a	5:1	3800	4900	9.7
3b	2:1	2500	3100	6.4
3c	3:2	2000	2450	5.0
3d	1:1	1500	2000	4.0
3e	1:2	1300	1500	3.3

^{a} Oligofluorene calibration (explanation see text).

The number average molecular weight of the oligomers decreases from 3800 g/mol to 1300 g/mol with increasing amounts of endcapper. The molecular weight distributions of **3a-e** can be seen in Figure 1 and for a simplified assignment the SEC scan of an independently synthesised trimer (n=1) is shown in addition. The peak next to the trimer at M_n=780 g/mol can be assigned to the dimer (n=0), the signal at 1500 g/mol corresponds to the tetramer (n=2) and higher molecular weight oligomers can be assigned up to the nonamer (n=7). With an increasing amount of bifunctional monomer **1** the intensity of high molecular weight part increases and in mixture **3a** the polymeric part becomes dominant. Each SEC scan shows only one homologous series of oligomers, which indicates that no side products were formed in the Yamamoto coupling.

For the molecular weight calibration the SEC scans depicted in Figure 1 have been used. From MALDI-TOF measurements we know that the peaks assigned in Figure 1 are the oligomers in which both sides are endcapped. Since the exact molecular weights of these oligomers are known, we set up a calibration curve for the oligofluorenes (Figure 2). From

this plot it becomes evident that for the molecular weights between 700 and 2000 g/mol the results from PS (polystyrene) and oligofluorene calibration are similar. For molecular weights above 2000 g/mol the real molecular weights are lower than calculated from polystyrene calibration. For the highest molecular weight oligomer **3a** with a M_n of 3800 g/mol the polystyrene calibration would give an overestimation of 1200 g/mol compared to the oligofluorene calibration. This is in accordance with literature results [2]. They showed in a combined SEC/LS (light scattering) experiment that in the case of high molecular weight polyfluorene the molecular weights are overestimated by a factor of 2.7 if a polystyrene calibration is used [24]. This is explained by the semi-rigid character of the polyfluorene backbone. In the low molecular weight region below 2000 g/mol the polystyrene chain cannot be described as random coil which explains that the molecular weights determined by oligofluorene and polystyrene calibration are similar.
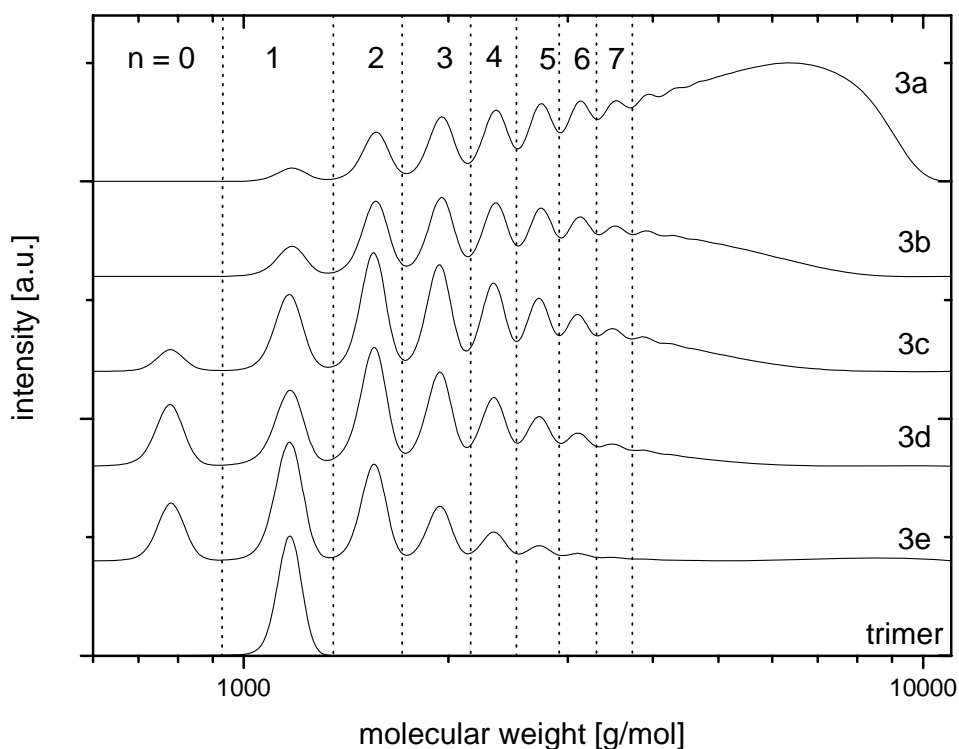
Figure 1. *SEC scans of the oligomers **3a-e** (oligofluorene calibration) and an independently synthesised trimer; n refers to Scheme 1.*
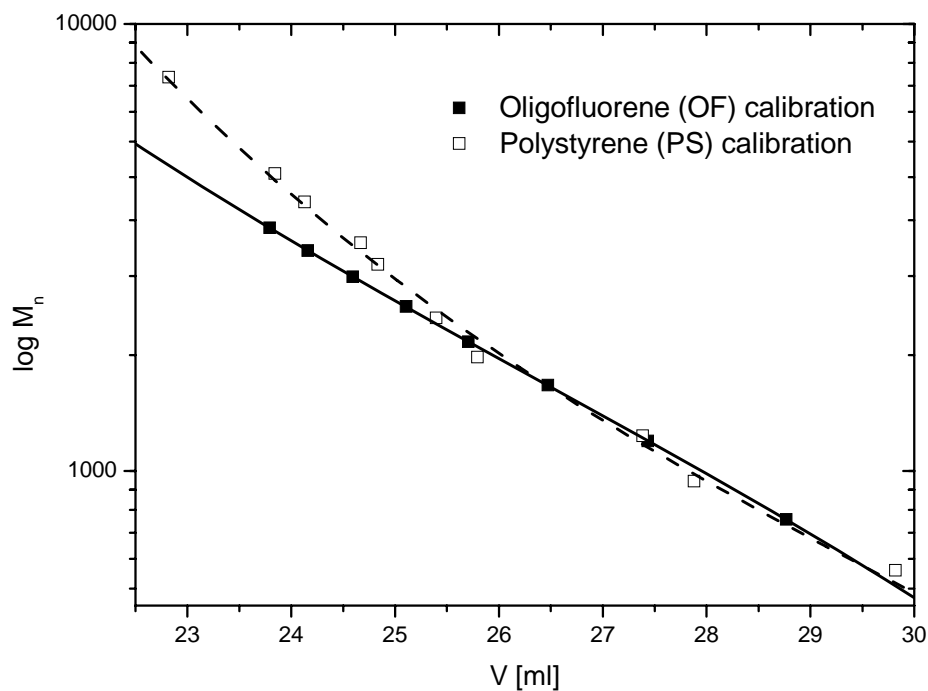
Figure 2. *Oligofluorene and polystyrene calibration curves; the lines correspond to the 3rd order polynomial fits of the experimental data points.*

Optical Properties

Figure 3 shows the UV-vis spectra of the fluorene oligomers. The data are given in Table 2.

With an increasing molecular weight the absorption maximum λ_{max} shifts to higher

wavelengths from **3e** to **3a**. For comparison the absorption spectrum of high molecular weight

poly[9,9-di(2-ethylhexyl)-2,7-fluorene-diyl] is also shown in Figure 3.
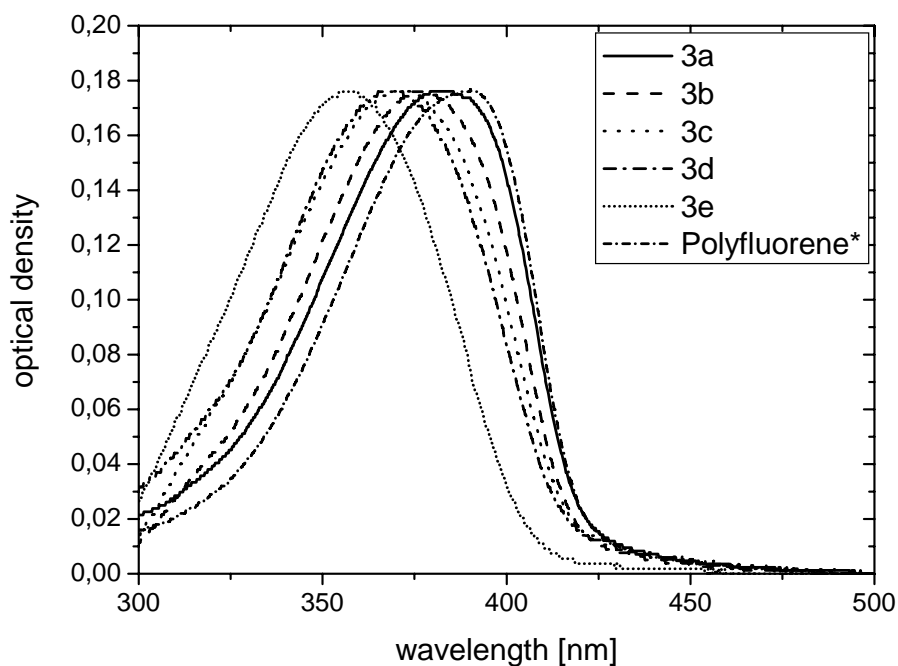
Figure 3. *Normalised UV-vis spectra of thin films of **3a-e** and poly[9,9-di(2-ethylhexyl)-2,7-fluorene-diyl), *M_n=20000, M_w=48000, synthesised via Yamamoto coupling.*

Table 2. *Absorption maxima, band edges and optical band gaps ΔE of **3a-e**.*

	λ_{max} [nm]	λ_{AE} [nm]	ΔE [eV]
3e	357	406	3.05
3d	368	416	2.98
3c	372	418	2.97
3b	377	418	2.97
3a	382	420	2.95
Polyfluorene*	389	421	2.94

*M_n=20000 g/mol, M_w=48000 g/mol.

From the absorption edge the optical band gap can be calculated (Table 2). The absorption

edges increase with an increasing molecular weight from 406 to 421 nm. This corresponds to

a decrease of the optical band gap from 3.05 eV for **3e** with a molecular weight of 1300 g/mol to 2.94 eV for polyfluorene.
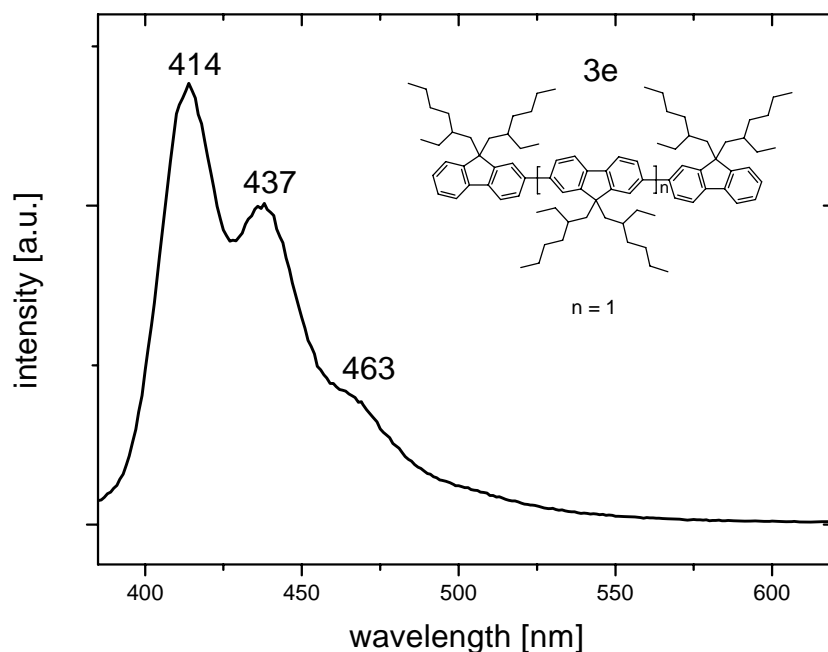
Figure 4. Fluorescence spectrum of a 20 nm thick film of 3e.

Figure 4 envisions a typical emission spectrum and shows the strong blue fluorescence. The most intense transition at 414 nm is assigned to the $S_{1,0}$-$S_{0,0}$ transition and further well resolved vibronic progressions are the $S_{1,0}$-$S_{0,1}$ (437 nm) and $S_{1,0}$-$S_{0,2}$ (463 nm) transitions. The energy differences between the peaks at 414 and 437 nm is 1272 cm^{-1} and between 437 and 463 nm is 1285 cm^{-1} and correspond to signals in the IR spectrum.

Thermal Properties

The glass transition temperatures were obtained by differential scanning calorimetry (DSC) and rise from 2°C for **3e** up to 34°C for **3b** (see Table 3). The glass transition of **3a** as well as the clearing temperatures of **3a-e** could not be detected by the DSC instrument and were therefore determined with polarisation microscopy. All mixtures except **3e** exhibit nematic

mesophases and the typical Schlieren textures were observed (Figure 5). From the SEC scans in Figure 1 it becomes clear, that **3e** mainly consists of the trimer and it is known that fluorene trimers do not exhibit LC phases [15]. However it has been shown that a reduction of the length of the alkyl chain in 9-position of the fluorene from C_8 to C_1 and the introduction of n-octyl or n-hexadecyl lateral side groups lead to the formation of smectic phases [25].

Table 3. Glass transition temperatures and isotropic-nematic transition temperatures of 3a-e.

sample	T_g [°C][a]	$T_{i->n}$ [°C][b]
3a	n.d.	> 360°C
3b	34	250
3c	22	150
3d	16	57
3e	2.0	n.d.

[a] determined by DSC, heating rate 20K/min. [b] determined by polarisation microscopy upon cooling with a rate of 0.1°C/min.
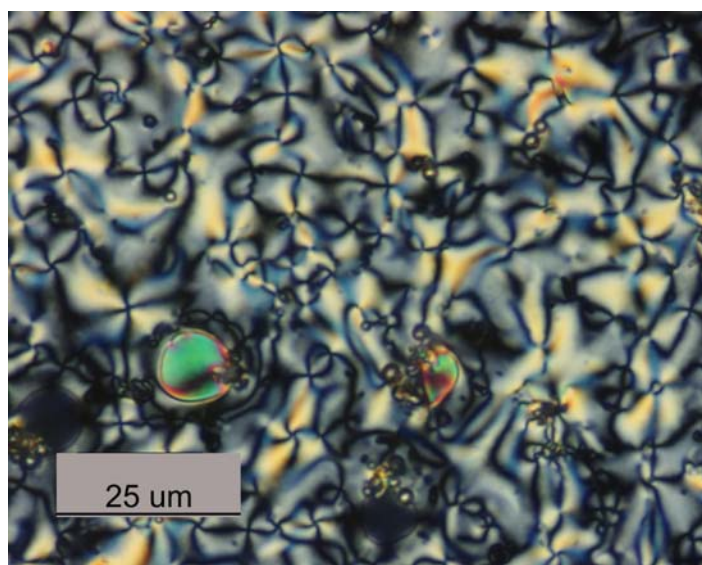
Figure 5. Nematic Schlieren texture of 3c observed upon cooling with 0.1°C/min between crossed polarisers; picture taken at 140°C.

The lowest clearing temperature of 57°C was observed for **3d** and the highest clearing point of 250°C for **3b**. The mixture **3a** with the highest molecular weight of 3800 g/mol exhibits a nematic phase up to decomposition at 360°C. Thus we could show that by varying the amount of endcapper the nematic mesophase of the fluorene oligomers **3a-e** can be shifted in a broad temperature range.
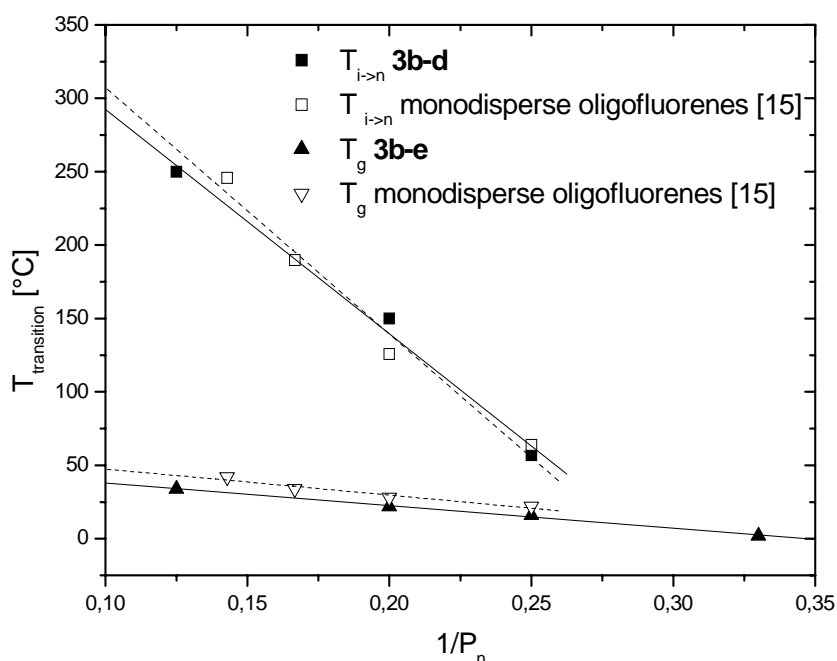
Figure 6. Glass transition temperature T_g and clearing temperature T_c versus reciprocal degree of polymerisation for *3b-e*. The transition temperatures of monodisperse oligomers from [15] are shown in addition. The full and dotted lines represent the linear regressions, the full lines refer to the data points of *3b-e*, the dotted lines refer to the monodisperse fluorene model compounds.

Figure 6 shows a plot of glass transition (T_g) and isotropic-nematic transition ($T_{i \to n}$) temperatures versus $1/P_n$ of **3b-e**. Both transition temperatures follow an almost linear dependence. The transition temperatures of monodisperse fluorene model compounds published in reference [15] are also displayed (open signs) and a good conformance between monodisperse and polydisperse oligomers can be observed. The glass transition temperatures of the monodisperse samples are slightly higher than those for the polydisperse ones. The

linear regression provides a T_g for the ideal polymer (with P_n->∞) of 53°C for the polydisperse fluorenes and 65°C for the monodisperse ones. The linear regression of the clearing temperatures leads to a value of > 440°C for high molecular weight polyfluorene. In practice this value cannot be achieved due to decomposition starting at 360°C.

Conclusion

Summing up we have developed an efficient 1-step synthesis of polydisperse fluorene oligomers **3a-e**. SEC analysis showed that the endcapping process is efficient and the molecular weights could be adjusted in the range from 1300 g/mol to 3800 g/mol by the amount of monofunctional endcapper.

The thermal behaviour was determined using DSC and polarisation microscopy. The glass transition temperatures vary between 2°C for the lowest molecular weight mixture and 34°C. The samples **3a-d** exhibit liquid crystalline phases and the clearing temperatures rise from 57°C to more than 360°C. The comparison of the thermal behaviour of the polydisperse oligomers **3a-e** with the monodisperse counterparts reported in reference [15] showed a good conformance. Thus the simple and efficient 1-step synthesis using a monofunctional endcapper enables us to tailor both the glass transition and the clearing temperature of oligofluorenes. In a forthcoming paper we will report the synthesis of analogous oligofluorenes with acrylate endgroups and the formation of micrometer sized patterns by photopolymerisation.

Experimental Section

General

^{1}H NMR spectra were recorded on a Bruker AC 250 spectrometer in CDCl$_3$ at 250 MHz with tetramethylsilane as reference. The molecular weights were determined by a Waters size exclusion chromatography system (SEC) for oligomers (analytical columns: crosslinked polystyrene gel, length 2 x 60 cm, width 0.8 cm, particle size 5 μm, pore size 100 Å, eluent THF (0.5 ml/min, 80 bar), oligofluorene calibration). UV-vis absorption spectra were recorded on a HITACHI U-3000 spectrophotometer and the fluorescence spectra on a SHIMADZU RF-5301 PC spectrofluorometer with 90° detection. Absorption and emission spectra were obtained at ambient temperature from thin films spin coated (1500 rpm, 0.5 wt%) from xylene solutions on cleaned glass substrates. The liquid crystalline behaviour was examined by a polarisation microscope Nikon Diaphot 300 with a Mettler FP 90 hotstage from films that were obtained by drop casting from CH$_2$Cl$_2$ solutions. For differential scanning calorimetry measurements (DSC) a Perkin-Elmer DSC-7 apparatus was used.

Absolute toluene and DMF were used as purchased from FLUKA. The catalyst Ni(COD)$_2$ was used as purchased from ABCR. 1,5-Cyclooctadiene and 2,2`-bipyridyl were used as received from Aldrich.

The synthesis of the monomers **1** and **2** (see Scheme 1) has been reported elsewhere [22].

Synthesis of the oligo[9,9-di(2-ethylhexyl)-2,7-fluorene-diyl]s 3a-e (see Table 4).

The synthesis of the mixture **3a** with a molar ratio of the bifunctional monomer **1** to the endcapper **2** of 5:1 is described in detail:

A schlenk flask was charged with 1.26 g (4.58 mmol) nickeldicyclooctadiene, 0.56 ml (4.58 mmol) cyclooctadiene, 0.715 g (4.58 mmol) 2,2`-bipyridyl and 25 ml dry DMF under argon. The mixture was degassed by 3 freeze-thaw cycles before it was heated to 80°C for 30 min under stirring. 0.74 g (1.35 mmol) dibromofluorene **1** and 0.13 g (0.27 mmol) monobromofluorene **2** were mixed in a separate flask. 60 ml dry toluene were added and the mixture was degassed by 3 freeze-thaw cycles. Subsequently the monomer mixture was added to the catalyst mixture using a cannula. The reaction mixture was stirred under argon at 80°C for 5 days in the dark. Afterwards it was poured into 240 ml MeOH/HCl(conc.) 1:1 and stirred at room temperature for 2 hours. The organic phase was separated from the HCl phase which was then washed with ether. The combined organic phases were washed with water and the solvent was evaporated. The crude product was filtered over a small alumina (neutral) column using toluene as eluent, then washed 5 times with alkaline EDTA solution (5%), reprecipitated twice from THF into MeOH and dried in vacuum yielding 0.551 g (87%) of **3a** as pale yellow powder.

^{1}H NMR (250 MHz, CDCl$_3$). δ (ppm): 7.5-7.9 (m, 5H), 7.3-7.45 (m, 1H), 1.9-2.25 (m, 4H), 0.4-1.1 (m, 30H)

^{13}C NMR (250 MHz, CDCl$_3$). δ (ppm): 151.7, 141.6, 140.8, 126.5, 123.5, 120.6, 55.5, 45.0, 35.2, 34.5, 28.7, 27.6, 23.2, 14.5, 10.8

IR (KBr) (cm^{-1}): 2957, 2921, 2855 (CH stretch); 1457 (aromatic ring vibration); 1377 (CH deformation); 813 (CH aromatic)

*Table 4. Molar amounts for monomer **1** and endcapper **2**, yields and molecular weights of oligofluorenes **3a-e**.*

	ratio[a] **1/2**	n_A[b] [mmol]	n_B[c] [mmol]	yield [%]	M_n (SEC)[d] [g/mol]
3a	5:1	1.35	0.27	87	3800
3b	2:1	1.89	0.95	61	2500
3c	3:2	1.77	1.18	73	2000
3d	1:1	0.18	0.18	76	1500
3e	1:2	1.18	2.36	92	1300

[a] monomer **1**/endcapper **2**. [b] monomer **1**. [c] endcapper **2**. [d] determined by SEC in THF with oligofluorene calibration.

Literature

1   Bernius, M.T., Inbasekaran, M., O`Brien, J., Wu, W., 2000, *Adv. Mater.*, **23**, 1737-1750.

2   Scherf, U., List, E. J. W., 2002, *Adv. Mater.* **7**, 477-487.

3   Grell, M., Bradley, D. D. C., Inbasekaran, M., Woo, E.. 1997, *Adv. Mater.*, **9**, 798-802.

4   O'Neill, M., Kelly, S.M., 2003, *Adv. Mater.,* **15**, 1135-1146.

5   Grell, M., Knoll, W., Lupo, D., Meisel, A., Miteva, T., Neher, D., Nothofer, H.-G., Scherf, U., Yasuda, A., 1999, *Adv. Mater.*, **11**, 671-675.

6   Whitehead, K.S., Grell, M., Bradley, D. D. C., Jandke, M., Strohriegl, P., 2000, *Appl. Phys. Lett.*, **76(20)**, 2946-2948.

7   Sirringhaus, H., Wilson, R.J., Friend, R.H., Inbasekaran, M., Wu, W., Woo, E.P., Grell, M., Bradley, D. D. C., 2000, *Appl. Phys. Lett.*, **77(3)**, 406-408.

8   Sims, M., Bradley, D.D.C., Ariu, M., Koeberg, M., Asimakis, A., Grell, M., Lidzey, D. G., 2004, *Adv. Func. Mater.*, **14**, 765-781.

9   Kulkarni, A. P., Kong, X., Jenekhe, S. A., 2004, *J. Phys. Chem. B*, **108**, 8689-8701.

10   List, E. J. W., Guentner, R., Scanducci de Freitas, P., Scherf, U., 2002, *Adv. Mater.*,
      14(5), 374-378.

11   Chi, C., Im, C., Engelmann, V., Ziegler, A., Lieser, G., Wegner, G., 2005, *Chem. Eur.
      J.*, **11**, 6833-6845.

12   Klaerner, G., Miller, R. D., 1998, *Macromolecules*, **31**, 2007-2009.

13   Geng, Y., Chen, A. C. A., On, J. J., Chen, S. H., Klubek, K., Vaeth, K., Tang, C. W.,
      2003, *Chem. Mater.*, **15**, 4352-4360.

14   Culligan, S. W., Geng, Y., Chen, S. H., Klubek, K., Vaeth, K., Tang, C.W., 2003, *Adv.
      Mater.*, **14**, 1176-1180.

15   Jo, J., Chi, C., Höger, S., Wegner, G., Yoon, D. Y., 2004, *Chem. Eur. J.*, **10**, 2681-2688.

16   Chi, C., Wegner, G., 2005, *Macromol. Rapid Comm.*, **26**, 1532-1537.

17   Chi, C., Im, C., Wegner, G. J., 2006, *Chem. Phys.*, **124**, 024907.

18   Anemian, R., Mulatire, J. C., Andraud, C., Stephan, O., Vial, J. C., 2002, *Chem. Comm.*,
      1608-1609.

19   Miteva, T., Meisel, A., Knoll, W., Nothofer, H. G., Scherf, U., Müller, D. C., Meerholz,
      K., Yasuda, A., Neher, D., 2001, *Adv. Mater.*, **13**, 565-570.

20   Knaapila, M., Stepanyan, R., Torkkeli, M., Lyons, B. P., Ikonen, T. P., Almasy, L.,
      Foreman, J. P., Serimaa, R., Güntner, R., Scherf, U., Monkman, A. P., 2005, *Phys. Rev.
      E.*, **71**, 041802.

21   Knaapila, M., Stepanyan, R., Lyons, B. P., Torkkeli, M., Hase, T. P. A., Serimaa, R.,
      Güntner, R., Seeck, O. H., Scherf, U., Monkman, A. P., 2005, *Macromolecules*, **38**,
      2744-2753.

22   Thiem, H., Strohriegl, P., Setayesh, S., De Leeuw, D., 2006, *Synth. Met.,* **165**, 582-589.

23   Kreyenschmidt, M., Klaerner, G., Fuhrer, T., Ashnenhurst, J., Karg, S., Chen, W. D.,

Lee, V. Y., Scott, J. C., Miller, R. D., 1998, *Macromolecules*, **31**, 1099-1103.

24   Grell, M., Bradley, D. D. C., Long, X., Chamberlain, T., Inbasekaran, M., Woo, E. P.,

Soliman, M., 1998, *Acta Polym.*, **49**, 439-444.

25   Güntner, R., Farrell, T., Scherf, U., Miteva, T., Yasuda, A., Nelles, G. J., 2004, *Mater.

Chem.,* **14**, 2622-2626.

12 Appendix:

# Single molecule spectroscopy of oligofluorenes: how molecular length influences polymorphism

Enrico Da Como[1]*, Esther Scheler[2], Peter Strohriegl[2], John M. Lupton[3], Jochen Feldmann[1]

[1] Photonics and Optoelectronics Group, Department of Physics and CeNS

Ludwig-Maximilians-Universität, 80799, Munich, Germany

[2] Makromolekulare Chemie I and Bayreuther Institut für Makromolekülforschung, University

of Bayreuth, 95440 Bayreuth, Germany

[3] Department of Physics, University of Utah, UT 84113-5036, Salt Lake City, USA

enrico.dacomo@physik.uni-muenchen.de
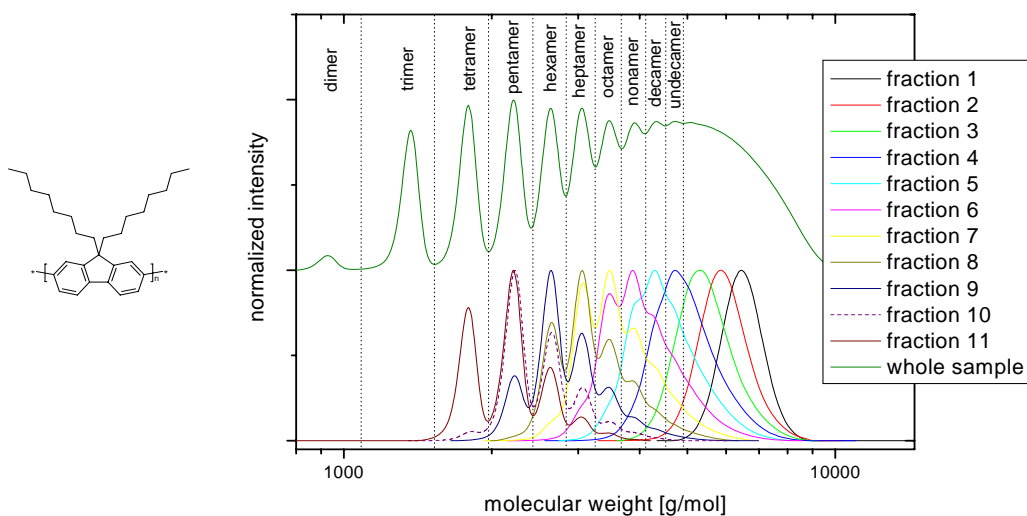
Abstract

Polyfluorene represents a unique model to study the influence of intramolecular conformation on the electronic properties of chromophores with an extended π-conjugation. According to the degree of planarity between the adjacent repeat units the electronic and optical properties can change substantially. This peculiar spectroscopic behaviour has been described by identifying different phases, namely the *glassy*, the γ- and the β-phase. Here we present the low-temperature single-molecule spectroscopy of a series of oligofluorenes differing in the number of monomeric units, in order to gain information on the influence of chain length on the polymorphism. By monitoring the energy of the zero-phonon line we have classified single molecules belonging to the different phases. We demonstrate that a large number of molecules starts to form the β-phase only when more than 9 repeat units are constituting the molecular chain. The implications for the control of morphology in polyfluorene thin films are discussed.

Introduction

Polyfluorene (PF) is one of the most remarkable conjugated polymers in terms of electrical and optical properties [1]. It is characterized by a wide energy band-gap which elects this material as an ideal system for deep-blue light emitting diodes (LEDs). In addition, the good charge-transport characteristics, which can show ambipolar character [2], have been exploited in optoelectronic applications such as lasers and LEDs [3].

In the fundamental research devoted to understand structure-property correlations in conjugated polymers, PFs emerged as model materials because of the rich polymorphic behaviour, achieved without the need for chemical modifications in the molecular structure. The polymorphism is, nevertheless, related to the type of side groups in position 9 to the fluorene moiety [4]. Poly(9,9-dioctyl)fluorene, hereafter termed PFO, shows at least three different phases in the solid state, which can be reproducibly obtained according to peculiar annealing or vapour swelling procedures [4,5]. Figure 1 (a) shows the chemical structure of the repeat unit of this conjugated polymer. Several experiments and theoretical models have unravelled the intramolecular nature of the different phases, which primarily resides in the degree of planarization between the repeat units [5-7]. Therefore, the polymer chain solid-state packing encountered in films seems to do not play a major role on the diverse photophysical responses characterizing the different phases. To review the previous studies, we start by pointing out that the extended planarization of the fluorene units leads to the formation of the β-phase [5-7]. Such a phase has a peculiar red-shifted emission (440 nm), with respect to the *glassy* phase, the latter showing the origin line (0-0) of the photoluminescence (PL) spectrum at 405 nm. These spectral properties have been explained considering an increase in the conjugation length for the planarized β-phase in contrast to the twisted *glassy*, where the larger dihedral angles partially disrupt the conjugation length [6,8]. Some recent studies have also demonstrated the existence of an intermediate phase, where the

planarization and long-range intrachain order does not reach the parameters of the β-phase. Such a phase has been called γ and could constitute a transition state between the ordered (β-) and disordered (*glassy*) phases of PFO [6]. Usually, thin films of PFO contain all of the phases in different amounts. In the absence of annealing and vapour swelling procedures, it is observed a large amount of chains in the *glassy* conformation with a lower amount of β-phase. The γ-phase is rare and was observed only in few reports [6].

Among the different polymorphs the β-phase has shown superior properties in terms of photochemical stability and charge transport [7,9]. As a consequence, many efforts were devoted to establish reproducible protocols to increase the relative amount of such planarized chains. In general annealing and vapour swelling protocols are effective in controlling the β-phase formation. However, a unified picture describing the thermodynamics and kinetics of phase transitions is still lacking. Some recent reports have shown that the conformation of the overall chain might have a role in regulating the phase transition and the correlated change in electronic properties [10].

The studies aiming to establish structure-property correlations in PFs have been principally performed on polymeric samples, which are disordered systems according to the large variance in molecular weights (polydispersity) [11,12]. In contrast to this approach experiments on oligomers have been used to shed light on the electronic structure of other families of conjugates polymers such as polyphenylene-vinylenes and polythiophenes [13,14]. PFO oligomers are expected to be equally important in order to understand the polymorphism. This approach has been exploited recently to study the optical properties of thin films of oligofluorenes [15]. However, oligomers can present an intrinsic polydispersity which can alter the conclusions drawn from ensemble experiments. It is, therefore, natural to consider techniques which can overcome the inhomogenity in the sample, such as single molecule

spectroscopy (SMS). SMS proved to be very effective in the comprehension of the optical properties of conjugated polymers as well as in revealing structure-property correlations at the single-chain level [14,16-18]. Moreover, information for the material characteristics in ensemble can be promptly obtained by statistical data on a large number of single molecules. In this paper, we present a systematic SMS study on oligo-FOs with an increasing number of repeat units. We have analyzed several samples differing in the relative abundance of one particular oligomer, which we termed n-FO, where n stands for the number of units in the dominating oligomer. By monitoring the 0-0 of the PL spectrum we counted molecules belonging to the *glassy* or *β*-phase in 5-FO, 6-FO. 7-FO and 8-FO. Interestingly, we have also observed a distribution of molecules peaking at 428 nm, which corresponds to an intermediate phase between the *glassy* (405 nm) and *β*-phase (440 nm). We have assigned this distribution to *γ*-phase molecules. The appearance of a considerable amount of *β*-phase molecules starts for fluorene oligomers with more than 9 repeat units. This result points to a molecular length dependence on the thermodynamic of *β*-phase formation and at the same time it shows directly the minimum delocalization length for excitons in *β*-phase chromophores. The results are important for the description of optical excitations in *β*-phase chromophores and for the understanding of the chain conformation and morphology control in PFO.

Experimental

Polydisperse oligofluorenes were obtained according to the procedure reported in reference [19], using 2,7-dibromofluorene and 2-bromofluorene precursors bearing dioctyl side chains in position 9. The Yamamoto coupling was performed using $Ni(COD)_2$ and 2,2`-bipyridyl in a mixture of dry DMF and dry toluene. The chemical structures were validated by ^{1}H NMR and ^{13}C NMR spectroscopy. The Yamamoto condensation results in samples characterized by a

broad molecular weight distribution. Therefore, preparative gel-permeations-chromatography (GPC) was performed in order to obtain samples with a low polydispersity. The whole oligomer mixture was hence separated into different fractions with low polydispersity indices, each fraction containing fluorene oligomers with different chain lengths. Figure 1 (b, c) show the GPC scan (light absorption versus molecular weight) of four different fractions separated by this method. All the studied fractions show well defined UV absorption peaks corresponding to an increasing discrete number of dioctyl-fluorene units in the molecular backbone. The calibration curve for the GPC was constructed from the knowledge of the exact molecular weight of the single oligomers derived from MALDI-TOF measurements. The different fractions were named according to the largest abundance of one particular oligomer. For example, in Fig.1 (b) the molecular weight distribution for the 5-FO (solid line) and 6-FO (dashed line) are reflecting the highest abundance of pentamer and hexamer, respectively. Table 1 summarizes the number average molecular weight (Mn) and the weight average molecular weight (Mw) [20], together with the polydispersity index (PDI) obtained by the oligofluorene calibration. The reported PDI are in the range of 1.04 demonstrating a reasonably defined separation in the oligomer concentration of the different fractions. Here we note that the relative abundance of one oligomer with respect to the others within the same fraction cannot be considered strictly quantitative, being slightly different the absorption cross-sections. Nevertheless, the differences are estimated to be well below the variance in absorbance between the peak molecular weight and the side distributions.

Table 1. *Average molecular weight by number (M_n) and by weight (M_w) for the four fractions. In the last column the polidispersity index (PDI) is reported. A GPC calibration based on oligofluorene was applied.*

Sample	M_n (g/mol)	M_w (g/mol)	PDI
5-FO	1870	1940	1.04
6-FO	2490	2580	1.04
7-FO	2830	2930	1.03
8-FO	3190	3300	1.03
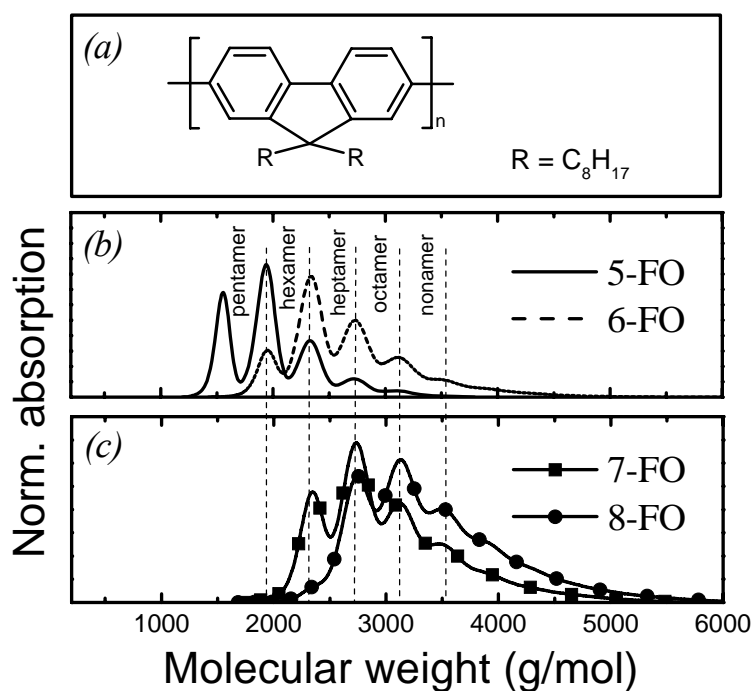
Figure 1. *(a) Chemical structure of the dioctyl-fluorene repeat units. Molecular weigth distributions obtained from a GPC separation for the four fractions. (b) fractions 5-FO (solid line) and 6-FO (dashed line). (c) fractions 7-FO (line + squares) and 8-FO (line + circles).*

Thin films for SMS were prepared by spin coating solutions of the different samples on aluminium-coated glass cover slides. These substrates reduce remarkably the scattered light which can be a serious problem for SMS in the near-UV spectral range, where fluorenes have to be excited [7,10]. The spin coated solutions consisted of the oligofluorenes dissolved at

very high dilution (10^{-8} g/l) in toluene in the presence of the inert polymer Zeonex (7g/l). Zeonex, a highly transparent matrix, was used for isolating oligofluorene molecules and ensures an optimal optical quality of the thin films. Spin coating was performed at 5000 rpm and all the samples were exposed to vapours of toluene for a period of 10 hours in a saturated chamber kept at 343 K. According to previous reports this receipt increases the number of β-phase molecules in the sample as a consequence of vapour swelling of the matrix [5,10]. The thin films were subsequently mounted on a cold finger liquid helium cryostat (5K) and kept under a dynamic vacuum of $<10^{-6}$ mbar for SMS experiments.

SMS was performed with a home built wide field microscope described in detail elsewhere [18,21]. Briefly, the second harmonic of a Ti:sapphire oscillator (398 nm, 80 MHz repetition rate) was used as excitation source. The PL of single molecules was imaged on a front illuminated charge coupled device camera, after passing through a spectrograph.

Results

Figure 2 shows three exemplary PL spectra from different single oligomers observed in the same sample (6-FO). In panel (a) the typical spectrum of a *glassy* phase molecule is observed, which is characterized by a broad 0-0 peak centered at 413 nm and a vibronic progression involving C=C stretching extending to the 0-2 peak [7,10]. In panel (b) we report a previously not observed SM spectrum, which appears at an intermediate wavelength (428 nm) between the *glassy* phase (panel a) and the narrow PL peak (FWHM= 1.8 meV) at 446nm of the β-phase (panel c). In agreement with previous reports, we have assigned the spectrum in panel (b) to the γ-phase [6]. The large differences in linewidth reported for the three spectra are entangled to the degree of intramolecular order. In the case of the β-phase a quasi-1D crystal is formed as demonstrated by polarization resolved measurements on the single polymer chain

[10]. For the other two conformations the inhomogeneous distribution of dihedral angles impacts directly on the electronic disorder of the chromophores resulting in a smooth transition to the large linewidth of the *glassy* phase (50 meV).
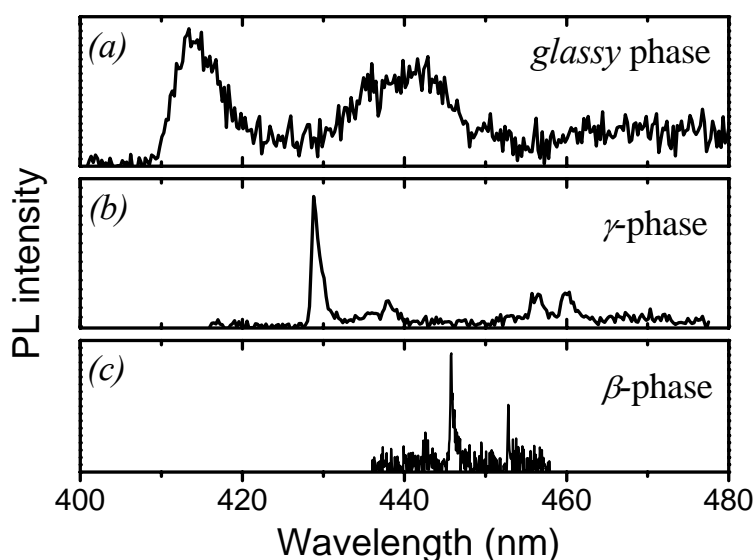
Figure 2. *Low temperature (5K) PL spectra of single oligofluorenes in the glassy (a), γ- (b) and β-phase (c) recorded from different single molecules out of the fraction 6-FO. The spectrum in panel (c) was recorded using a high resolution grating and shows the spectral features only in a limited range. Excitation was performed at 400 nm.*

We have used these very different spectral features to distinguish and count the number of molecules belonging to the different phases for the four fractions separated from the GPC (see Fig.1). In figure 3 we report a histogram of the peak emission wavelength of the 0-0 for 80 single molecules from the sample 5-FO (panel a) and 115 single molecules from 6-FO (panel b). For 5-FO molecules the histogram peaks at 410 nm demonstrating that this sample is almost completely constituted of fluorene oligomers in the *glassy* phase. The occurrence of emission spectra in the spectral range beyond 420 nm (γ- and β-phase) becomes apparent in the 6-FO fraction where the histogram extends to the red part of the spectrum. According to

the Mw distributions of figure 1 (b), we note that the 6-FO fraction presents an increased

amount of oligomers with more than 9 repeat units when compared to 5-FO.
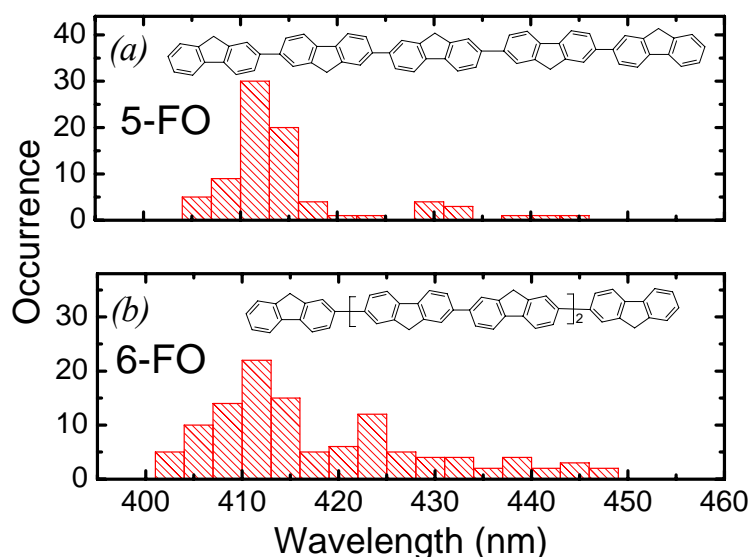
Figure 3. *0-0 emission wavelength histograms for 80 single molecules from the 5-FO fraction (a) and 115 single molecules from the 6-FO fraction (b). The insets show the chemical structures for the most abundant oligomer in the respective fractions. The octyl side groups are not shown for the sake of clarity.*

We performed the same type of experiment for 7-FO and 8-FO. The histograms are reported

in figure 4. In the 7-FO fraction (panel a) the number of oligomers in the *glassy* conformation

is still dominant. However, a clear distribution peaking at about 440 nm is appearing,

suggesting an increased number of molecules in the β-phase. It is interesting to note that in

contrast to the case of the polymer, where no emission peaks are observed between the *glassy*

and the β-phase [7,10], an almost continuous distribution of emission peaks is present in the

range between 420-440 nm. The distribution in this spectral range evolves to two

distinguishable peaks in the histogram of 8-FO (Figure 4 b). In this case a negligible amount

of molecules in the *glassy* phase is observed and a bimodal distribution peaking at 425 and

440 nm is left.
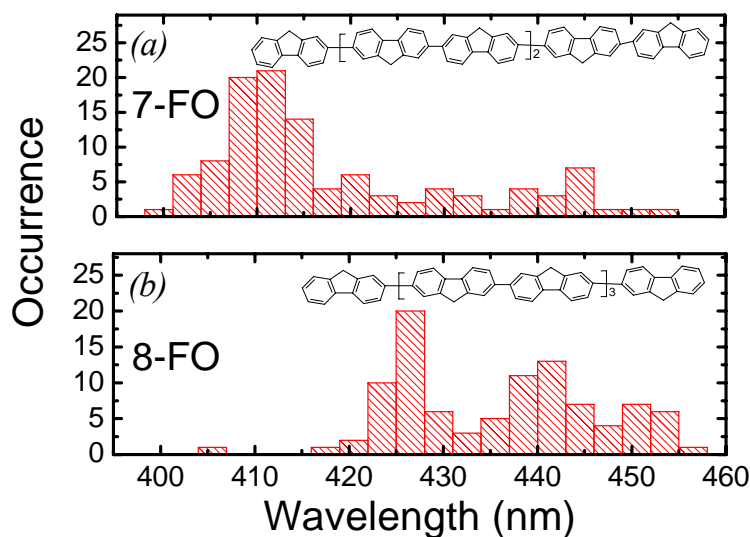
Figure 4. *0-0 emission wavelength histograms for 110 single molecules from the 7-FO fraction (a) and 97 single molecules from the 8-FO fraction (b). The insets show the chemical structures for the most abundant oligomer in the respective fractions.*

Discussion

According to the Mw distribution of figure 1 the fraction 5-FO shows a relatively low absorption signal for oligomers longer than 8 repeat units. The corresponding histogram in figure 3 clearly shows a negligible number of molecules in the γ- or β- phase. A small number of β-phase molecules is instead observed in the 6-FO fraction, where the Mw distribution extends to more than 9 repeat units. Therefore, from these results we deduce that 9 or more repeat units are necessary to form a planarized chain of fluorene repeat units. The β-phase content increases further when we look at the histograms for 7-FO and 8-FO (figure 4). Since all the samples were prepared with the same procedure and exposed to the vapour swelling, we conclude that β- phase formation in PFO is a molecular length dependent process. The minimum number of repeat units necessary to generate the β-phase should be larger than 9. According to the histogram of 8-FO, we speculate that 8 and 7 repeat units should give the chain length necessary to observe an intermediate γ-phase. As mentioned before such a phase was rarely observed in previous studies on PFO. The reason might be related to the fact that in

polymers the large number of repeat units favours the formation of β-phase segments whenever planarization occurs. The energetically lower β-phase chromophores act as very efficient emitting sites, precluding the observation of emission in intermediate states involved in the exciton funnelling. This interpretation is consistent with the results on thin films where both intrachain and interchain energy transfer takes place [11]. The absence of emission from γ-phase segments in single isolated polymer chains is interesting and points to a very efficient intrachain energy transfer along the polymer backbone. Efficient intrachain energy transfer has been previously demonstrated by SMS on dye endcapped PFs and is likely to take place in PFO with a similar efficiency [22].

Very recently Tsoi et al. reported a systematic study on the conjugation length of polyfluorene in the β-phase [15]. In the optical experiments a PFO sample was compared with a statistical oligomer comprising molecules with 5 to 19 repeat units and a very pure oligomer with 5 units. In qualitative agreement with our results it was concluded that a molecular length of more than 5 units is required to generate the β-phase. Our study considers oligomers with a lower polydispersity and moves the lower limit to 9 units. However, we point out that this value should not be considered as an absolute number. Indeed an oligomeric chain of 9 units could still not form the β-phase if the chain does not adopt an extended conformation.

Indeed, in a previous report we demonstrated a direct correlation between the planarity of the fluorene units and the degree of chain extension in space by using polarization anisotropy measurements [10]. In particular, the planarized β-phase tends to have an elongated shape of the chromophores, while the *glassy* phase has a more collapsed structure. While this behaviour could be related to the different number of chromophoric units in the chain, the planarization should induce rigidity to the chain which in turn assumes a more elongated structure. As a preliminary result of such kind of correlations on oligomers we report in

figure 5 a polarization anisotropy trace. In such an experiment the polarization of the exciting laser beam is rotated with respect to the fixed position of the single molecule and the PL intensity is recorded. The PL intensity is governed by the coupling between the transition dipole moment of the chromophore and the electric field vector of the laser light. The superimposed white diamonds are the data points obtained by integrating the PL intensity on the 0-0 shown in the color contour plot as a function of the polarization angle. The data are perfectly fitted by a $\cos^2$ function, describing the vectorial coupling. A quantitative measure of the anisotropy is given by the anisotropy degree defined as $P = (I_{max} - I_{min})/(I_{max} + I_{min})$ [16]. Where I_{max} and I_{min} are the maximum and minimum intensity extracted from the trace. The oligomer molecule in figure 5 presents an P value of 0.74, witnessing a rather elongated conformation as expected for a β-phase chromophore. Future investigations will concern the measurement of the chain extension in larger oligomers to establish the critical chain length for folding, a critical parameter for obtaining PFO with a large amount of chains in the β-phase. In addition, these experiments should give further insights about the unique photophysical properties of β-phase chromophores, where the multi-chromophoric picture has failed [7,10].
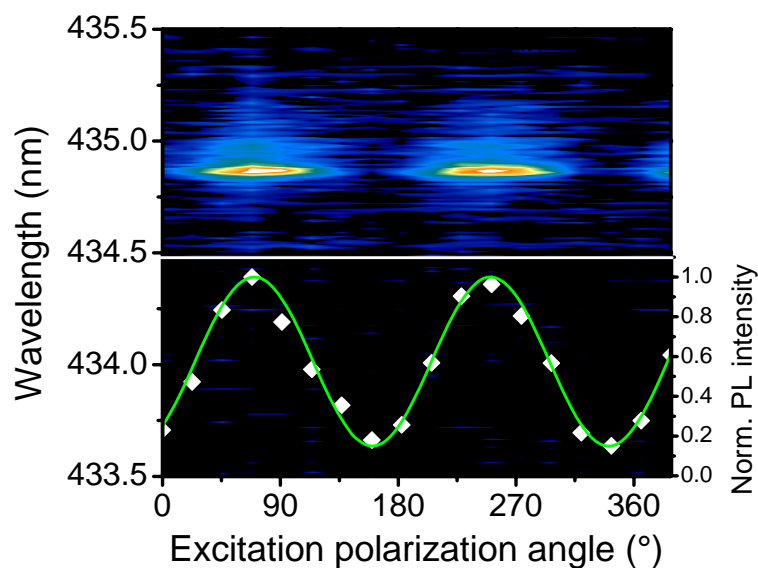
Figure 5. *Color contour plot of the temporal evolution (trace) of the PL spectrum of a single β-phase molecules from sample 8-FO recorded during the rotation of the polarization of the excitation light. The PL spectrum shows the 0-0 transition 434.8 nm. The superimposed white diamonds are an effective measure of the polarization anisotropy. The green line is a fit according to a $\cos^2(\theta)$ function. The resulting polarization anisotropy for this molecule is P = 0.74.*

Conclusions

In summary, we have performed low temperature (5K) SMS on fluorene oligomers with diverse molecular weights. By counting single molecules belonging to the different phases we have established the minimum number of repeat units necessary to form the *β*-phase. In addition we have observed the spectroscopical signatures of an intermediate phase (*γ*-phase), previously observed only in ensemble studies. Further studies will involve polarization anisotropy measurements to clarify the role of chain extension in oligomers. The results presented here provide new strategies for the morphological control of polyfluorene films and information for the theoretical modelling of polymorphism in polyfluorenes.

References

1   M. Grell, W. Knoll, D. Lupo, A. Meisel, T. Miteva, D. Neher, H. G. Nothofer, U. Scherf, A. Yasuda: Adv. Mater. **11**, 671 (1999); U. Scherf, E. J. W. List: Adv. Mater. **14**, 477 (2002).

2   L. L. Chua, J. Zaumseil, J. F. Chang, E. C. W. Ou, P. K. H. Ho, H. Sirringhaus, R. H. Friend: Nature (London) **434**, 194 (2005).

3   J. M. Lupton: Nature (London) **453**, 459 (2008); Y. Yang, G. A. Turnbull, I. D. W. Samuel: Appl. Phys. Lett. **92**, 163306 (2008); R. D. Xia, G. Heliotis, D. D. C. Bradley: Appl. Phys. Lett. **82**, 3599 (2003).

4   E. J. W. List, R. Guentner, P. S. de Freitas, U. Scherf: Adv. Mater. **14**, 374 (2002).

5   M. Grell, D. D. C. Bradley, G. Ungar, J. Hill, K. S. Whitehead: Macromolecules **32**, 5810 (1999).

6   W. Chunwaschirasiri, B. Tanto, D. L. Huber, M. J. Winokur: Phys. Rev. Lett. **94**, 107402 (2005).

7   K. Becker, J. M. Lupton: J. Am. Chem. Soc. **127**, 7306 (2005).

8   I. Franco, S. Tretiak: J. Am. Chem. Soc. **126**, 12130 (2004).

9   P. Prins, F. C. Grozema, B. S. Nehls, T. Farrell, U. Scherf, L. D. A. Siebbeles: Phys. Rev. B **74**, 113203 (2006).

10   E. Da Como, K. Becker, J. Feldmann, J. M. Lupton: Nano Lett. **7**, 2993 (2007).

11   M. Ariu, M. Sims, M. D. Rahn, J. Hill, A. M. Fox, D. G. Lidzey, M. Oda, J. Cabanillas-Gonzalez, D. D. C. Bradley: Phys. Rev. B **67**, 195333 (2003).

12   A. L. T. Khan, P. Sreearunothai, L. M. Herz, M. J. Banach, A. Kohler: Phys. Rev. B **69**, 085201 (2004).

13   E. Da Como, M. A. Loi, M. Murgia, R. Zamboni, M. Muccini: J. Am. Chem. Soc. **128**, 4277 (2006); B. J. Schwartz: Nature Mater. **7**, 427 (2008); M. Muccini, E. Lunedei, A. Bree, G. Horowitz, F. Garnier, C. Taliani: J. Chem. Phys. **108**, 7327 (1998).

14   K. Becker, E. Da Como, J. Feldmann, F. Scheliga, E. T. Csanyi, S. Tretiak, J. M. Lupton: J. Phys. Chem. B **112**, 4859 (2008).

15   W. C. Tsoi, A. Charas, A. J. Cadby, G. Khalil, A. M. Adawi, A. Iraqi, B. Hunt, J. Morgado, D. G. Lidzey: Adv. Funct. Mater. **18**, 600 (2008).

16   D. H. Hu, J. Yu, K. Wong, B. Bagchi, P. J. Rossky, P. F. Barbara: Nature (London) **405**, 1030 (2000).

17   T. Huser, M. Yan, L. J. Rothberg: Proc. Natl. Acad. Sci. USA **97**, 11187 (2000); J. G. Müller, U. Lemmer, G. Raschke, M. Anni, U. Scherf, J. M. Lupton, J. Feldmann: Phys. Rev. Lett. **91**, 267403 (2003).

18   F. Schindler, J. M. Lupton, J. Feldmann, U. Scherf: Proc. Natl. Acad. Sci. USA **101**, 14695 (2004).

19   E. Scheler, P. Strohriegl: Liq. Cryst. **34**, 667 (2007).

20   M. P. Stevens, *Polymer Chemistry: an introduction*. (Oxford University Press, New York, 1999).

21   J. G. Müller, M. Anni, U. Scherf, J. M. Lupton, J. Feldmann: Phys. Rev. B **70**, 035205 (2004).

22   K. Becker, J. M. Lupton: J. Am. Chem. Soc. **128**, 6468 (2006); K. Becker, J. M. Lupton, J. Feldmann, B. S. Nehls, F. Galbrecht, D. Q. Gao, U. Scherf: Adv. Funct. Mater. **16**, 364 (2006); K. Becker, J. M. Lupton, J. Feldmann, S. Setayesh, A. C. Grimsdale, K. Müllen: J. Am. Chem. Soc. **128**, 680 (2006).

13   List of publications

Esther Scheler, Irene Bauer, Peter Strohriegl

Synthesis and photopatterning of fluorene based reactive mesogens

Macromolecular Symposia **2007**, *254*, 203

Esther Scheler, Peter Strohriegl

Tailoring fluorene-based oligomers for fast photopatterning

Journal of Macromolecular Chemistry **2009**, *19*, 3207

Esther Scheler, Peter Strohriegl

Three color random fluorene- based oligomers for fast micron scale photopatterning

submitted to *Chemistry of Materials*

Esther Scheler, Peter Strohriegl

Synthesis of oligofluorenes by endcapping

Liquid crystals **2007**, *34*, 667

Enrico Da Como, Esther Scheler, Peter Strohriegl, John M. Lupton, Jochen Feldmann

Single molecule spectroscopy of oligofluorenes: how molecular length influences polymorphism

Applied Physics A: Materials Science and Processing **2009***, 95*, 61

Esther Scheler, Peter Strohriegl

Bookchapter in: Liquid Crystalline Semiconductors: Materials, Properties and Applications, Canopus Academic Publishing Ltd, submitted.

Mein Dank gilt auch den ehemaligen und derzeitigen Mitgliedern im Labor 595: Dr. Martin Sonntag, Dr. Heiko Thiem, Andreas Ringk, Andrea Jahreis und Pamela Schrögel für das Korrekturlesen und ihre Hilfsbereitschaft bei den größeren und kleineren Dingen des Laboralltags und vor allem für das angenehme Laborklima. Die Studenten Thomas Czubak, Michael Schrempf und Eva Betthausen haben auch durch ihre Mitarbeit an einigen Projekten zu dieser Arbeit beigetragen.

Meinen Eltern möchte ich für ihre Unterstützung während des gesamten Studiums und der Anfertigung dieser Doktorarbeit ganz herzlich danken, da sie dies alles überhaupt erst ermöglicht haben.

Vor allem meinem Freund Michi möchte ich für die große Unterstützung bei all den größeren und kleineren Problemen innerhalb und außerhalb des Labors danken. Sein Verständnis und seine Geduld haben maßgeblich zum Gelingen und Anfertigen meiner Doktorarbeit beigetragen.

Erklärung

Die vorliegende Arbeit habe ich selbst verfasst und keine anderen als die von mir angegebenen Quellen und Hilfsmittel benutzt.

Ferner erkläre ich, dass ich nicht versucht habe, anderweitig mit oder ohne Erfolg eine Dissertation einzureichen oder mich der Doktorprüfung zu unterziehen.

Bayreuth, Juli 2009

....

Esther Scheler